

Crystal Nucleation in Liquids: Open Questions and Future Challenges in Molecular Dynamics Simulations

Gabriele C. Sosso,¹ Ji Chen,¹ Stephen J. Cox,¹ Martin Fitzner,¹ Philipp Pedevilla,¹ Andrea Zen,¹ and Angelos Michaelides¹

Thomas Young Centre, London Centre for Nanotechnology and Department of Physics and Astronomy, University College London, Gower Street WC1E 6BT London, UK.

The nucleation of crystals in liquids is one of nature's most ubiquitous phenomena, playing an important role in areas such as climate change and the production of drugs. As the early stages of nucleation involve exceedingly small time and length scales, atomistic computer simulations can provide unique insight into the microscopic aspects of crystallization. In this review, we take stock of the numerous molecular dynamics simulations that in the last few decades have unraveled crucial aspects of crystal nucleation in liquids. We put into context the theoretical framework of classical nucleation theory and the state of the art computational methods, by reviewing simulations of e.g. ice nucleation or crystallization of molecules in solutions. We shall see that molecular dynamics simulations have provided key insight into diverse nucleation scenarios, ranging from colloidal particles to natural gas hydrates, and that in doing so the general applicability of classical nucleation theory has been repeatedly called into question. We have attempted to identify the most pressing open questions in the field. We believe that by improving (i) existing interatomic potentials; and (ii) currently available enhanced sampling methods, the community can move towards accurate investigations of realistic systems of practical interest, thus bringing simulations a step closer to experiments.

Keywords: crystal nucleation, supercooled liquids, molecular dynamics

CONTENTS

Abbreviations	2
I. Introduction	3
A. Theoretical Framework	3
1. Classical Nucleation Theory	3
2. Two-step nucleation	5
3. Heterogeneous Nucleation	6
4. Nucleation at Strong Supercooling	7
B. Experimental Methods	8
C. Molecular Dynamics Simulations	9
1. Brute Force Simulations	9
2. Enhanced Sampling Simulations	11
II. Selected Systems	12
A. Colloids	12
B. Lennard-Jones Liquids	14
C. Atomic Liquids	17
D. Water	19
1. Homogeneous Nucleation	19
Nucleation rates	19
Nucleation mechanism	22
2. Heterogeneous Ice Nucleation	23
E. Nucleation from Solution	27
F. Natural Gas Hydrates	30
III. Future Perspectives	35
Acknowledgement	36
References	37

ABBREVIATIONS

BCC	Body Centered Cubic
cDFT	Classical Density Functional Theory
CNT	Classical Nucleation Theory
CNT	Classical Nucleation Theory
DFT	Density Functional Theory
DSC	Differential Scanning Calorimetry
FCC	Face Centered Cubic
FES	Forward Flux Sampling
FTIRS	Fourier Transform Infrared Spectroscopy
HDL	High Density Liquid
LCH	Labile Cluster Hypothesis
LDL	Low Density Liquid
LSH	Local Structure Hypothesis
MD	Molecular dynamics
MetaD	Metadynamics
PNC	Pre-Nucleation Cluster
RHCP	(Random)Hexagonal Close Packed
SEM	Scanning Electron Microscope
sH	Structure H
sI	Structure I
sII	Structure II
SMRT-TEM	Single-Molecule-Real-Time - TEM
TEM	Transmission Electron Microscope
TIS	Transition Interface Sampling
UMD	Unbiased Molecular Dynamics
US	Umbrella Sampling
XPS	X-Ray Photoelectron Spectroscopy

I. INTRODUCTION

Crystal nucleation in liquids has countless practical consequences in science and technology, and it also affects our everyday experience. One obvious example is the formation of ice, which influences global phenomena like climate change^{1,2} as well as processes happening at the nanoscale, like intracellular freezing^{3,4}. On the other hand, controlling nucleation of molecular crystals from solutions is of great importance to pharmaceuticals and particularly in the context of drug design and production, as the early stages of crystallization impact on the crystal polymorph obtained^{5,6}. Even the multibillion-dollar oil industry is affected by the nucleation of hydrocarbon clathrates, which can form inside pipelines endangering extraction^{7,8}. Finally, crystal nucleation is involved in many processes spontaneously happening in living beings, from the growth of the beautiful Nautilus shells⁹ to the dreadful formation in our own brains of amyloid fibrils, which are thought to be responsible for many neurodegenerative disorders like Alzheimers disease^{10,11}.

Each of the above scenarios start from a liquid below its melting temperature. This *supercooled liquid*¹² is doomed, according to thermodynamics, to face a first-order phase transition leading into a crystal^{13,14}. Before this can happen, however, a sufficiently large cluster of crystalline atoms (or molecules, or particles) must form within the liquid, such that the free energy cost of creating an interface between the liquid and the crystalline phase will be overcome by the free energy gain of having a certain volume of crystal. This event stands at the heart of crystal nucleation, and how the latter has been, is, and will be modeled by means of computer simulations is the subject of this review.

The last few decades have witnessed an impressive body of experimental work devoted to crystal nucleation. For instance, thanks to novel techniques like e.g. Transmission Electron Microscopy at very low temperatures (cryo-TEM microscopy), we are now able to peek in real-time into the early stages of crystallization¹⁵. A substantial effort has also been made to understand which materials, in the form of impurities within the liquid phase, can either promote or inhibit nucleation events¹⁶, a common scenario known as heterogeneous nucleation. However, our understanding of crystal nucleation is far from being complete. This is because the molecular (or atomistic) details of the process are largely unknown due to the very small length scale involved (nm), which is exceedingly challenging to probe in real time even by state of the art measurements. Hence the need for computer simulations and particularly molecular dynamics (MD), where the temporal evolution of the liquid into the crystal is more or less faithfully reproduced. Unfortunately, crystal nucleation is a rare event, which can happen on timescales of e.g. seconds, far beyond the reach of any conventional MD framework. In addition, a number of approximations within the computational models, the algorithms and the theoretical framework used have

been severely questioned for several decades. While the rush for computational methods able to overcome this *timescale problem* is more competitive than ever, we are almost always forced to base our conclusions upon the ancient grounds of classical nucleation theory (CNT), a powerful theoretical tool that nonetheless dates back 90 years to Volmer and Weber¹⁷.

Nonetheless, these are exciting times for the crystal nucleation community, as demonstrated by the many reviews covering several aspects of this diverse field^{18–24}. This particular review will focus almost exclusively on MD simulations of crystal nucleation of supercooled liquids and supersaturated solutions. We take into account several systems, from colloidal liquids to natural gas hydrates, highlighting long standing issues as well as recent advances. While we will review a substantial fraction of the theoretical efforts in the field, mainly from the last decade, our goal is not to discuss in detail every contribution. Instead, we try to pinpoint the most pressing issues that still prevent us from furthering our understanding of nucleation.

This paper is structured into three parts. In the first part we introduce the theoretical framework of CNT (Sec. IA), the state of the art experimental techniques (Sec. IB) and the MD-based simulation methods (Sec. IC) that in the last few decades have provided insight into nucleation. In Sec. II we then put such computational approaches into context, describing achievements as well as open questions concerning the molecular details of nucleation for different kinds of systems, namely colloids (Sec. IIA), Lennard-Jones (LJ) liquids (Sec. IIB), atomic liquids (Sec. IIC), water (Sec. IID), nucleation from solution (Sec. IIE) and natural gas hydrates (Sec. IIF). In the third and last part of the paper (Sec. III) we highlight future perspectives and open challenges in the field.

A. Theoretical Framework

1. Classical Nucleation Theory

Almost every computer simulation of crystal nucleation in liquids invokes some elements²⁵ of classical nucleation theory (CNT). The latter has been discussed in great detail elsewhere^{26–28} and we include it here for the sake of completeness and also to introduce various terms used throughout the review. Nonetheless, readers familiar with CNT can skip to Sec. IB.

CNT was formulated 90 years ago thanks to the contributions of Volmer and Weber¹⁷, Farkas^{29,30}, Becker and Döring³¹ and Zeldovich³², on the basis of the pioneering ideas of none other than Gibbs himself³³. CNT was created to describe the condensation of supersaturated vapors into the liquid phase, but most of the concepts can also be applied to the crystallization of supercooled liquids and supersaturated solutions. According to CNT, clusters of crystalline atoms (or particles, or molecules) of

any size are treated as macroscopic objects, that is homogeneous chunks of crystalline phase separated from the surrounding liquid by a vanishingly thin interface. This apparently trivial assumption is known as the capillarity approximation, which encompasses most of the strengths and weaknesses of the theory. By embracing the capillarity approximation, the interplay between the interfacial free energy γ_S , and the free energy difference $\Delta\mu_V$ between the liquid and the crystal fully describes the thermodynamics of crystal nucleation. In three dimensions³⁴, the free energy of formation ΔG_N for a spherical crystalline nucleus of radius r can thus be written as the sum of a surface term and a volume term:

$$\Delta G_N = \underbrace{4\pi r^2 \gamma_S}_{\text{Surface term}} - \underbrace{\frac{4\pi}{3} r^3 \Delta\mu_V}_{\text{Volume term}}. \quad (1)$$

This function, sketched in Fig. 1, displays a maximum corresponding to the so called critical nucleus size n^*

$$n^* = \frac{32\pi\rho_C}{3} \frac{\gamma_S^3}{\Delta\mu_V^3}, \quad (2)$$

where ρ_C is the number density of the crystalline phase. The critical nucleus size represents the number of atoms that must be included in the crystalline cluster for the free energy difference $\Delta\mu_V$ to match the free energy cost due to the formation of the solid liquid interface. Clusters of crystalline atoms occur within the supercooled liquid by spontaneous, infrequent fluctuations, which eventually lead the system to overcome the free energy barrier for nucleation

$$\Delta G_N^* = \frac{16\pi}{3} \frac{\gamma_S^3}{\Delta\mu_V^2}, \quad (3)$$

triggering the actual crystal growth (see Fig. 1).

The kinetics of crystal nucleation is typically addressed by assuming that no correlation exists between successive events increasing or reducing the number of constituents of the crystalline nucleus. In other words, the time evolution of the nucleus size is presumed to be a Markov process, in which atoms in the liquid either order themselves one by one in a crystalline fashion or dissolve one by one into the liquid phase. In addition, we state that every crystalline nucleus lucky enough to overcome the critical size n^* quickly grows to macroscopic dimensions on a timescale much smaller than the long time required for that fortunate fluctuation to come about. If the above mentioned conditions are met³⁵ the nucleation rate, i.e. the probability per unit time per unit volume of forming a critical nucleus does not depend on time, leading to the following formulation of the so called steady-state nucleation rate \mathcal{J} :

$$\mathcal{J} = \mathcal{J}_0 \exp\left(-\frac{\Delta G_N^*}{k_B T}\right), \quad (4)$$

where k_B is the Boltzmann constant and \mathcal{J}_0 is a prefactor which we discuss later. The steady-state nucleation rate is the central quantity in the description of crystallization kinetics, as much as the notion of critical nucleus size captures most of the thermodynamics of nucleation.

All quantities specified up to now depend on pressure and most notably temperature. In most cases, the interfacial free energy γ_S is assumed to be linearly dependent on temperature, while the free energy difference between the liquid and the solid phase $\Delta\mu_V$ is proportional to the supercooling $\Delta T = T_M - T$ (or the supersaturation). Several approximations exist to treat the temperature dependence of γ_S ³⁶ and $\Delta\mu_V$ ³⁷, which can vary substantially for different supercooled liquids³⁸. In any case, it follows from Eq. 3 that the free energy barrier for nucleation ΔG_N^* decreases with supercooling. In other words, the further we are from the melting temperature T_M , the larger the thermodynamic driving force for nucleation.

Interestingly, in the case of supercooled liquids kinetics goes the other way, as the dynamics of the liquid slow down with supercooling, thus hindering the occurrence of nucleation events. In fact, while a conclusive expression for the prefactor \mathcal{J}_0 is still lacking^{39,40}, \mathcal{J}_0 is usually written within CNT as²⁷:

$$\mathcal{J}_0 = \rho_S \cdot \mathcal{Z} \cdot \mathcal{A}_{kin} \quad (5)$$

where ρ_S is the number of possible nucleation sites per unit volume, \mathcal{Z} is the Zeldovich factor^{27,41} (accounting for the fact that several postcritical clusters may still shrink without growing into the crystalline phase), and \mathcal{A}_{kin} is a kinetic prefactor³⁹. The latter should represent the *attachment rate*, that is the frequency with which the particles in the liquid phase reach the cluster re-arranging themselves in a crystalline fashion. However, in a dense supercooled liquid \mathcal{A}_{kin} also quantifies the ease with which the system explores configurational space, effectively regulating the amplitude of the fluctuations possibly leading to the formation of a crystalline nucleus. In short, we can safely say that \mathcal{A}_{kin} involves the atomic or molecular mobility of the liquid phase, more often than not quantified in terms of the self-diffusion coefficient \mathcal{D} ²⁷, which obviously decreases with supercooling. Thus, for a supercooled liquid the competing trends of ΔG_N^* and \mathcal{A}_{kin} lead - in the case of diffusion-limited nucleation⁴² - to a maximum in the nucleation rate, as depicted in Fig. 2. The same arguments apply when dealing with e.g. solidification of metallic alloys^{43,44}. In the case of nucleation from solutions, γ_S and $\Delta\mu_V$ depend mainly on supersaturation. However, the dependence of the kinetic prefactor on supersaturation is much weaker than the temperature dependence of \mathcal{A}_{kin} characteristic of supercooled liquids. As a result, there is usually no maximum in the nucleation rate as a function of supersaturation for nucleation from solutions⁴⁵.

Although \mathcal{A}_{kin} is supposed to play a minor role compared to the exponential term in Eq. 4, the kinetic prefactor has been repeatedly blamed for the quantitative

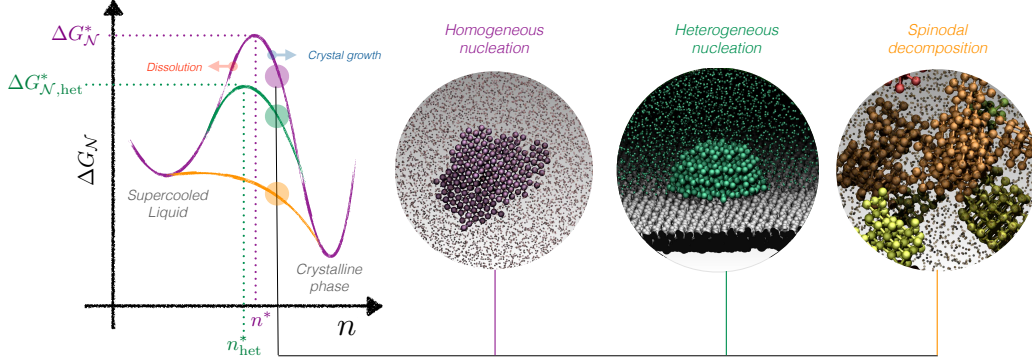


Figure 1. Sketch of the free energy difference ΔG_N as a function of the crystalline nucleus size n . A free energy barrier for nucleation ΔG_N^* must be overcome in order to proceed from the - metastable - supercooled liquid state to the thermodynamically stable crystalline phase via homogeneous nucleation (purple). Heterogeneous nucleation (green) can be characterized by a lower free energy barrier $\Delta G_N^*,\text{het}$ and a smaller critical nucleus size n^*,het , while in the case of spinodal decomposition (orange) the supercooled liquid is unstable with respect to the crystalline phase, and the transformation to the crystal proceeds in a barrierless fashion. The three snapshots depict a crystalline cluster nucleating within the supercooled liquid phase (homogeneous nucleation) or thanks to the presence of a foreign impurity (heterogeneous nucleation), as well as the simultaneous occurrence of multiple crystalline clusters in the unstable liquid. This scenario is often labeled as spinodal decomposition, albeit the existence of a genuine spinodal decomposition from the supercooled liquid to the crystalline phase has been debated (see text).

disagreement between experimental measurements and computed crystal nucleation rates^{39,46}. Atomistic simulations could in principle help to clarify the temperature dependence as well as the microscopic origin of \mathcal{A}_{kin} and also of the thermodynamic ingredients involved in the formulation of CNT. However, quantities like e.g. γ_S are not only infamously difficult to converge within decent levels of accuracy^{47,48}, but can even be ill-defined in many situations. For instance, it remains to be seen whether γ_S , which in principle refers to a planar interface under equilibrium conditions, can be safely defined when dealing with small crystalline clusters of irregular shapes. In fact, the early stages of the nucleation process often involve crystalline nuclei whose size and morphology fluctuate on a timescale shorter than the structural relaxation time of the surrounding liquid. On top of that, the dimensions of such nuclei can be of the same order of the diffuse interface between the liquid and the solid phases, thus rendering the notion of a well defined γ_S quite dangerous. As an example, Joswiak *et al.*⁴⁹ have recently shown that for liquid water droplets γ_S could strongly depend on the curvature of the droplet. The mismatch between the macroscopic interfacial free energy and its curvature dependent value can spectacularly affects water droplets nucleation, as reported by atomistic simulations of droplets characterized by radii of the order of ~ 0.5 - 1.5 nm. Some other quantities, like the size of the critical cluster, depend in many cases rather strongly on the degree of supercooling. This is the case of e.g. the critical nucleus size n^* that can easily span two orders of magnitude in just ten degrees of supercooling^{50,51}.

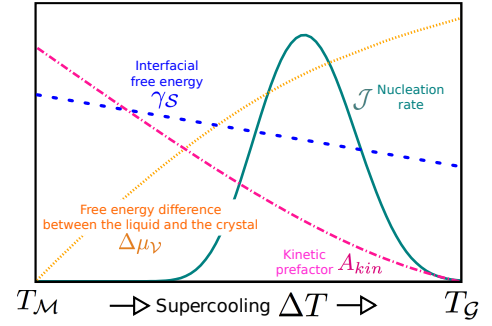


Figure 2. Illustration of how certain quantities from CNT vary as a function of supercooling ΔT for supercooled liquids. The free energy difference between the liquid and the solid phase $\Delta\mu_V$, the interfacial free energy γ_S and the kinetic prefactor \mathcal{A}_{kin} are reported as a function of ΔT in a generic case of diffusion-limited nucleation, characterized by a maximum in the steady state nucleation rate \mathcal{J} . $\Delta\mu_V$ is zero at the melting temperature T_M and \mathcal{A}_{kin} are vanishingly small at the glass transition temperature T_G .

2. Two-step nucleation

Given the old age of CNT, it is no surprise that substantial efforts have been devoted to extend and/or improve its original theoretical framework. The most relevant modifications possibly concern the issue of two-step nucleation. Many excellent works have reviewed this subject extensively (see e.g. Refs. 18,24,52,53), so that in here we supply to the reader the essential concepts only.

In the original formulation of CNT, the system has to overcome a single free energy barrier, corresponding to a crystalline nucleus of a certain critical size, as depicted in Fig. 3. When dealing with crystal nucleation from the melt, it is rather common to consider the number of crystalline particles within the largest connected cluster, n , as the natural reaction coordinate describing the whole nucleation process. In many cases, the melt is dense enough so that local density fluctuations are indeed not particularly relevant, while the slow degree of freedom is in fact the crystalline ordering of the particles within the liquid network. However, one can easily imagine that in the case of e.g. crystal nucleation of molecules in solutions the situation can be quite different. Specifically, in a realistically supersaturated solution, a consistent fluctuation of the solute density (concentration) could be required to just bring a number n_ρ of solute molecules close enough to form a connected cluster. Assuming that the molecules involved in such a density fluctuation will also order themselves in a crystalline fashion on exactly the same timescale is rather counterintuitive.

In fact, the formation of crystals from molecules in solution often happens according to a two-step nucleation mechanism that has no place in the original formulation of CNT. In the prototypical scenario depicted in Fig. 3, a first free energy barrier $\Delta G_{n_\rho, two-step}^*$ has to be overcome by means of a density fluctuation of the solute, such that a cluster of connected molecules of size n_ρ^* is formed. This object does not have any sort of crystalline order yet, and according to the system under consideration can be either unstable or stable with respect to the supersaturated solution (see Fig. 3). Subsequently, the system has to climb a second free energy barrier $\Delta G_{n, two-step}^*$ to order the molecules within the dense cluster in a crystalline-like fashion. A variety of different nucleation scenarios have been loosely labeled as two-step, from crystal nucleation in colloids (see Sec. IIA) or Lennard-Jones liquids (see Sec. IIB) to the formation of crystals of urea or NaCl (see Sec. IIE), not to mention biomineralization (see e.g. Refs. 18,53) and protein crystallization (see e.g. Refs. 54,55).

In all these cases, CNT as it is simply not capable to deal with two-step nucleation. This is why in the last few decades a number of extensions and/or modifications of CNT have been proposed and indeed successfully applied in order to account for the existence of a two-step mechanism. In here we mention the phenomenological theory of Pan *et al.*⁵⁴, who wrote an expression for the nucle-

ation rate assuming a free energy profile similar to the one sketched in Fig. 3, where dense metastable states are involved as intermediates toward the final crystalline structure. The emergence of so-called pre-nucleation clusters (PNCs), i.e. stable states within supersaturated solutions which are known to play a very important role in the crystallization of e.g. biominerals, has also been recently fit into the framework of CNT by Hu *et al.*⁵⁶. The authors proposed a modified expression for the excess free energy of the nucleus taking into account shape, size and free energy of the PNCs as well as the possibility for the PCNs to be either metastable or stable with respect to the solution. A comprehensive review on the subject is offered by the work of Gebauer *et al.*¹⁸. It is worth noticing that these *extensions* of CNT are mostly quite recent, as they have been triggered by overwhelming experimental evidence for two-step nucleation mechanisms.

3. Heterogeneous Nucleation

CNT is also the tool of the trade for heterogeneous crystal nucleation, that is when nucleation occurs thanks to the presence of a foreign phase (see Fig. 1). As a matter of fact, nucleation in liquids happens heterogeneously more often than not, since in some cases the presence of foreign substances in contact with the liquid can lower significantly the free energy barrier $\Delta G_{\mathcal{N}}^*$. A typical example is given by the formation of ice: as we shall see in Sec. IID 1 and IID 2, it is surprisingly difficult to freeze pure water, which invariably takes advantage of a diverse portfolio of impurities - from clay minerals to bacterial fragments¹⁶ - in order to facilitate the formation of ice nuclei.

Heterogeneous nucleation is customarily formulated within the CNT framework in terms of geometric arguments²⁷. Specifically:

$$\Delta G_{\mathcal{N}(\text{heterogeneous})}^* = \Delta G_{\mathcal{N}(\text{homogeneous})}^* \cdot f(\theta) \quad (6)$$

where $f(\theta) \leq 1$ is the *shape factor*, a quantity that accounts for the fact that we have to balance three different interfacial free energies: $\gamma_{S(\text{crystal}, \text{liquid})}$, $\gamma_{S(\text{crystal}, \text{foreign phase})}$ and $\gamma_{S(\text{liquid}, \text{foreign phase})}$. For instance, considering a supercooled liquid nucleating on top of an ideal planar surface offered by the foreign phase, we obtain the so called Young's relation:

$$\gamma_{S(\text{liquid}, \text{foreign phase})} = \gamma_{S(\text{crystal}, \text{foreign phase})} + \gamma_{S(\text{crystal}, \text{liquid})} \cdot \cos \theta$$

where θ is the contact angle, i.e. a measure of the extent to which the crystalline nucleus *wets* the foreign surface. Thus, the contact angle determines whether and

how much it could be easier for a critical nucleus to form in an heterogeneous fashion, as for $0 \leq \theta < \pi$ the volume to surface energy ratio $\frac{\Delta \mu v}{\gamma_s}$ is larger for the spherical

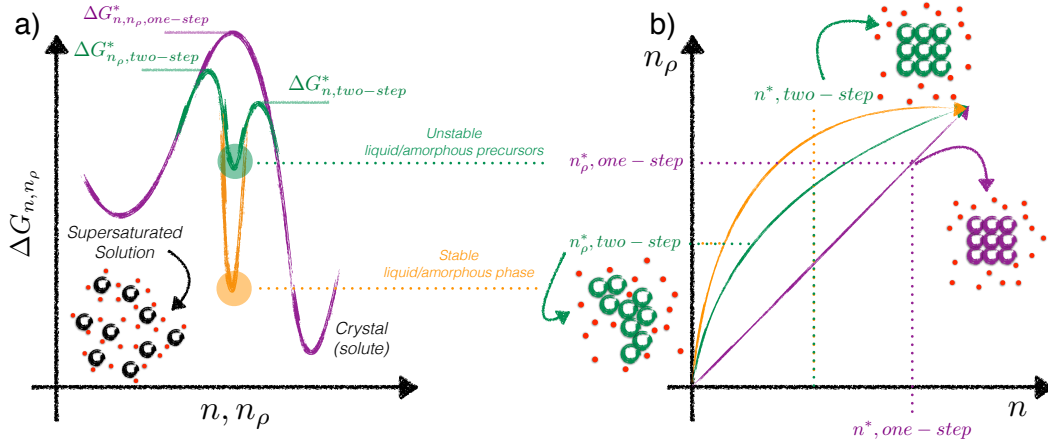


Figure 3. Schematic comparison of one-step versus two-step nucleation for a generic supersaturated solution. a) Sketch of the free energy difference $\Delta G_{n,n_\rho}$ as a function of the number of solute molecules in the largest "connected" cluster (they can be ordered in a crystalline fashion or not) (n_ρ) and of the number of crystalline molecules within the largest connected cluster (n). The one-step mechanism predicted by CNT (purple) is characterized by a single free energy barrier for nucleation $\Delta G_{n,n_\rho,one-step}^*$. In contrast, the two-step nucleation requires a free energy barrier $\Delta G_{n_\rho,two-step}^*$ to be overcome via a local density fluctuation of the solution, leading to a dense, but not crystalline-like precursor. The latter can be unstable (green) or stable (orange) with respect to the liquid phase, being characterized by an higher (green) or lower (orange) free energy basin. Once this dense precursor has been obtained, the second step consists in climbing a second free energy barrier $\Delta G_{n,two-step}^*$ corresponding to the ordering of the solute molecules within the precursor from a disordered state to the crystalline phase. b) One-step (purple) and two-step (green and orange) nucleation mechanism visualized in the density (n_ρ) - ordering (n) plane. The one-step mechanism proceeds along the diagonal, as both n_ρ and n increase at the same time, in such a way that a single free energy barrier has to be overcome. In this scenario, the supersaturated solution transforms continuously into the crystalline phase. On the other hand, within a two-step nucleation scenario the system has to experience a favorable density fluctuation along (n_ρ) first, forming a disordered precursor which in a second step orders itself in a crystalline fashion, moving along the (n) coordinate and ultimately leading into the crystal.

cap nucleating on the foreign surface compared to the sphere nucleating in the liquid. This simple formulation is clearly only a rough approximation of what happens in reality. At first, the contact angle is basically a macroscopic quantity, of which the microscopic equivalent is in most cases ill-defined on the typical length scales involved in the heterogeneous nucleation process⁵⁷. In addition, in most cases the nucleus will not be shaped like a spherical cap, and to make things more complicated, typically many different nucleation sites with different morphologies can exist on the same impurity. Finally, the kinetic prefactor \mathcal{A}_{kin} in heterogeneous nucleation becomes even more obscure, as it is plausible that the foreign phase will affect the dynamical properties of the supercooled liquid.

4. Nucleation at Strong Supercooling

Moving towards strong supercooling, several things can happen to the supercooled liquid phase. Whether or not one can avoid the glass transition largely depends on the specific liquid under consideration and on the cooling rate (see e.g. Ref. 58). Assuming we are able to cool the system sufficiently slowly, hence avoiding both the glass transition and crystal nucleation, one can in principle en-

ter a supercooled regime where the liquid becomes unstable with respect to the crystalline phase. This region of the phase diagram is known as the *spinodal region*, where the tiniest perturbation of e.g. the local density or the degree of ordering leads the system toward the crystalline phase without paying anything in terms of free energy (see Fig. 1). In fact, below a certain critical temperature T_{SP} , the free energy barrier for nucleation is zero, and the liquid transforms spontaneously into the crystal on very short timescales. The same picture holds for molecules in solution, as nicely discussed by e.g. Gebauer *et al.*¹⁸, and it cannot, by definition, be described by conventional CNT, according to which a small $\Delta G_{\mathcal{N}}^*$ persists even at the strongest supercoolings⁵⁹.

While spinodal regimes have been observed in a variety of scenarios⁶⁰ the existence of a proper spinodal decomposition from the supercooled liquid to the crystalline phase has been debated (see e.g. Ref. 61). Enhanced sampling MD simulations⁶² which we discuss in Sec. II B have suggested that barrierless crystal nucleation is possible at very strong supercooling, while other works claim that this is not the case (see e.g. Ref. 63). In here, we just note that at strong supercooling - not necessarily within the presumed spinodal regime - a number of assumptions upon which CNT rely become, if not erroneous, ill-defined. The list is long, and in fact a number of nu-

cleation theories²⁷ able to at least take into account the emergence of a spinodal decomposition exist, although they have been mostly formulated for condensation problems. In any case the capillarity approximation is most likely to fail at strong supercoolings, since the size of the critical nucleus becomes exceedingly small, down to loosing its meaning in the event of a proper spinodal decomposition. On top of that, we shall see for instance in Sec. II B that the shape of the crystalline clusters is anything but spherical at strong supercooling, and that at the same time the kinetic prefactor assumes a role of great importance. As a matter of fact, nucleation at strong supercooling may very well be dominated by \mathcal{A}_{kin} , as the mobility of the supercooled liquid is what really matters when the free energy barrier for nucleation approaches vanishingly small values. We care about strong supercooling because this is the regime in which most computational studies have been performed. Large values of ΔT imply high nucleation rates and smaller critical nuclei, although as much as we move away from T_M we progressively invalidate most of the assumptions of CNT.

At this point, having highlighted some of the substantial approximations of CNT⁶⁴, and especially in light of its old age, the reader might be waiting for us to introduce the much more elegant, accurate and comprehensive theories that experiments and simulations surly embrace nowadays. Sadly, this is not the case. Countless flavors of nucleation theories exist. Many of them, like e.g. Dynamical Nucleation Theory⁶⁵, Mean-field Kinetic Nucleation Theory⁶⁶, and Coupled Flux Theory^{67–70}, are mainly limited to condensation problems, and some others have only rarely been applied to e.g. crystallization in glasses²⁶, such as the Diffuse Interface Theory^{71,72}. Several improvements upon CNT have been proposed, targeting specific aspect like the shape of the crystalline nuclei⁷³ or the finite size of the non-sharp crystal-liquid interface⁴⁹. Nucleation theories largely unrelated to CNT can also be found, like classical Density Functional Theory (cDFT)^{74–77} (*classical*, not to be misinterpreted with the celebrated quantum mechanical framework of Hohenberg and Kohn⁷⁸). A fairly complete inventory of nucleation theories, together with an excellent review of nucleation in condensed matter, can be found elsewhere⁷⁹. In here, we do not enter into the details of any of these approaches, as indeed none of them has been consistently used to model crystal nucleation in liquids. This is because CNT, while having many shortcomings, is a simple yet powerful theory, able to capture at least qualitatively the thermodynamics and kinetics of nucleation for very different systems, from liquid metals to organic crystals. It has been easily extended to include heterogeneous nucleation, and it is fairly easy to take into consideration multicomponent systems like binary mixtures as well^{27,79}.

B. Experimental Methods

Several different experimental approaches have been employed to understand the thermodynamics and the kinetics of crystal nucleation in liquids. While this review discusses almost exclusively theory and simulations, we present in this section a concise overview of the state of the art experimental techniques, in order to highlight their capabilities as well as their limitations.

A schematic synopsis focusing on both spatial and temporal resolutions is sketched in Fig. 4, while an inventory of notable applications is reported in Table I. As we have said nucleation is a dynamical process usually happening on very small time and length scales (ns and nm respectively). Thus, obtaining the necessary spatial and temporal resolutions is a tough technical challenge.

Indeed, true microscopic⁸⁰ insight has rarely been achieved. For instance, colloids offer a playground where simple microscopy can image the particles involved in the nucleation events, which in turn happen on such long timescales (seconds) that a full characterization in time of the process has been achieved^{81,82}. Specifically, confocal microscopy has lead to 3D imaging of colloidal systems, unraveling invaluable information about e.g. the critical nucleus size^{83,84}.

In a similar fashion Sleutel *et al.* achieved molecular resolution of the formation of two-dimensional glucose-isomerase crystals by means of atomic force microscopy⁸⁵. This particular investigation features actual movies showing crystal growth as well as the dissolution of pre-critical clusters, also providing information about the influence of the substrate. In addition, cryo-TEM techniques have recently delivered 2D snapshots of nucleation events at very low temperatures. In selected cases, where the timescales involved are again on the order of seconds, dynamical details have been obtained, as e.g. in the case of CaCO_3 ^{86,87}, metal phosphate⁸⁸ or magnetite⁸⁹.

However, more often than not crystal nucleation in liquids takes place within time windows too small (ns) to allow for a sequence of snapshots to be taken with high spatial-resolution instruments. In these cases, microscopic insights cannot be obtained, and much more *macroscopic* measurements have to be performed. In this context, several experimental approaches aim at examining a large number of independent nucleation events for a whole set of rather small configurations of the system, basically performing an ensemble average. For example in *droplet experiments*, nucleation is characterized as a function of time or temperature. Freezing is identified for each nucleation event within the ensemble of available configurations by techniques such as femtosecond X-Ray scattering^{90,91}, optical microscopy^{81,82,92,93} or powder X-Ray diffraction^{94–96}. From these data the nucleation rate is often reconstructed by either measuring metastable zone widths^{97–104} or induction times^{105–110}, (several examples are listed in e.g. Refs. 111–115), providing in this way a solid connection to theoretical frameworks such as

CNT (see Sec. I A).

An essential technical detail within this class of measurements is that the volume available for each nucleation event has to be as small as possible, in order to reduce the occurrence of multiple nucleation events within the same configuration. High throughput devices such as the lab-on-a-chip¹¹⁶ can significantly improve the statistics of the nucleation events, thus enhancing the capabilities of these approaches.

Another line of action focuses on the study of large, macroscopic systems. Freezing is detected by e.g. differential scanning calorimetry^{117–122}, Fourier transform infrared spectroscopy (FTIRS)^{123–127}, analytical ultracentrifugation¹²⁸ or some flavor of chamber experiments^{2,129–135}. In this case, the frozen fraction of the overall system and/or the nucleation temperatures can be obtained, and in some cases nucleation rates have been extracted (see Table I).

Finally, experimental methods that can detect nucleation and the formation of the crystal (predominantly by means of optical microscopy) but do not provide any microscopic detail have helped to shed light on issues such as the role of the solvent or impurities. This is usually possible by examining the amount of crystalline phase obtained along with its structure.

Even though there are a large number of powerful experimental techniques and new ones emerging (e.g. ultrafast X-ray⁹⁰), it is still incredibly challenging to obtain microscopic level insight into nucleation from experiments. As we shall see now MD simulations provide a powerful complement to experiment.

C. Molecular Dynamics Simulations

1. Brute Force Simulations

When dealing with crystal nucleation in liquids, atomistic simulations should provide a detailed picture of the formation of the critical nucleus. The simplest way to achieve this is by so-called brute force MD simulations, which involve cooling the system to below the freezing temperature and then following its time evolution until nucleation is observed. Brute force simulations are the antagonist of enhanced sampling simulations, where specific computational techniques are used to alter the dynamics of the system so as to observe nucleation on a much smaller timescale. Monte Carlo (MC) techniques, although typically coupled with enhanced sampling techniques, can be used to recover $\Delta G_{\mathcal{N}}^*$ ^{146–148}, but the calculation of \mathcal{A}_{kin} requires other methods, like Kinetic Monte Carlo (KMC)³⁹. The natural choice to simulate nucleation event is instead in MD simulations, which provide directly the temporal evolution of the system.

MD simulations aimed at investigating nucleation are usually performed in the isothermal-isobaric ensemble NPT, where P (usually ambient pressure) and $T < T_m$ are kept constant by means of a barostat and a thermostat respectively. Such computational tweaking is a double-edged sword. In fact, nucleation and most notably crystal growth are exothermic processes¹⁴⁹, and within the length scale probed by conventional atomistic simulations (1-10⁴ nm) is necessary to keep the system at constant temperature. On the other hand, in this way dynamical and structural effects in both the liquid and the crystalline phases due to the heat developed during the nucleation events are basically neglected^{150–152}. Although the actual extent of these effects is not yet clear, forcing the sampling of the canonical ensemble is expected to be especially dangerous when dealing with very small systems affected by substantial finite size effects. More importantly, thermostats and barostats affect the dynamics of the system. Small coupling constants and clever approaches (e.g. stochastic thermostats¹⁵³) can be employed to limit the effects of the thermostats, but in general care must be taken. The same reasoning applies for P and barostats as well. A density change of the system is usually associated with nucleation¹⁵⁴, the crystalline phase being more (or less, in the case of e.g. water) dense than the liquid parent phase.

Three conditions must be fulfilled to extract \mathcal{J} from brute force MD simulations:

1. The system must be allowed to evolve in time until spontaneous fluctuations lead to a nucleation event.
2. The system size must be significantly larger than the critical nucleus.
3. A significant statistics of nucleation events must be collected.

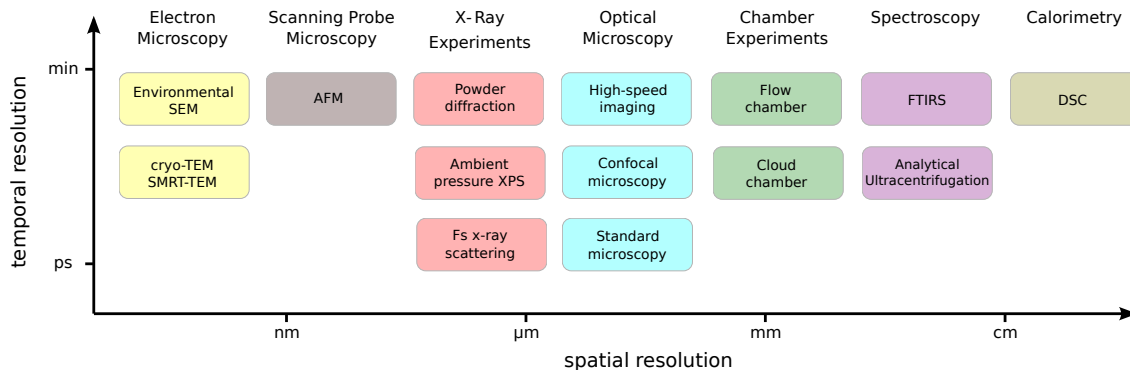


Figure 4. Overview of some of the experimental methods that have been applied to characterize nucleation. A schematic of the spatial and temporal resolution typical of each approach is reported on the x- and y-axis, respectively.

Methods	Examples
Confocal Scanning Microscopy	colloids ^{83,84} , oogenesis in <i>Xenopus</i> ¹³⁶
AFM	glucose-isomerase ⁸⁵
SMRT-TEM, HREM	organic crystals ^{137,138} , metal phosphate ⁸⁸
cryo-TEM	CaCO ₃ ^{86,87} , magnetite ⁸⁹ , mcm41 ¹³⁹
fs X-Ray Scattering	ice ^{90,91}
high speed VIS or IR imaging	ice ¹⁴⁰
Analytical Ultracentrifugation	CaCO ₃ ¹²⁸
Powder Diffraction	colloids ^{94,95} , ice ⁹⁶
FTIRS	ice ¹²³⁻¹²⁵ , glycine ¹²⁶ , paracetamol ^{127,141}
Optical Microscopy	colloids ^{81,82} , ice ^{92,93}
Ambient Pressure XPS	ice ^{142,143}
DSC	glass fibers ¹¹⁷ , hydrates ¹¹⁸ , ice ¹¹⁹⁻¹²¹ , metal-alloy ¹²²
Environmental SEM	CaP ¹⁴⁴ , ice ¹⁴⁵
Flow Chamber	ice ¹²⁹⁻¹³¹ , <i>n</i> -pentanol ¹³²
Cloud Chamber	ice ^{2,133-135}

Table I. Selection of experimental approaches that have been employed to study nucleation phenomena, along with some examples of systems examined.

Each one of these conditions is surprisingly difficult to fulfill. The most daunting obstacle is probably the first one because of the so-called *timescale problem*^{155,156}. In most cases, nucleation is a rare event, meaning that it usually happens on a very long timescale; precisely how long depends strongly on ΔT . A rough estimate of the number of simulation steps required to observe a nucleation event within a molecular dynamics run is reported in Fig. 5. Under the fairly optimistic assumption that classical MD simulations can cope with up to $\sim 10^5$ molecules on a timescale of nano/micro-seconds, there is only a very narrow sets of conditions for which brute force classical MD simulations could be used to investigate nucleation, usually only at strong supercooling. Timescales typical of first principles simulations, also reported in Fig. 5 assuming up to $\sim 10^2$ molecules, indicate that unbiased *ab initio* simulations of nucleation events are unfeasible.

The second important condition is the size of the system. The number of atoms (or molecules) in the system defines the timescale accessible to the simulation, and thus the severity of the timescale problem. The reason

we need large simulation boxes, i.e. significantly larger than the size of the critical nucleus, is because periodic boundary conditions will strongly affect nucleation (and growth) if even the precritical nuclei are allowed to interact with themselves. This usually leads to unrealistically high nucleation rates. This issue worsens at mild supercooling, where the critical nucleus size rapidly increases towards dimensions not accessible by MD simulations.

Third, it is not sufficient to collect information on just one nucleation event. Nucleation is a stochastic event following a Poisson distribution (at least ideally, see Sec. IA), and so to obtain the nucleation rate, one needs to pile up decent statistics.

Taking these issues into consideration, various approaches for obtaining \mathcal{J} have emerged. One approach, known as the Yasuoka-Matsumoto method¹⁵⁷, involves simulating a very large system, so that different nucleation events can be observed within a single run. In this case large simulation boxes are needed in order to collect sufficient statistics and to avoid spurious interactions between different nuclei. Another family of methods involves running many different simulations using

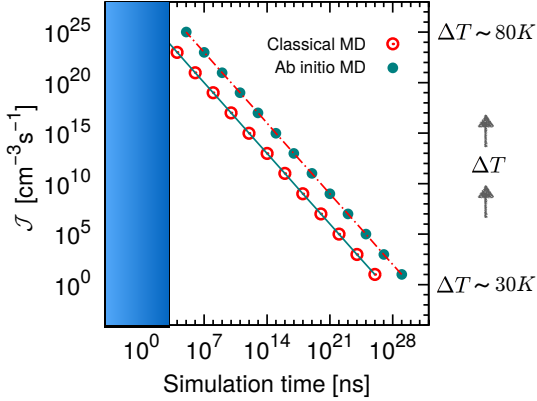


Figure 5. Nucleation rate \mathcal{J} as a function of the simulation time needed within a MD simulation to observe a single nucleation event. The blue shaded region highlights the approximate simulation times currently affordable by classical MD simulations; clearly only very fast nucleation processes can be simulated with brute force MD. For homogeneous ice nucleation, $\mathcal{J} = 10^0$ and $\mathcal{J} = 10^{25}$ can typically be observed for $\Delta T = 30K$ and $\Delta T = 80K$ respectively. 10^5 and 10^2 molecules have been considered in the derivation of classical and *ab initio* simulation times respectively, together with the number density of a generic supercooled liquid $\rho_L = 0.01 \text{ molecules} \cdot \text{\AA}^{-3}$

much smaller systems, which is usually computationally cheaper. Once a collection of nucleation events has been obtained, several ways to extract \mathcal{J} can be employed. The simplest ones (Mean Lifetime¹⁵⁸, Survival Probability^{159,160} methods) involve the fitting of the nucleation times to Poisson statistics. A more in-depth technique, the so-called Mean First-Passage method¹⁶¹ allows for a detailed analysis of the nuclei population, but requires a probability distribution in terms of nucleus size.

The literature offers a notable number of works in which brute force MD simulations have been successfully applied. Most of them rely on one way to circumvent the above mentioned issues, particularly the time scale problem. As we shall see in Sec. II, in order to simulate nucleation events we almost always have to either choose a very simple system, or to increase the level of approximation sometimes dramatically, for instance by coarse-graining the interatomic potential used.

2. Enhanced Sampling Simulations

In the previous section we introduced the timescale problem, the main reason brute force MD simulations are generally not feasible when studying crystal nucleation. Enhanced sampling methods alter how the system explores its configurational space, so that nucleation events can be observed within a reasonable amount of

computational time. Broadly speaking, one can distinguish between free energy methods and path sampling methods, both of which have been extensively discussed elsewhere (see e.g. Refs. 156,162–164). Thus, only the briefest of introductions is needed here.

Of the many enhanced sampling methods, only an handful have been successfully used to compute crystal nucleation rates. This is because we need information about both the thermodynamics of the system (the free energy barrier for nucleation ΔG_N^*) and the kinetics of the nucleation process (the kinetic prefactor \mathcal{A}_{kin}). When dealing with crystal nucleation in supercooled liquids, free energy based methods are rather common, such as umbrella sampling (US)^{165–167} or metadynamics^{168–170}. In both cases, and indeed in almost all enhanced sampling methods currently available, the free energy surface of the actual system is coarse grained by means of one or more order parameters, or collective variables. The choice of the order parameter is not trivial and can have dramatic consequences. An external bias is then applied to the system, leading to a modified sampling of the configurational space that allows for the reconstruction of the free energy profile with respect to the chosen order parameter, and thus for the computation of the free energy barrier. This approach has been successful in a number of cases. However, there is a price to be paid: by introducing an extra term into the system Hamiltonian, the actual dynamics of the system is to some extent hampered, and much of the insight into the nucleation mechanism is lost. Besides, ΔG_N^* is only half of the story. In order to obtain \mathcal{A}_{kin} , one needs complementary methods, usually aimed at estimating the probability for the system on top of the nucleation barrier - in the space of the selected order parameter - to get back to the liquid phase or to evolve into the crystal. Most frequently such methods are based on some flavor of transition state theory^{171–174}, like the Bennet-Chandler formulation^{175,176}, and require a massive set of MD or KMC simulations to be performed.

On the other hand, the ever growing family of path sampling methods can provide direct access to the kinetics of the nucleation process. These approaches rely again on the definition of an order parameter, but instead of applying an external bias potential, an importance sampling is performed so as to enhance the naturally occurring fluctuations of the system. Within the majority of the path sampling approaches used nowadays, including Transition Interface Sampling^{177–179} (TIS) and Forward Flux Sampling^{180,181} (FFS), the ensemble of paths connecting the liquid and the crystal is divided into a series of interfaces according to different values of the order parameter. By sampling the probability with which the system crosses each one of these interfaces, a cumulative probability directly related to the nucleation rate can be extracted. Other path sampling techniques such as Transition Path Sampling^{182,183} (TPS) rely instead on the sampling of the full ensemble of the reactive trajectories. In both cases, by means of additional simu-

lations involving e.g. committor analysis distribution¹⁸⁴ and thermodynamic integration¹⁸⁵, one can subsequently extract the size of the critical nucleus and the free energy difference between the solid and the liquid phases respectively. Many different path sampling methods are available, but to our knowledge only TPS, TIS and most prominently FFS have allowed for estimates of crystal nucleation rates. Under certain conditions, path sampling methods do not alter the dynamics of the system, allowing for invaluable insight into the nucleation mechanism. However, they are particularly sensitive to the slow dynamics of strongly supercooled systems, which hinder the sampling of the paths and makes them exceedingly expensive computationally. While the last few decades have taught us that enhanced sampling techniques are effective in tackling crystal nucleation of colloids (see Sec. II A), Lennard-Jones melts (see Sec. II B) or other atomic liquids (see Sec. II C), only recently have these techniques been applied to more complex systems. One exceedingly challenging scenario for simulations of nucleation is provided by the formation of crystals from solutions characterized by very low solute concentration. While this occurrence is often encountered in real systems of practical interest, it is clearly extremely difficult for MD simulations, even if aided by conventional enhanced sampling techniques, to deal with just a few solute molecules dissolved within 10^3 – 10^6 solvent molecules. In these cases, the diffusion of the solute plays a role of great relevance, and the interaction between solvent and solute can enter the nucleation mechanism itself. Thus, obtaining information about the thermodynamics, let alone the kinetics of nucleation at very low solute concentration is presently a formidable task. However, efforts have been devoted to further our understanding of e.g. solute migration and solute-nuclei association, as demonstrated by the pioneering works of Gavezzotti *et al.*^{186,187} and more recently by Kawska *et al.*^{188,189}. In the latter work the authors illustrate an approach that relies on the modeling of subsequent growth step, where solute particles (often ions) are progressively added to the (crystalline or not) cluster. After each one of these growth steps, a structural optimization of the cluster and the solvent by means of MD simulations is performed. While this method cannot offer quantitative results in terms of the thermodynamics and/or the kinetics of nucleation, it can in principle provide valuable insight into the very early stages of crystal nucleation when dealing with solutions characterized by very low solute concentration.

On a final note, we mention seeded MD simulations. This technique relies on simulations in which a crystalline nucleus of a certain size is inserted into the system at the beginning of the simulation. While useful information about critical nucleus size can be obtained in this way^{51,190–192}, the method does not usually allow for a direct calculation of the nucleation rate. However, seeded MD simulations are one of the very few methods by which we can currently investigate solute precipitate nucleation (see e.g. Knott *et al.*¹⁹³). There, the exceedingly slow at-

tachment rate of the solute often prevents both free energy as well as transition path sampling enhanced sampling methods from being applied effectively.

As we shall see in the next few sections, the daunting computational cost, together with the delicate choice of order parameter and the underlying framework of CNT, still make enhanced sampling simulations of crystal nucleation in liquids an intimidating challenge.

II. SELECTED SYSTEMS

We have chosen to review different classes of systems, which we shall present in order of increasing complexity. We start in Secs. II A and II B with colloids and Lennard-Jones liquids respectively. These systems are described by simple interatomic potentials that allow large scale MD simulations, and thus with them many aspects of CNT can be investigated and nucleation rates calculated. In some cases, the latter can be directly compared to experimental results. As such, colloids and Lennard-Jones liquids represent a sort of benchmark for MD simulations of crystal nucleation in liquids, although we shall see that our understanding of crystal nucleation is far from satisfactory even within these relatively easy playgrounds. In Sec. II C we discuss selected atomic liquids of technological interest such as liquid metals, supercooled liquid silicon and phase change materials for which nucleation happens on exceedingly small timescales. As the first example of a molecular system, we then focus on the most important liquid of them all, water. We review the body of computational work devoted to unravel the homogeneous (Sec. II D 1) as well as the heterogeneous (Sec. II D 2) formation of ice, offering an historical perspective guiding the reader through the many advances that have furthered our understanding of ice nucleation in the last decades.

Following this, we present an overview of nucleation from solution (Sec. II E), where simulations have to deal with solute and solvent. We take into account systems of great practical relevance such as urea molecular crystals, highlighting the complexity of the nucleation mechanism which is very different from what CNT predicts. Finally, Sec. II F is devoted to the formation of gas hydrates.

As a rule of thumb, increasing the complexity of the system raises more questions about the validity of the assumptions underpinning CNT. The reader will surely notice that simulations have revealed many drawbacks of CNT along the way, and that reaching decent agreement for the nucleation rate \mathcal{J} between experiments and simulations still remains a formidable task.

A. Colloids

Hard sphere model systems take a special place in nucleation studies. One reason for this is the simplicity of the interatomic potential customarily used to model

them: the only interaction a hard sphere particle experiences comes from elastic collisions with other particles. Because there is no attractive force between particles, a hard sphere system is entirely driven by entropy. As a consequence, the phase diagram is very simple, and can be entirely described with one single parameter, the volume fraction Φ . Only two different phases are possible: a fluid and a crystal. At a volume fraction $\Phi < 0.494$ the system is in its fluid state, at $0.492 < \Phi < 0.545$ it will be a mix between fluid and crystalline states, and at $\Phi > 0.545$ the thermodynamically most stable phase is the crystal. The transformation from fluid to crystal happens via a first order phase transition¹⁹⁴. Despite their simplicity, systems behaving like hard spheres can be prepared experimentally. Colloids made of polymers are commonly used for this purpose, the most prominent example being poly-methylmethacrylate (PMMA) spheres coated with a layer of poly-12-hydroxystearic acid. After synthesizing the spheres, they are dissolved in a mixture of cis-decaline and tetraline, which enables the use of a wide range of powerful optical techniques in order to, for example, investigate nucleation^{195,196}. The possibility of using these large hard spheres in nucleation experiments has two major advantages: First, a particle size larger than the wavelength used in microscopy experiments makes it possible to track the particle trajectories in real space. Second, the timescale of the nucleation process happens on the second scale, which allows the experimentalists to follow the complete nucleation process in detail. Compared to other systems it is therefore possible to directly observe the critical nucleus by e.g. confocal microscopy (see Sec. IB) which is of crucial importance for understanding nucleation. These qualities of hard sphere systems make them ideal candidates to advance our understanding of nucleation. As such it is not surprising that the freezing of hard spheres is better characterized than any other nucleation scenario, and in fact a number of excellent reviews in this field already exist^{197–202}. Our aim here is therefore not to give a detailed overview of the field, but to highlight some of the milestones and key discoveries and connect them to other nucleation studies. In order to keep the discussion reasonably brief, we limit the latter to neutral and perfectly spherical hard sphere systems. However, we note that a sizable amount of work has been devoted to a diverse range of colloidal systems, such as non-spherical particles^{203–208}, charged particles and mixtures of different colloidal particles^{209–214} just to name a few.

Readers interested in the state of the art around 2000 are referred to other reviews^{197,198}. In the early 2000's two major advances in the field were made, one on the theoretical side, the other experimentally. In 2001 Auer and Frenkel³⁹ computed absolute nucleation rates of a hard sphere system using KMC simulations. They did so by calculating P_{crit} , the probability of forming a critical nucleus spontaneously, and \mathcal{A}_{kin} , the kinetic prefactor separately and without any parameters. This made a direct comparison between simulations and experiments

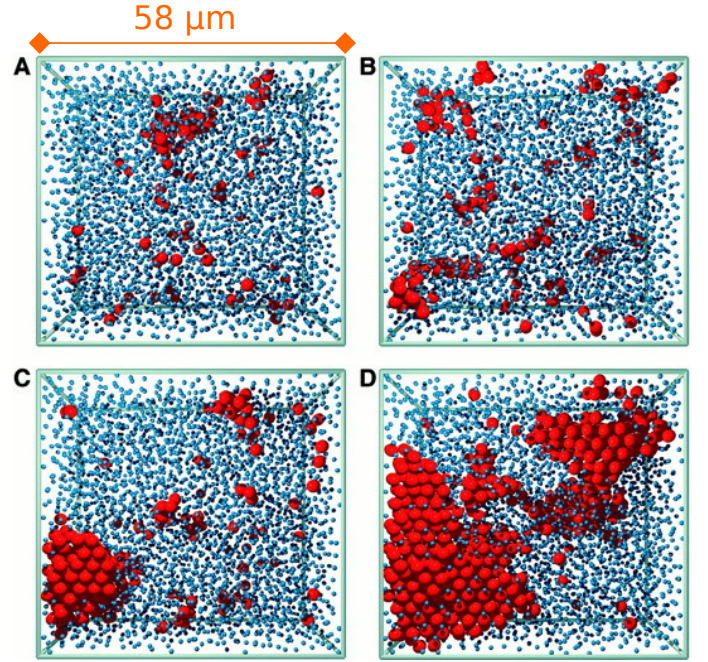


Figure 6. Crystallization of PMMA with $\Phi = 0.45$ observed by confocal microscopy. Red (large) and blue (small) spheres show crystal- and liquid-like particles respectively. The size of the observed volume is $58 \mu\text{m}$ by $55 \mu\text{m}$ by $20 \mu\text{m}$, containing about 4000 particles. After shear melting the sample, snapshots were taken after 20 min (A), 43 min (B), 66 min (C) and 89 min (D). The time series shows how an aspherical nucleus forms and grows over time. Reprinted with permission from Ref. 83. Copyright 2001, The American Association for the Advancement of Science.

possible. The outcome was surprising and worrisome. They found that experimental and theoretical nucleation rates disagreed by several orders of magnitude. This was surprising, because simulations did really well in describing all sorts of properties of hard spheres before. It was worrisome because only very few sound approximations were made by Auer and Frenkel to obtain their nucleation rates. Their theoretical approach seemed to be as good as it gets. The authors' suggestion, that the problem lay in experiments, or more precisely in the interpretation of experiments, showed a possible way to resolve the discrepancy. In the same year, Gasser *et al.*⁸³ conducted ground-breaking experiments. The authors imaged the nucleation of a colloidal suspension in real space using confocal microscopy. Four snapshots of their system containing approximately 4000 particles are shown in Fig. 6. This was a big step, because previously nucleation had been investigated indirectly, using for example the structure factor obtained from light scattering experiments. In their study, they were able to directly measure the size of a critical nucleus for the first time. Achieving sufficient temporal and spatial resolution at the same time so far is only possible for colloidal systems (for more details about experimental techniques see Sec. IB). They found that the nucleus was rather aspherical with a rough

surface, both of these effects are completely neglected in CNT. Note that the aspherical nucleus also appears in e.g. LJ systems (see sec 2.2.1). In addition, a random hybrid close-packed structure (RHCP) stacking for the hard spheres was observed, in good agreement with Auer and Frenkel³⁹. This is interesting, because slightly different systems such as soft spheres and Lennard Jones particles seem to favor BCC stacking. However, Gasser's study did not resolve the discrepancy between experimental and simulated nucleation rates, as their results were in agreement with earlier small-angle light scattering experiments²¹⁵.

Much of the subsequent work focused on trying to resolve this discrepancy between experiments and simulation. A step forward was made in 2006 and 2007^{216,217}. Schöpe *et al.* found experimental evidence supporting a two step crystallization (see Sec. I A 2) process in hard sphere systems. Other systems such as proteins or molecules in solution (see Sec. I I E) were well known at that time to crystallize via a more complex mechanism than that assumed by CNT. Even for hard sphere systems, two step nucleation processes were reported before 2006^{218–220}; the occurrence of that mechanism was attributed to details of the polydispersity of the hard spheres however. The new insight Schöpe *et al.* provided in 2006 and 2007 was that the two step nucleation process is general, and as such does not depend on either polydispersity or volume fraction. In 2010, simulations performed by Schilling *et al.*²²¹ supported these experimental findings. Using unbiased MC simulations the authors were able to reproduce the evolution of the structure factor from previous experiments. Not even the simplest model system seemed to follow the traditional picture assumed in CNT. Could this two step mechanism explain, why the computational rates³⁹ disagree with experiments? At first this seems like a tempting explanation, because Auer and Frenkel had to introduce order parameters to calculate absolute nucleation rates. That however automatically presupposes a reaction pathway, which might not necessarily match the nucleation pathway taken in experiments. Filion *et al.*²²² showed in the same year however, that very different computational approaches (brute force MD, US and FFS which we described earlier (see Sec. I C 2)) led to the same nucleation rates, all in agreement with Auer and Frenkel. They therefore concluded that the discrepancy between simulations and experiments did not lie in the computational approach employed by Auer and Frenkel. They offered two possible explanations, one being that hydrodynamic effects, completely neglected in the simulations, might play a role; the other possible difficulties in interpreting the experiments. Schilling *et al.*¹⁴⁷ tried to address one of the key issues when comparing experiments with simulations: uncertainties and error estimation. Whilst the determination of the most characteristic quantity in hard sphere systems, the volume fractions, is straightforward for simulations, experimentalists are confronted with a more difficult task there. The typical error in determin-

ing the volume fraction experimentally is about ± 0.004 , which translates into an uncertainty in the nucleation rate of about an order of magnitude. On taking these considerations into account, the authors concluded that the discrepancy can be explained by statistical errors and uncertainties.

Does this mean the last 10 years of research tried to explain a discrepancy which actually is not there? Filion *et al.*²²³ rightfully pointed out, that whilst the rates between experiments and simulations coincide at high volume fraction, they still clearly disagree in the low volume fraction regime. No simple rescaling justified by statistical uncertainty could possibly resolve that. In their paper, they also addressed a different issue. In a computational study in 2010, Kawasaki and Tanaka²²⁴ obtained, by means of Brownian Dynamics²²⁵, nucleation rates in good agreement with experiments, contrary to the nucleation rates computed by Auer and Frenkel using brute force MD. It should be noted that they did not use a pure hard sphere potential, but a Weeks-Chandler-Andersen potential instead. Was the approximation of a hard sphere system, something that can never be fully realized in experiments, the problem all the time? What Filion *et al.* showed is that different computational approaches (brute force MD, US and FFS) all lead to the same nucleation rates, all of them in disagreement with what Kawasaki and Tanaka found. Through a detailed evaluation of their approach and that of Kawasaki and Tanaka they agreed that their rates are more reliable. The discrepancy was back on the table, where it still remains, and is as large as ever.

For a detailed comparison between experimental and computational rates, the reader is referred to Ref. 202. What we want to leave the reader with here is that still today, the disagreement between simulations and experiments in the simplest system persists. It is worth mentioning, that this fundamental disagreement between simulations and experiments is not unique to colloids. Other systems such as water (Sec. I I D 1 and I I D 2) and molecules in solution (Sec. I I E) also show discrepancies of several orders of magnitude in nucleation rates. This long standing debate is of great relevance to all investigations dealing with systems modeled via any flavor of hard sphere potential. A notable example in this context is the crystallization of proteins, which are usually treated as hard spheres. While basically neglecting most of the complexity of these systems, this substantial approximation has allowed for a number of computational studies^{226–236} that, although outside the scope of this review, certainly contributed to furthering our understanding of the self-assembly of biological particles.

B. Lennard-Jones Liquids

Having discussed hard spheres, the first step towards more realistic systems involves the inclusion of attractive interactions. The Lennard-Jones liquid is a widely stud-

ied model system that achieves this. It can be seen as the natural extension of the hard-sphere model, to which it becomes equivalent when the strength of the attractive interactions goes to zero. LJ liquids were first reported in 1924²³⁷, and since then they have been the subject of countless computational studies. LJ potentials allow for exceedingly fast MD simulations, and a wide range of thermodynamic information is available for them, such as the phase diagram^{238–242} and the interfacial free energy^{243–245}.

The stable structure of the LJ system up to T_M is a face centered cubic (FCC) crystal, slightly less stable in free energy is an hexagonal close packed (HCP) structure which in turn is significantly more stable than a third body centered cubic (BCC) phase^{246,247}. With his study of liquid argon in 1964, Rahman reported what is probably the first LJ MD simulation²⁴⁸. His findings showed good agreement with experimental data for the pair distribution function and the self diffusion coefficient, thus demonstrating that LJ potentials can properly describe noble elements in their liquid form at ambient pressure. This conclusion was validated later by Verlet²⁴⁹ and McGinty²⁵⁰. As far as we know, nucleation of LJ liquids was investigated for the first time in 1969 by de Wette²⁴⁰ and in 1976 by Mandell *et al.*²⁵¹ for two-dimensional and three-dimensional systems, respectively.

Non-spherical Nuclei

Early simulations^{252,253} investigating the condensation of LJ vapors into liquid already indicated a substantial discrepancy with CNT rates. It is worth noticing that the order parameter for crystal-like particles presented by ten Wolde *et al.*²⁵² fostered a considerable amount of later work devoted to improve the order parameters customarily used to describe crystal nucleation from the liquid phase (see e.g. Ref. 254). In 2008, Kalikmanov *et al.*²⁵⁵ compared CNT and cDFT (see Sec. IA) simulations with condensation data of argon. It turned out that CNT spectacularly failed to reproduce experimental condensation rates, underestimating them by up to 26 orders of magnitude. This disagreement triggered a number of computational studies aimed at clarifying the assumption of the sphericity of the critical nucleus within the freezing of LJ liquids. By embedding pre-existing spherical clusters into supercooled LJ liquids, Bai and Li^{256,257} found values of the critical nucleus size in excellent agreement with CNT within a broad range of temperatures. However, these results have been disputed by e.g. the umbrella sampling simulations of Wang *et al.*²⁵⁸ and the path sampling investigation of Moroni *et al.*²⁵⁹. In both cases the nuclei became less spherical with increasing ΔT . In addition, Moroni *et al.* pointed out that the critical nucleus size is determined by a non trivial interplay between the shape, the size and the degree of crystallinity of the cluster. Such a scenario is clearly much more complex than the usual CNT picture as it violates the capillarity approximation (see IA 1). Non-spherical nuclei have also been observed by Trudu *et al.*⁶², who extended the con-

ventional CNT formula to account for ellipsoidal nuclei. Such a tweak gave much better estimations of both the critical nucleus size and the nucleation barrier. Recall that the shape of the critical nuclei can be observed experimentally in very few cases (see Sec. IB and II A).

However, at very strong supercooling things fell apart because of the emergence of spinodal effects (see Sec. IA). Note that CNT fails at strong supercooling even without the occurrence of spinodal effects, as the time lag (transient time) needed for the structural relaxation into the steady-state regime results in a time dependent nucleation rate¹⁹. For instance, Huitema *et al.*²⁶⁰ have shown that incorporating the time dependence into the kinetic prefactor yields an improved estimate of nucleation rates. In fact, by embedding extensions to the original CNT framework one can recover in some cases a reasonable agreement between simulations and experiments even at strong supercooling. As an example, Peng *et al.*²⁶¹ have also shown that including enthalpy-based terms in the formulation of the temperature dependence of γ_S substantially improves the outcomes of CNT.

Polymorphism

Another aspect that has been thoroughly addressed within crystal nucleation of LJ liquids is the structure of the crystalline clusters involved. The mean-field theory approach of Klein and Leyvraz²⁶² suggests a decrease of the nucleus density as well as an increase of BCC character when moving towards the spinodal region. These findings were confirmed by the umbrella sampling approach of ten Wolde *et al.*^{252,263,264} who reported a BCC shell surrounding FCC cores. Furthermore, Wang *et al.*²⁵⁸ have shown that the distinction between the crystalline clusters and the surrounding liquid phase falls off as a function of ΔT . In fact, the free energy barrier for nucleation, computed by means of umbrella sampling (see Sec. IC 2) simulations, turned out to be of the order of $k_B T$ at $\Delta T = 52\%$. In addition, the nuclei undergo substantial structural changes towards non-symmetric shapes, a finding validated by the metadynamics simulations of Trudu *et al.*⁶². The same authors investigated the nucleation mechanism close to the critical temperature T_{SP} for spinodal decomposition (see Sec. IA 4), where the free energy basin corresponding to the liquid phase turned out to be ill-defined, i.e. already overlapping with the free energy basin of the crystal. Such a finding, basically suggested that below T_{SP} there is no free energy barrier for nucleation, indicating that the liquid is unstable rather than metastable and that the crystallization mechanism has changed from nucleation towards the more collective process of spinodal decomposition (see Sec. IA 4 and Fig. 1).

Insights into the interplay between nucleation and polymorphism have been provided by the simulations of e.g. ten Wolde *et al.*^{252,263,264}, suggesting that within the early stages of the nucleation process the crystalline clusters are BCC-like, turning into FCC crystalline kernels surrounded by BCC shells later on. These findings were

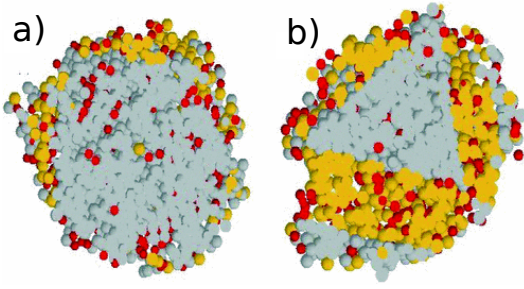


Figure 7. Cross section of post-critical crystalline clusters of 5000 LJ particles for a) $\Delta T = 10\%$ and b) $\Delta T = 22\%$. FCC-, HCP- and BCC-like particles are depicted in gray, yellow and red respectively. At $\Delta T = 22\%$ substantial HCP domains form within the crystallite, while at $\Delta T = 10\%$ HCP particles can be found almost exclusively on the surface of the FCC core. Reprinted with permission from Ref. 247. Copyright 2007, American Physical Society.

validated by Desgranges *et al.*²⁶⁵ and Wang *et al.*²⁵⁸.

More recently, Wang *et al.*²⁶⁶ performed a cDFT study in order to determine the difference between the free energy barrier for nucleation required for the creation of a FCC or a BCC critical nucleus. In addition the difficulty for nucleation of the three different crystal orientations for FCC was ranked $(100) > (110) > (111)$. These studies confirm the presence of a two-step mechanism (see Sec. IA 2) and the validity of Ostwald’s step rule²⁶⁷ for the LJ model. As we will see later (e.g. homogeneous ice nucleation, Sec. IID 1), nucleation via metastable phases has also been observed for more complicated liquids. Important contributions regarding polymorph control during crystallization have been made by Desgranges and Delhommelle^{247,265,268} who investigated nucleation under different thermodynamic conditions. While keeping the temperature constant and altering the pressure, they were able to influence the amount of BCC particles. This reached up to a point where the nucleus was almost purely BCC-like. By calculating the BCC-liquid line in the phase diagram it was shown that these nucleation events had occurred in the BCC existence-domain. Additionally the transformation from HCP to FCC during crystal growth, well after the critical nucleus size has been reached, was studied by changing temperature under constant pressure conditions. As depicted in Fig. 7, at $\Delta T = 10\%$ a small number of HCP atoms were observed surrounding the FCC core, while at $\Delta T = 22\%$ much larger HCP domains formed within the crystallite, suggesting that the conversion from HCP to FCC is hindered at higher temperatures. On a final note, we underline that many findings related to polymorphism are often quite dependent on the choice of the order parameters employed. This issue is not limited to LJ systems, and it is especially important when dealing with similarly dense liquid and crystalline phases (e.g. metallic liquids), where order parameters usually struggle to dis-

tinguish properly the different crystalline phases from the liquid²⁶⁸. In particular, it remains to be seen whether the fractional BCC, FCC and HCP content of the LJ nuclei we have discussed will stand the test of the last generation of order parameters.

Heterogeneous Nucleation

Heterogeneous crystal nucleation has also been investigated for a variety of LJ systems. For instance, Wang *et al.*²⁵⁸ calculated by means of umbrella sampling simulations (see Sec. IC 2) the free energy barrier for heterogeneous nucleation of a LJ liquid on top of an ideal impurity, represented by a single layer of LJ particles arranged in an honeycomb lattice. By explicitly varying the lattice spacing a_{Sub} of the substrate, they calculated ΔG_N^* as a function of $a_{Sub} - a_{Equi}$, a_{Equi} being the lattice spacing of the equilibrium crystalline phase²⁶⁹. It turned out that ΔG_N^* displays a minimum for $a_{Sub} - a_{Equi} = 0$, while for large $a_{Sub} - a_{Equi}$ nucleation proceeds within the bulk of the supercooled liquid phase. These findings support the early argument of the zero lattice mismatch introduced by Turnbull and Vonnegut²⁷⁰ to justify the striking effectiveness of AgI crystals in promoting heterogeneous ice nucleation. In fact, in several situations one can define a disregistry or lattice mismatch δ as

$$\delta = \frac{a_{Sub} - a_{Equi}}{a_{Equi}}. \quad (7)$$

Values of δ close or even better equal to zero have often been celebrated as the main ingredient that makes a crystalline impurity particularly effective in promoting heterogeneous nucleation. However, the universality of this concept has been severely questioned in the last few decades, as we shall see in Sec. IID 2 for heterogeneous ice nucleation. Nonetheless, it seems that the zero lattice mismatch argument can hold for certain simple cases, as demonstrated by e.g. Mithen and Sear²⁷¹, who studied heterogeneous nucleation of LJ liquids on the (111) and (100) faces of a FCC crystal by means of FFS simulations (see Sec. IC 2). They reported a maximum in the heterogeneous nucleation rate for a small, albeit non-zero, value of δ (see Fig. 8). The difference between this study and Wang *et al.*²⁵⁸ is simply because many more values of δ were taken into account by Mithen and Sear²⁷¹, thus allowing the maximum of \mathcal{J} to be determined more precisely. On a different note, Dellago *et al.*²⁷² also investigated by TIS (see Sec. IC 2) simulations the heterogeneous crystal nucleation of LJ supercooled liquids on very small crystalline impurities. They found that even tiny crystalline clusters of just ~ 10 LJ particles can actively promote nucleation, and that the morphology of the substrate can play a role as well. Specifically, while FCC-like clusters were rather effective in enhancing nucleation rates, no substantial promotion was observed for icosahedrally ordered seeds.

MC simulations performed by Page and Sear²⁷³ have demonstrated that confinement effects can be of great rel-

evance as well. They computed heterogeneous nucleation rates for a LJ liquid wallled in two flat crystalline planes characterized by a certain angle θ_{Sub} . A maximum of \mathcal{J} was found for a specific value of θ_{Sub} , boosting the nucleation rate by several orders of magnitude with respect to the promoting effect of a flat crystalline surface. In addition, different values of θ_{Sub} led to the formation of different crystalline polymorphs.

Finally, Zhang *et al.*²⁷⁴ recently probed the influence of structured and structurless LJ potential walls on nucleation rates. Both types of wall were found to increase the temperature at which nucleation occurs. However, this effect became negligible when moving towards vanishingly small liquid-wall interaction strengths. We shall see in Sec. IID 2 that the interplay between the morphology of the substrate and the strength of the liquid-substrate interaction can lead to a diverse range of nucleation behavior.

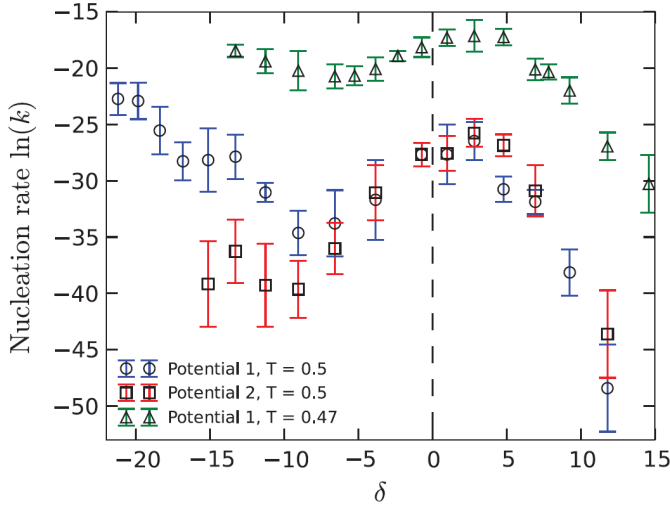


Figure 8. Nucleation rates computed with the FFS method for a rigid hexagonal surface of LJ atoms in contact with a LJ liquid. Potential 1 and 2 describe the interaction between substrate and liquid and differ only slightly by the σ they use. Error bars are standard deviations from 5 FFS runs. These results show that the maximum in the nucleation rate occurs at non-zero values of the lattice mismatch δ . Reprinted with permission from Ref. 271. Copyright 2014, AIP Publishing LLC.

Finite Size Effects

MD simulations of LJ liquids are computationally cheap, making them the perfect candidates to examine how finite-size effects impact upon crystal nucleation. The seminal work of Honeycutt and Andersen²⁷⁵ took into account up to 1300 LJ particles at $\frac{k_B T}{\epsilon_{LJ}} = 0.45$, which turned out to be too few to completely rule out the effect of periodic boundary conditions. In fact, the authors suggested that extra care had to be taken because of the diffuseness of the interface between the supercooled li-

quid phase and the crystalline nucleus, which can induce an artificial long range order in the system leading to a nonphysically fast nucleation rate. These findings are particularly relevant as the critical nucleus size at this ΔT is of the order of just a few tens of particles, representing a tiny fraction of the whole system. Only a few years later Swope and Andersen²⁷⁶ investigated the same effects by taking into account up to 10^6 LJ particles subjected to the same strong supercooling probed by Honeycutt and Andersen²⁷⁵. According to their large scale MD simulations, 15,000 particles seem to be sufficient to avoid finite-size effects. This outcome must be carefully pondered, as nowadays the vast majority of simulations dealing with crystallization of realistic systems cannot obviously afford to take into account system sizes three order of magnitude larger than the size of the critical nucleus. Consistent with Honeycutt and Andersen²⁷⁵, Huitema *et al.*²⁶⁰ examined the nucleation of a LJ liquid in a wide range of temperatures (70-140 K). While non-physical, instantaneous crystallization was observed for systems of the order of ~ 500 particles, simulation boxes containing about 10,000 particles seem to be free from finite-size effects.

It is also worth pointing out that Peng *et al.*²⁶¹ have recently described a novel class of finite-size effects unrelated to periodic boundary conditions. In fact, they have shown that the equilibrium density of critical nuclei \mathcal{P}_{Equi} ²⁷⁷ can effectively influence the absolute value of nucleation rates. Specifically, at very strong supercooling the critical nuclei will on average form very shortly after the transient time, while at mild ΔT the stochastic nature of nucleation will lead to a consistent scatter of the nucleation times. In other words, in this latter scenario either exceedingly large systems must be taken into account, or a sizable number of independent simulations must be performed in order to deal with the long tails of the distribution of nucleation times.

C. Atomic Liquids

Various interatomic potentials have been developed to deal with atomic liquids. Examples include the Sutton-Chen potentials²⁷⁸ for several metals and the Tosi-Fumi potential²⁷⁹ for molten salts like NaCl. Terms accounting for the directionality of covalent bonds have been included in e.g. the Stillinger-Weber potential²⁸⁰ for Si, the bond order potentials of Tersoff^{281,282} for Si, GaAs and Ge or the reactive potential of Brenner²⁸³ for carbon-based systems. Another class of interatomic potential is based on the concept of local electronic density, and includes for instance the Finnis-Sinclair potentials^{278,284} for metallic systems, the whole family of the Embedded Atoms Method (EAM) potentials²⁸⁵ and the Glue potential^{286,287} for Au and Al.

Many of these potentials are still incredibly cheap in terms of computer time, thus allowing for large scale, unbiased MD simulations. Recently, massively parallel

MD runs succeeded in nucleating supercooled liquid Al²⁸⁸ and Fe²⁸⁹ using an EAM and a Finnis-Sinclair potential respectively. As up to 10^6 atoms were taken into account, actual grain boundaries were observed, providing unprecedented insight in to the crystal growth process. The nucleation of BCC Fe crystallites and the evolution of the resulting grain boundaries at different temperatures can be appreciated in Fig. 9a. The sizable dimension of the simulation boxes (~ 50 nm) allowed nucleation events to be observed within hundreds of ps, and grain coarsening, i.e. the process by which small crystallites end up incorporated into the bigger ones, is also clearly visible. Mere visual inspection of the nucleation trajectories depicted in Fig 9a suggests different nucleation regimes as a function of temperature. In fact, the same authors have calculated a temperature profile for the nucleation rate, shown in Fig 9b, which demonstrates the emergence of a maximum of \mathcal{J} characteristic of diffusion limited nucleation (see Sec. I A 1).

A field that has greatly benefited from MD simulations is the crystallization of metal clusters, as nicely reviewed by Aguado *et al.*²⁹¹. For instance, it is possible to probe the interplay between the size of the clusters and the cooling rate upon crystal nucleation and growth. In this context, Shibuta²⁹² reported three different outcomes for supercooled liquid Mo nanoparticles - modeled by means of a Finnis-Sinclair potential - namely the formation of a BCC single crystal, a glassy state or a polycrystalline phase. In some cases, nucleation rates obtained from simulations were consistent with CNT, as in the case of Ni nanodroplets²⁹³ where nucleation events were again observed by means of brute force MD simulations using the Sutton-Chen potential. The influence of the redox potential on the nucleation process has also been investigated. Milek and Zahn²⁹⁴ employed an enhanced flavor of the EAM potential to study the nucleation of Ag nanoparticles from solution. They established that the outcome of nucleation events is strongly influenced by the strength of the redox potential, able to foster either a rather regular FCC phase or a multi-twinned polycrystal. Similar to what was done for LJ liquids, the effects of confinement were assessed for Au nanodomains modeled via the Glue potential by Pan and Shou²⁹⁵. According to their findings, smaller domains facilitate crystal nucleation. Lü and Chen²⁹⁶ have instead investigated surface layering-induced crystallization of Ni-Si nanodroplets, using a modified EAM potential. It seems that for this particular system atoms proximal to the free surface of the droplet assume a crystalline-like ordering on very short timescales, thus triggering crystallization in the inner regions of the system. No such effect has been reported instead in the case of surface-induced crystallization in supercooled tetrahedral liquids like Si and Ge, investigated by Li *et al.*²⁹⁷ via FFS simulations employing both Tersoff or Stillinger-Weber potentials. The presence of the free surface facilitates crystal nucleation for this class of systems as well, but surface layering was not observed. Instead, the authors claimed that the sur-

face reduces the free energy barrier for nucleation as it introduces a pressure-dependent term in the volume free energy change expected for the formation of the crystalline clusters. The situation is quite different for surface induced ice nucleation, at least according to the coarse-grained mW model of Molinero and Moore²⁹⁸. In fact, Haji-Akbari *et al.*²⁹⁹ have recently investigated ice nucleation in free-standing films of supercooled mW water using both FFS and US, finding that in these systems crystallization is inhibited in the proximity of the vapor-liquid interface. Very recently, Gianetti *et al.*³⁰⁰ extended the investigation of Haji-Akbari *et al.*²⁹⁹ to the crystallization of a whole family of modified Stillinger-Weber liquids with different degrees of *tetrahedrality* λ , locating a crossover from surface-enhanced to bulk-dominated crystallization in free-standing films as a function of λ . Another seminal study by Li³⁰¹, again using FFS, focused on homogeneous ice nucleation within supercooled mW water nano-droplets, where nucleation rates turned out to be strongly size dependent and in general consistently smaller (by several orders of magnitude) than the bulk case. FFS was also applied by Li *et al.*³⁰² to examine homogeneous nucleation of supercooled Si. FFS has also been successful in predicting homogeneous crystal nucleation rates in molten NaCl, modeled via a Tosi-Fumi potential by Valeriani *et al.*³⁰³. Large discrepancies between their results and experimental nucleation rates can be appreciated when CNT is used to extrapolate the calculations to the milder supercooling probed by the actual measurements. Given that the authors obtained consistent results using two different enhanced sampling methods, this study hints again at the many pitfalls of CNT.

Phase Change Materials

A unique example of a class of materials for which nucleation can be effectively addressed by brute force MD simulations is given by the so called phase change materials^{304,305}. Phase change materials are systems of great technological interest as they are widely employed in optical memories (e.g. DVD-RW) and in a promising class of non volatile memories known as Phase Change Memory (PCM)³⁰⁶, based on the fast and reversible transition from the amorphous to the crystalline phase. While crystal nucleation in amorphous systems, especially metallic and covalent glasses is outside the scope of this review, we refer the reader to the excellent work of Kelton and Greer²⁶ for a detailed introduction. Phase change materials used in optical and electronic devices are typically tellurium based chalcogenide alloys (see Ref. 305). The family of the pseudobinary compounds $(\text{GeTe})_x(\text{Sb}_2\text{Te}_3)_y$ represents a prototypical system. Although both the structure and the dynamics of these systems is far from trivial, nucleation from the melt takes place within the ns timescale for a wide range of supercooling³⁰⁴⁻³⁰⁶. Thus with phase change materials we have a great opportunity to investigate nucleation in a complex system by means of brute force MD simulations. We note that the crys-

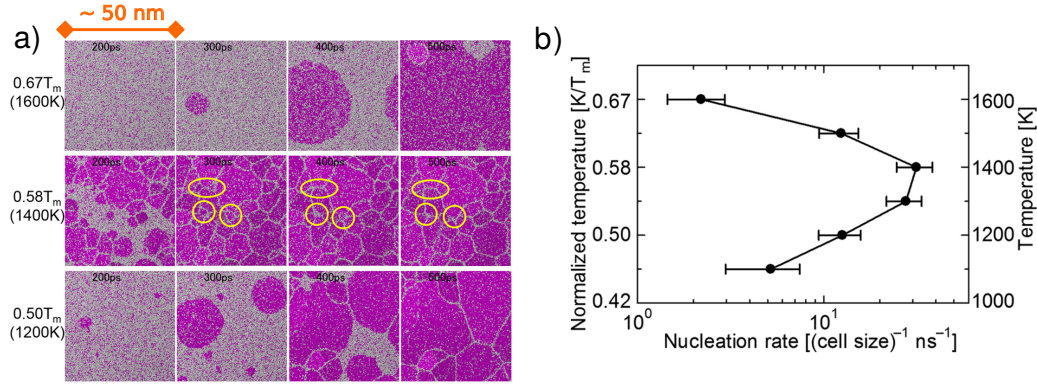


Figure 9. Crystal nucleation of supercooled Fe by means of large scale MD simulations. a) Snapshots of trajectories at different temperatures. Crystalline (BCC) atoms are depicted in purple. Yellow circles highlight small crystalline grains doomed to be incorporated into the bigger ones later on because of grain coarsening. b) Nucleation rate as a function of temperature. Reprinted with permission from Ref. 290. Copyright 2015, Nature Publishing Group.

tallization of these systems has been extensively characterized by different experimental techniques (particularly TEM and AFM, see Sec. IB; the crystallization kinetics has also been recently investigated by means of ultrafast-heating calorimetry³⁰⁷ and ultrafast X-ray imaging³⁰⁸), but because of the exceedingly high nucleation rates, it is difficult to extract information about the early stages of the nucleation process. Thus, in this scenario simulations could play an important role. Unfortunately, Phase Change Materials require *ab initio* methods or sophisticated interatomic potentials with first principles accuracy. In fact, several attempts have been made to study nucleation in phase change materials by *ab initio* MD in very small systems^{309,310}. While these studies provided useful insights into the nucleation mechanism, severe finite size effects prevented the full characterization of the crystallization process. The limited length and timescale typical of first principles calculations has recently been outstripped in the case of the prototypical phase change material GeTe by the capabilities of a neural network interatomic potential³¹¹. Those potentials allow for a computational speedup of several orders of magnitude compared to conventional *ab initio* methods, while retaining an accuracy close to that of the latter³¹². While nucleation rates have not been calculated yet, detailed investigations of homogeneous and heterogeneous nucleation have already been reported^{313,314}. For instance, as shown in Fig. 10, a single crystalline nucleus formed in a 4000-atom model of supercooled liquid GeTe in the 625-675 K temperature regime. Within a few hundred picoseconds, several nuclei appear below 600 K, suggesting that the free energy barrier for nucleation is vanishingly small for this class of materials just above the glass transition temperature. This is because of the *fragility*³¹⁵ of the supercooled liquid, which displays a substantial atomic mobility even at large supercoolings³¹⁶. Thus, in this particular case the kinetic prefactor \mathcal{A}_{kin} (see Eq. 5) is not hindered that much by the strong supercooling,

while the free energy difference between the liquid and the crystal $\Delta\mu_V$ (see Eq. 1) skyrockets as expected, leading to the exceedingly high nucleation rates characteristic of these materials.

In conclusion, while MD simulations have by no means exhausted the field of crystal nucleation of atomic liquids, they have certainly provided insight into a number of interesting systems and paved the way for the study of more complex systems, as we shall see in the following sections.

D. Water

1. Homogeneous Nucleation

Ice nucleation impacts many different areas, ranging from aviation^{317,318} to biological cells³¹⁹ and Earth's climate^{320,321}. It is therefore not surprising that a considerable body of work has been carried out to understand this fundamental process. We cannot cover it all here, instead we give a general overview of the field, starting with a discussion of nucleation rates. This allows us to directly compare experiments and simulations and to identify strengths and weaknesses of different approaches. We then discuss insights into the nucleation mechanism.

Nucleation rates

An important goal for both experiments and simulations is to extract nucleation rates. Experimental nucleation rates have been measured over a broad range of temperatures, most often with micrometer sized water droplets so as to avoid heterogeneous nucleation. In Fig. 11 we bring together nucleation rates obtained from various experiments. Along with this we also report computed nucleation rates.

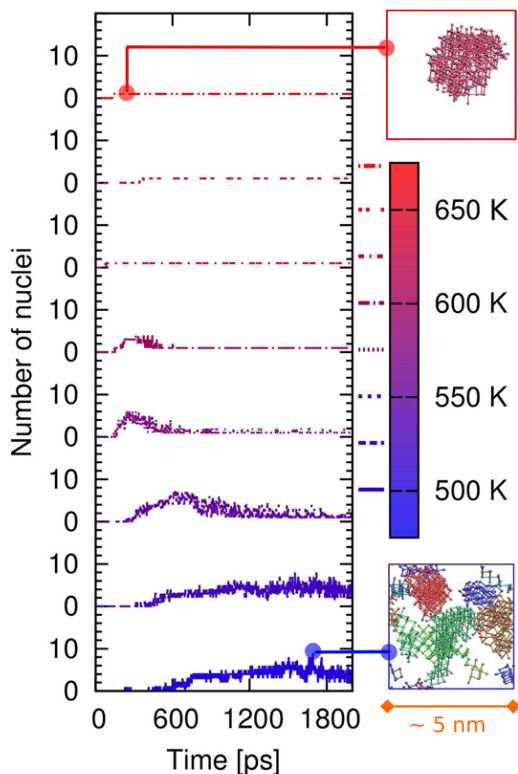


Figure 10. Fast crystallization of supercooled GeTe by means of MD simulations with neural network derived potentials. The number of crystalline nuclei larger than 29 atoms at different temperatures in the supercooled liquid phase is reported as a function of time (notice the exceedingly small timescale at strong supercooling). Two snapshots at the highest and lowest temperatures showing only the crystalline atoms are also reported. At high temperature, a single nucleus is present, while several nuclei (each one depicted in a different color) appear at low temperature. The number of nuclei first increases and then decreases due to coalescence. Reprinted with permission from Ref. 313. Copyright 2013, American Chemical Society.

Accessing nucleation rates from MD simulations became feasible only in the past few years due to advances in force fields (such as the coarse-grained mW²⁹⁸ potential) and enhanced sampling techniques described earlier (see Sec. IC 2). These methods have therefore been widely used, not only for homogeneous but also heterogeneous nucleation studies (see Sec. IID 2). From the comparison of experimental and computational nucleation rates reported in Fig. 11 few things are apparent. First, nucleation rates vary hugely with supercooling, by a factor of more than 10^{35} . Second, nucleation rates differ substantially (approximately 10 orders of magnitude) between simulations (filled symbols) and experiments (crossed symbols) at relatively small supercooling (≈ 30 -50 K). At larger supercoolings the agreement appears to be slightly better, even though very few simulations have been reported at very strong supercooling.

The third striking feature is that whilst experimental results agree well with each other (within 1-2 orders of magnitude) the computational rates differ much more from each other by a factor of approximately 10^{10} .

What is the cause of disagreement between different computational approaches? Part of the reason is certainly that different water models lead to different rates, see for example Espinosa *et al.*³²⁶. But even if the same water model is employed, rates do not agree with each other very well. A neat example is offered by nucleation rates obtained using the mW model. An early study by Moore *et al.*³³⁶ succeeded in calculating the Avrami exponent^{337,338} for the crystallization kinetics of ice from brute force MD simulations at very strong supercooling, obtaining results remarkably similar to experiment^{339,340}. However, mW nucleation rates turned out to be far less encouraging. In fact, Li *et al.*³²² and Reinhardt and Doye³²⁴ both performed simulations using the mW model, obtaining nucleation rates that differed by around 5 orders of magnitude. The only major difference was the enhanced sampling technique employed, FFS by Li *et al.* and US in Reinhardt and Doye. The statistical uncertainty of both approaches (1-2 orders of magnitude) is much smaller than the 5 orders of magnitude discrepancy between the two studies. It was also shown that both methods agree very well with each other for e.g. colloids³⁴¹ (see Sec. IIA). The use of different computational approaches therefore also seems to be an unlikely source of the disagreement. What the cause is remains elusive.

Because we cannot cover all of the work shown in Fig. 11 in detail here, we now discuss just two studies. First Sanz *et al.*⁵¹, which agrees best with the experimental rates. The authors used the TIP4P/2005 as well as the TIP4P/Ice water models in combination with the *seeding technique* (for more details the reader is referred to the original paper). Seeding involves considerably more assumptions than for example US or FFS. In particular, the approach assumes a CNT-like free energy profile - albeit it does not usually employ the macroscopic interfacial free energy. Furthermore, the temperature dependence of key quantities such as γ_S and $\Delta\mu_V$ (see Sec. IA 1) is approximated. Nevertheless, the agreement between their nucleation rates and experiment seemingly outperforms other approaches. In a more recent paper, Espinosa *et al.*³²⁶ obtained nucleation rates for a few other water models as well. However, it should be noted that the good agreement between the nucleation rates reported in Refs. 51,326 and the experimental data could originate from error cancellation. In fact, while the rather conservative definition of crystalline nucleus adopted in these works will lead to small nucleation barriers (and thus to higher nucleation rates), the TIP4P family of water models is characterized by small thermodynamic driving forces to nucleation³²⁷, which in turn results in smaller nucleation rates.

The second work we briefly discuss is the very recent study (2015) of Haji-Akbari and Debenedetti³²⁷. The

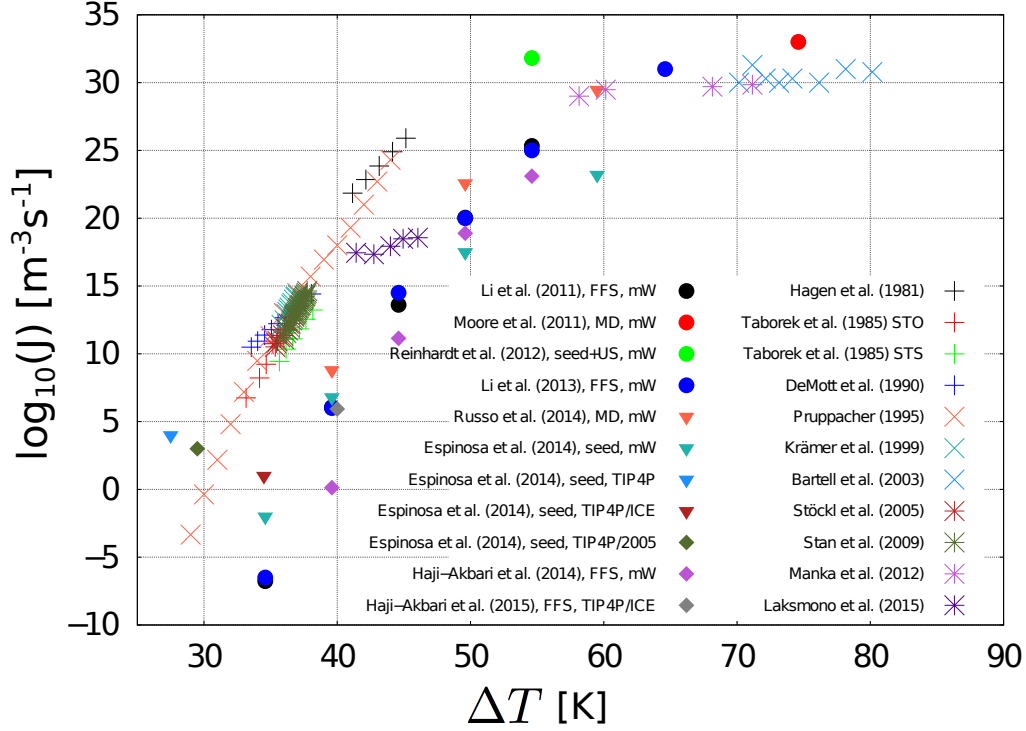


Figure 11. Compilation of homogeneous nucleation rates for water, obtained by experiments and simulations. The x-axis shows the supercooling with respect to the melting point of different water models or 273.15 K for experiment. The y-axis shows the logarithm of the nucleation rate in $m^{-3}s^{-1}$. Rates obtained with computational approaches are shown as filled symbols, experimental rates are shown otherwise. For all computational studies, the method as well as the water force field used are specified. The nucleation study of Sanz *et al.*⁵¹ is not included in the graph, because this study was conducted at a small supercooling (20 K) which results in a very low estimated nucleation rate far outside this plot (would correspond to -83 on y-axis). Taborek *et al.* performed measurements with different setups, namely using sorbitan tristearate (STS) and sorbitan trioleate (STO) as surfactants, with different droplet volumes (specified in the legend in μm , e.g. STS [surfactant] 6 [μm]). Data for the graph was taken from Refs. 124,299,301,322–335.

authors directly calculated the nucleation rate at 230 K of an all-atom model of water (TIP4P/ICE) using a novel FFS sampling approach³²⁷. This was a *tour de force* but strikingly, their rates differed from experiment by around 11 orders of magnitude. The authors point that this might be as close as one can actually get to experiment with current classical water models. This is because of the extreme sensitivity of nucleation rates to thermodynamic properties such as γ_S and $\Delta\mu_V$, which according to CNT enter exponentially (Sec. I A 1) in the definition of \mathcal{J} . For instance, an uncertainty of only 6-7% for γ_S at 235 K leads to an error of about 9 orders of magnitude in \mathcal{J} ³²². Experimental estimates for γ range from 25 to 35 mN/m³⁴², computational estimates from about 20³⁴³ to 35 mN/m³⁴⁴. As another example, Haji-Akbari and Debenedetti³²⁷ have explicitly quantified the extent to which the TIP4P/Ice model underestimates the free energy difference $\Delta\mu_V$ between the crystalline and liquid phase. It turned out that the mismatch between $\Delta\mu_V(TIP4P/Ice)$ and $\Delta\mu_V(Experimental)$ alone leads to an overestimation of the free energy barrier for nucleation of about 60%, which translates in nucleation rates

up to 9 orders of magnitude larger. In fact, taking into account such a discrepancy brings the results of Haji-Akbari and Debenedetti within the confidence interval of the experimental data. Thus, it is clear that we simply do not know some key quantities accurately enough to expect perfect agreement between simulations and experiments.

Besides issues of modeling water/ice accurately, finite size effects can be expected to also play a role (as they do with Lennard-Jones systems (Sec. II B) and molecules in solution (Sec. II E)). Only recently was this issue addressed explicitly for ice nucleation by English and Tse³⁴⁵ in unbiased simulations with the mW model. They were able to simulate systems containing nearly 10 million waters on a microsecond timescale, and found that larger systems favor crystallization precursor formation compared to smaller ones. Interestingly, lifetimes of the precursors were found to be less sensitive to system size. A quantitative understanding of finite size effects on the nucleation rates remains elusive nevertheless.

In summary it can be said that in terms of accurate nucleation rates, experiments are still clearly superior to

simulation. However, the advantage of simulations is that the nucleation mechanism can also be obtained, which at present is not accessible from experiments, although femtosecond X-ray laser spectroscopy might be able to partially overcome this limitation in the near future⁹⁰.

Nucleation mechanism

In 2002 Matsumoto *et al.*³⁴⁶ were the first to report a nucleation event in an unbiased simulation based on an all-atom model of water (TIP4P). Their landmark paper opened the doors to the study of ice nucleation at an atomistic level. They found that nucleation took place once a sufficient number of long-lived hydrogen bonds were formed with a nucleus of ice. Recent evidence suggests, that most likely their nucleation trajectory was driven by finite size effects⁵¹. Together with the simulations of Vrbka *et al.*³⁴⁷, also affected by severe finite size effects⁵¹, the work of Matsumoto remains to date the only seemingly unbiased MD simulation observing homogeneous ice nucleation with an all atom force field.

What really enabled the community to investigate ice formation at a molecular level was the development of the coarse grained mW potential for water²⁹⁸ in the early 2010's. Using unbiased MD simulations based on the mW force field Moore and Molinero in 2011³²³ provided evidence that in the supercooled regime around T_h the fraction of four fold coordinated water molecules increases sharply prior to a nucleation event. In a separate work the same authors suggested³⁴⁸ that at very strong supercooling the critical nucleus is mostly made of cubic ice, which subsequently evolves into a mixture of stacking disordered cubic and hexagonal ice layers. In the same year, Li *et al.*³²² identified another structural motif that might play a role in ice nucleation. They consistently observed a topological defect structure in growing ice nuclei in their FFS simulations based on the mW representation of water. This defect, depicted in Fig. 12a, can be described as a twin boundary with 5-fold symmetry, and it has also been observed³⁰² in nucleation simulations of tetrahedral liquids simulated via the Stillinger-Weber potential, upon which the mW coarse-grained model is built.

In 2012 another big leap in understanding the nucleation mechanism of ice from a structural point of view was made by combining experimental and computational techniques³⁴³. Malkin *et al.* showed, that ice forming homogeneously is stacking disordered (the corresponding ice structure was called I_{sd}), meaning that it is made out of cubic and hexagonal ice layers stacked in a random fashion.

In 2014 two studies substantiated the potential relevance of precursor structures prior to ice formation. Palmer *et al.* provided evidence for a liquid-liquid transition in supercooled water in a molecular model of water (ST2)³⁵⁰. In their study, the authors sampled the energy landscape of supercooled water and found two metastable liquid basins corresponding to low (LDL) and high den-

sity (HDL) water. The appealing idea behind the transition from HDL to LDL prior to ice nucleation is that LDL is structurally closer to ice than HDL. Note that the existence of two metastable liquid basins was not a general finding, the mW model does not have a basin for LDL for example³²³. Indeed the presence of this liquid-liquid phase transition is a highly debated issue^{351,352}.

Another conceptually similar idea is ice formation via ice 0, I_0 , proposed by Russo *et al.*³²⁵. Instead of a liquid-liquid phase transition which transforms water into another liquid state prior to nucleation, the authors propose a new ice polymorph (I_0) to bridge the gap between supercooled water and ice. I_0 is a metastable ice polymorph and is structurally similar to the supercooled liquid. It has a low interfacial energy with both, liquid water and ice I_c/I_h . Russo *et al.* therefore proposed I_0 to bridge liquid water to crystalline I_c/I_h . And indeed, the authors found I_0 at the surface of growing ice nuclei in MD simulations, we show part of a nucleation trajectory in Fig. 12b. Furthermore, they showed that the shape of the nucleation barrier is much better described by a core-shell-like model (I_c/I_h core surrounded by I_0) compared to the classical nucleation model. This is important, because it suggests that models which are solely based on CNT assumptions might not be appropriate to describe homogeneous ice nucleation.

However, the emergence of I_0 has not yet been reported by any other nucleation study, including the recent work of Haji-Akbari and Debenedetti³²⁷ we have previously mentioned in the context of nucleation rates. In there, the authors performed a topological analysis of the nuclei, validated by the substantial statistics provided by the FFS simulations. As depicted in Fig. 13, the majority of nuclei that reach the critical nucleus size contain a large amount of double-diamond cages (DDC, the building blocks of I_c), while nuclei rich in hexagonal cages (HC, the building blocks of I_h) have an exceedingly low probability to overcome the free energy barrier for nucleation. In addition, even postcritical nuclei have a high content of DDC cages, while HC cages do not show any preference to appear within the core of the postcritical nuclei. This evidence is consistent with the findings reported in Ref.³²³ and in contrast with the widely invoked scenario in which a kernel of thermodynamically stable polymorph (in this case I_h) is surrounded by a shell of a less stable crystalline structure (in this case I_c).

In the past few years the understanding of homogeneous ice nucleation has improved dramatically. We now have a good understanding of the structure of ice that forms through homogeneous nucleation, stacking disordered ice. Furthermore there is very good agreement (within two orders of magnitude) between experimental nucleation rates at a certain temperature range. Computational methods face the problem of being very sensitive to some key thermodynamic properties, the nucleation rates they predict are therefore less accurate. On the other hand they allow us to study conditions which are very challenging to probe experimentally, and also pro-

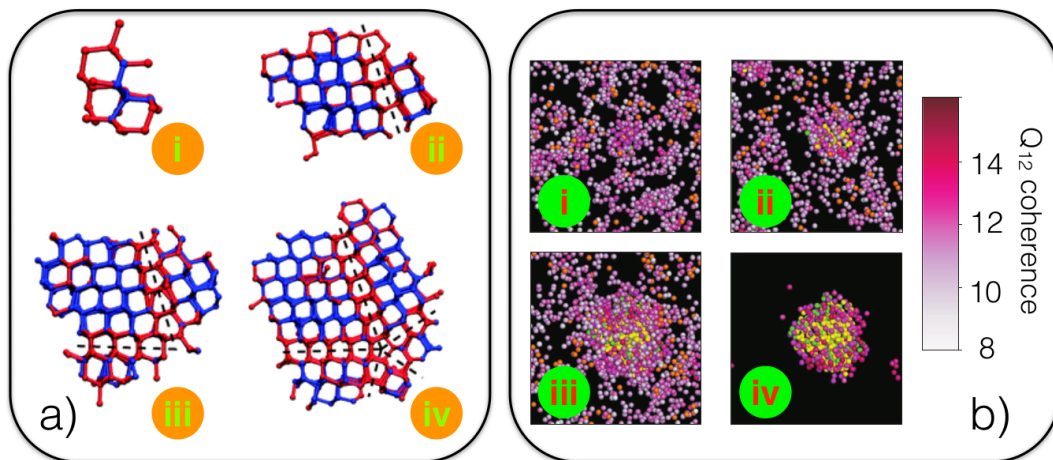


Figure 12. a) Formation of a topological defect with 5-fold symmetry during homogeneous ice nucleation. The snapshots (i-iv) show the time evolution of the defect structure, indicated by black dashed lines. I_c and I_h water molecules are shown in blue and red respectively. Reprinted with permission from Ref. 322 (Copyright 2011, Royal Society of Chemistry), in which Li *et al.* performed FFS simulations of models containing about 4000 mW water molecules. b) Nucleation of an ice cluster forming homogeneously from I_0 -rich pre-critical nuclei. Water molecules belonging to I_c , I_h , a clathrate-like phase and I_0 are depicted in yellow, green, orange and magenta respectively. i-ii: a critical nucleus forms in a I_0 -rich region. iii: the crystalline cluster evolves in a post critical nucleus, formed by a I_c -rich core surrounded by a I_0 -rich shell. iv: the same post critical nucleus depicted in iii, but only particles with 12 or more connections (among ice-like particles) are shown. The colormap refers to the order parameter Q_{12} specified in Ref. 325, from which this picture has been reprinted with permission (Copyright 2014, Nature Publishing Group). The unbiased MD simulations on which the analysis is based feature 10,000 mW molecules.

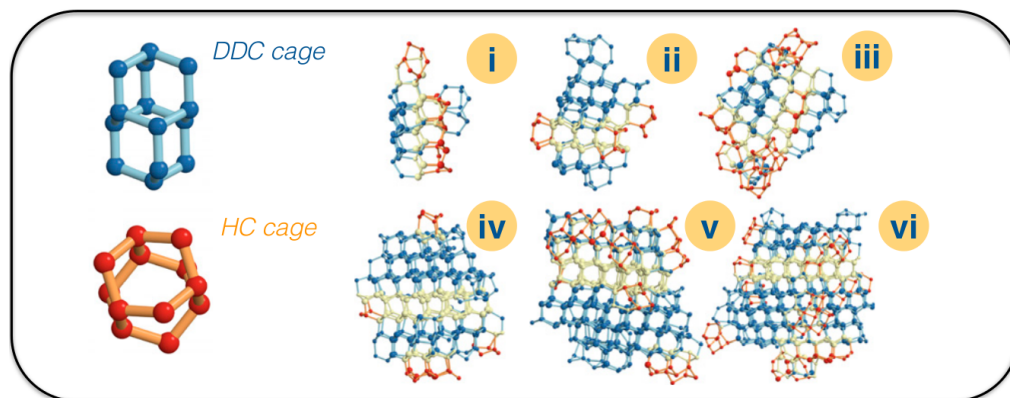


Figure 13. On the left, a typical double-diamond cage (DDC, blue) and an hexagonal cage (HC, red), the building blocks of I_c and I_h respectively. i-vi: temporal evolution of an ice nucleus from the early stages of nucleations (i-ii) up to post-critical dimensions (v-vi), as observed in the FFS simulations of Haji-Akbari and Debenedetti³²⁷. About 4,000 water molecules, modeled via the TIP4P/Ice potential³⁴⁹ have been considered in the NPT ensemble at $\Delta T \sim 40$ K. One can clearly notice the abundance of DDC cages throughout the whole temporal evolution. In contrast, HC-rich nuclei have only a marginal probability to cross the nucleation barrier (see text). Reprinted with permission from Ref. 327. Copyright 2015, National Academy of Sciences.

vide insight into the molecular mechanisms involved in the crystallization process.

2. Heterogeneous Ice Nucleation

As mentioned in the previous section, homogeneous ice nucleation becomes extremely slow at moderate supercooling. This seems at odds with our everyday expe-

rience – we do not, for example, have to wait for temperatures to reach -30°C before we have to use a deicer on our car windows. In fact, the formation of ice in nature happens almost exclusively heterogeneously, thanks to the presence of foreign particles. These ice nucleating agents facilitate the formation of ice by lowering the free energy barrier for nucleation (see Fig. 1). Indeed, the work of Sanz *et al.*³⁵³, in which homogeneous ice nucleation was studied using seeded MD (see Sec. IC 1) found

rates so low at temperatures above $\Delta T = 20$ K that they concluded that all ice nucleation above this temperature must occur heterogeneously. Homogeneous nucleation is still of great importance in atmospheric processes and climate modeling, as in certain conditions both heterogeneous and homogeneous nucleation are feasible routes toward the formation of ice in clouds, as reported in e.g. Ref. 354.

In addition to the challenges (both computational and experimental) faced when investigating homogeneous ice nucleation, one also has to consider the structure of water-surface interface and how this impacts on the nucleation rate. Generally, the experimental data for the rates and characterization of the interfacial structure come from two different communities: climate scientists have provided us with much information on how various particles, often dust particles or biological matter such as pollen, affect ice nucleation (as depicted in Fig. 14), while surface scientists have invested a lot of effort in trying to understand, at the molecular level, how water interacts with and assembles itself at surfaces (see e.g. Ref. 355). This means that there is a huge gap in our understanding, as the surfaces of the particles used to obtain rates are often not characterized, whereas surface science experiments are generally carried out at pristine, often metallic, surfaces under ultra-high vacuum conditions. We will see in this section that computational studies have gone some way to bridging this gap, although there is still much work to be done should we wish to quantitatively predict a material’s ice nucleating efficacy.

Water on crystalline surfaces

From a computational perspective, it is the surface science experiments that lend themselves most readily to modeling. In fact, even relatively expensive computational methods such as Density Functional Theory (DFT), which have not featured much in this article, have proven indispensable in furthering our understanding of how water behaves at surfaces, especially when used in conjunction with experiment (see e.g. Refs. 357, and 355 for an overview). As such, early computational studies focused on understanding how the surface affected the first few layers of water, especially with respect to the concept of lattice mismatch (see Sec. IIB), where a surface that has a structure commensurate with ice acts as a template for the crystal. Nutt and Stone^{358–360} investigated the adsorption structures of water at a model hexagonal surface and at BaF_2 (111), using interaction potentials derived from *ab initio* calculations. Although the surfaces under investigation had structures that matched the basal face of ice well, Nutt and Stone found disordered structures of water to be more favorable than ice-like overlayers. Using DFT, Hu and Michaelides investigated the adsorption of water on the (001) face of the clay mineral kaolinite^{361,362}, a known ice nucleating agent in the atmosphere. (The (001) surface of kaolinite exposes a pseudo-hexagonal arrangement of OH groups that were proposed to be the cause of its

good ice nucleating ability³⁶³.) While they found that a stable ice-like layer could form at the surface, the amphoteric nature of the kaolinite surface, depicted in Fig. 15 meant that all water molecules could participate in four hydrogen bonds, making further growth on top of the ice-like layer unfavorable. Croteau *et al.*^{364,365} investigated adsorption of water on kaolinite using the CLAYFF+SPC/E potentials^{366,367} and grand canonical Monte Carlo (GCMC). While some hexagonal patches of water were seen in the contact layer, the overall structure was mostly disordered, and the hexagonal structures that did form were strained relative to those found in ice. Also using GCMC, Cox *et al.*³⁶⁸ investigated the role of lattice mismatch using model hexagonal surfaces and TIP4P water³⁶⁹. It was found that for atomically flat surfaces, a nominally zero lattice mismatch produced disordered contact layers comprised of smaller sized rings (i.e. pentagons and squares), and hexagonal ice-like layers were only observed for surfaces with larger lattice constants.

Prior to *ca.* 2010, the above types of study were state-of-the-art for simulations of heterogeneous ice nucleation. While they provide evidence that properties such as lattice match alone are insufficient to explain a material’s ice nucleating ability, as ice nucleation itself was not directly observed, only inferences could be drawn about how certain properties may actually affect ice nucleation. Yan and Patey³⁷⁰ investigated the effects of electric fields on ice nucleation using brute force molecular dynamics (the electric fields were externally applied and were not due to an explicit surface). They found that the electric field need only act over a small range (e.g. 10 Å) and that the ice that formed near the ‘surface’ was ferroelectric cubic ice, although the rest of the ice that formed above was not. Cox *et al.* performed simulations of heterogeneous ice nucleation³⁷¹ in which both the atomistic nature of the water and the surface was simulated explicitly, using TIP4P/2005 water³⁷² and CLAYFF³⁶⁶ to describe kaolinite. Despite the fact that the simulations were affected by finite size effects, the simulations revealed that the amphoteric nature of the kaolinite^{361,362} was important to ice nucleation. In the liquid, a strongly bound contact layer was observed, and that for ice nucleation to occur, significant rearrangement in the above water layers was required. It was found that ice nucleated with its prism face, rather than its basal face, bound to the kaolinite, which was unexpected based on the theory that the pseudo-hexagonal arrangement of OH groups at the surface was responsible for templating the basal face. Cox *et al.* rationalized the formation of the prism of ice at the kaolinite due to its ability to donate hydrogen bonds both to the surface and to the water molecules above (see Fig. 15), whereas the basal face maximizes hydrogen bonding to the surface only^{361,362}. More recent simulation studies, employing rigid or constrained models of kaolinite have also found the amphoteric nature of the kaolinite surface to be important³⁷³. However, the heterogeneous nucleation mechanism of water on clays is yet to be validated by unconstrained simulations unaffected

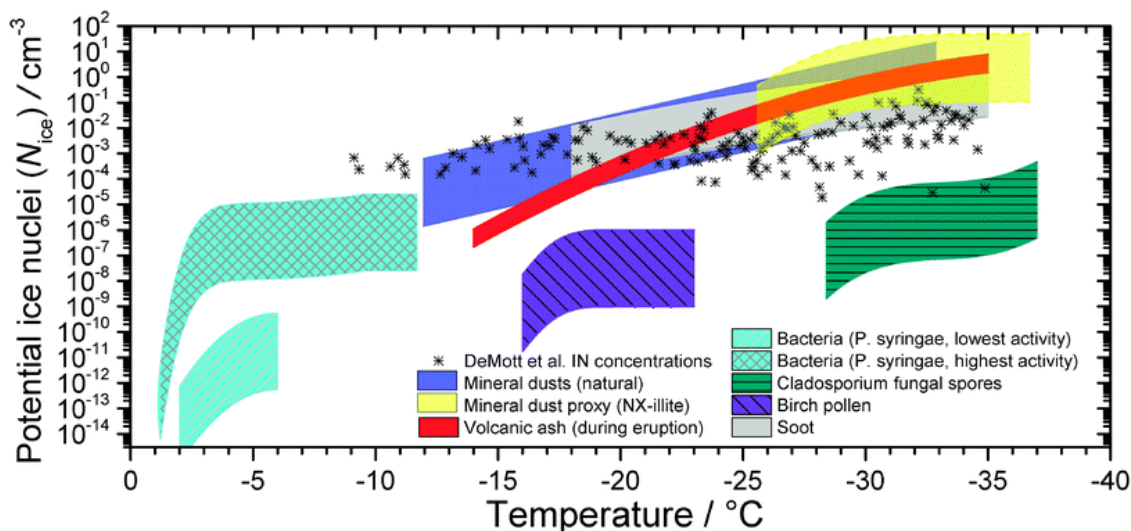


Figure 14. The *potential immersion mode ice nuclei concentrations* N_{ice} , a measure of the efficiency of a given substance to boost heterogeneous ice nucleation, is reported as a function of temperature for a range of atmospheric aerosol species. Note the wide range of nucleating capability for materials as diverse as soot or bacterial fragments over a very broad range of temperatures. Reprinted with permission from Ref. 356. Copyright 2012, Royal Society of Chemistry.

by substantial finite size effects.

Hydrophobicity and Surface Morphology

As in the case of simulations of homogeneous ice nucleation, the use of the coarse grained mW potential²⁹⁸ has seen the emergence of computational studies that actually quantify the ice nucleating efficiency of different surfaces. Recently, Lupi *et al.*³⁷⁴ investigated ice nucleation at carbonaceous surfaces (both smooth graphitic and rough amorphous surfaces) using cooling ramps to measure non-equilibrium freezing temperatures $\Delta T_f \equiv T_f - T_f^{\text{homo}}$, where T_f is the temperature at which ice nucleates in the presence of a surface, and $T_f^{\text{homo}} = 201 \pm 1$ K is the temperature at which homogeneous ice nucleation is observed. It was found that the rough amorphous surface did not enhance ice nucleation ($\Delta T_f = 0$ K) whereas the smooth graphitic surfaces promoted ice nucleation ($\Delta T_f = 11$ –13 K). This was attributed to the fact that the smooth graphitic surface induced a *layering* in the density profile of water above the surface, whereas the rough amorphous surface did not. (Lupi and Molinero quantified the extent of layering as $\mathcal{L} = \int_0^{z_{\text{bulk}}} [\frac{\rho(z)}{\rho_0} - 1]^2 dz$, where $\rho(z)$ is the density of water at a height z above the surface, and $\rho_0 \equiv \rho(z_{\text{bulk}})$ where z_{bulk} is a height where the density profile is bulk-like.) In a subsequent paper using the same methodology, Lupi and Molinero³⁷⁵ investigated how the hydrophilicity of graphitic surfaces affected ice nucleation. The hydrophilicity of the surface was modified in two different ways: first, by uniformly modifying the water-surface interaction strength; and second, by introducing hydrophilic species at the surface. It was found that the two ways produced qualita-

tively different results - uniformly modifying the interaction potential lead to enhanced ice nucleation, whereas increasing the density of hydrophilic species was detrimental to ice nucleation (although the surfaces still enhanced nucleation relative to homogeneous nucleation). It was concluded that the hydrophilicity is not a good indicator of the ice nucleating ability of graphitic surfaces. As for the difference between increasing the hydrophilicity by uniform modification of the interaction potential and by introducing hydrophilic species, Lupi and Molinero again saw that the extent of layering in water's density profile above the surface correlated well with the ice nucleating efficacy. The general applicability of the layering mechanism, however, was left as an open question.

Cox *et al.*^{376,377} addressed the question of the general applicability of the layering mechanism by investigating ice nucleation rates over a wider range of hydrophilicities (by uniformly changing the interaction strength) on two surfaces with different morphologies: (1) the (111) surface of a face centered cubic LJ crystal (FCC-111) that provided distinct adsorption sites for the water molecules; and (2) a graphitic surface, similar to that of Lupi *et al.*³⁷⁴. While it was found that the layering mechanism (albeit with a slight modification to the definition used by Lupi *et al.*) could describe the ice nucleating behavior of the graphitic surface, at the FCC-111 surface no beneficial effects of layering were observed. This was attributed to fact that the FCC-111 surface also affected the structure of the water molecules in the second layer above the surface, in a manner detrimental to ice nucleation. It was concluded that layering of water above the surface can be beneficial to ice nucleation, but only if

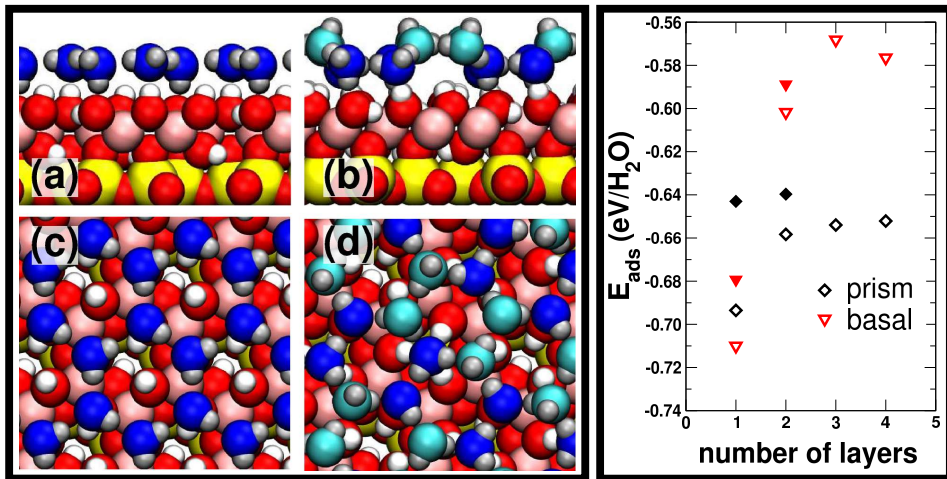


Figure 15. The amphoteric nature of kaolinite is important to its ice nucleating ability. The left panel shows ice-like contact layers at the kaolinite surface, with (a) the basal face of ice adsorbed on kaolinite, and (b) with its prism face adsorbed. The structure in (c) is the same as (a) viewed from above, likewise for (d) and (b). The right panel shows the adsorption energy of ice on kaolinite when bound either through its basal face (red data) or prism face (blue data), for a varying number of layers of ice. (The empty symbols were obtained with a classical force field and the filled symbols with DFT.) When only the contact layer is present, the basal face structure is more stable than the prism face, but as soon as more layers are present, the prism face becomes more stable. This can be understood by the ability of the prism face to donate hydrogen bonds to the surface, and to the water molecules above, due to the ‘dangling’ hydrogen bonds seen in (b) and (d). Figure reprinted with permission from Ref. 371. Copyright 2013, Royal Society of Chemistry.

the surface presents a relatively smooth potential energy surface to the water molecules.

The studies at the carbonaceous and FCC-111 surfaces^{374–377} discussed above hinted that the heterogeneous nucleation mechanism could be very different at different types of surfaces. While there is experimental evidence that e.g. different carbon nanomaterials are capable of boosting ice nucleation (see e.g. Ref. 378), most experiments can only quantify the ice nucleating ability of the substrates (see Sec. IB). However, the structure of the water-substrate interface and any insight into the morphology of the nuclei are typically not available, making simulations essential to complement the experimental picture. In this respect, Zhang *et al.*³⁷⁹ have assessed that the (regular) patterning of a generic crystalline surface at the nano scale can strongly affect ice formation. More generally, the interplay between hydrophobicity and surface morphology has been recently elucidated by Fitzner *et al.*³⁸⁰. Brute force MD simulations of heterogeneous ice nucleation were performed for the mW water model on top of several crystalline faces of a generic FCC crystal, taking into account different values of ϵ_{WS} as well as different values of the lattice parameter. The latter is involved in the rather dated²⁷⁰ concept of the zero lattice mismatch, which we introduced in Sec. IIB (see Eq. 7) and that has been often quoted as the main requirement of an effective ice nucleating agent. However, a surprisingly non-trivial interplay between hydrophobicity and morphology was observed, as depicted in Fig. 16. Clearly neither the layering nor the lattice mismatch alone are enough to explain such a

diverse scenario. In fact, the authors proposed three additional microscopic factors that can effectively aid heterogeneous ice nucleation on crystalline surfaces: (i) An in-plane templating of the first water overlayer on top of the crystalline surface; (ii) A first overlayer buckled in an ice-like fashion; and (iii) Enhanced nucleation in regions of the liquid beyond the first two overlayers, possibly aided by dynamical effects and/or structural templating effects of the substrate extending past the surface-water interface. In addition, it turned out that different lattice parameters can lead to the nucleation and growth of up to three different faces of ice (basal, prismatic, secondary prismatic ($\{11\bar{2}0\}$)) on top of the very same surface, adding a layer of complexity to the nucleation scenario. Insights into the interplay between hydrophobicity and morphology have also very recently been obtained by Bi *et al.*³⁸¹, who investigated heterogeneous ice nucleation on top of graphitic surfaces by means of FFS simulations using the mW model. Among their findings, the authors suggested that the efficiency of ice nucleating agents can be a function not only of surface chemistry and surface crystallinity, but of the elasticity of the substrate as well.

Computational Methods and Models

Enhanced sampling techniques have also been used to investigate heterogeneous ice nucleation. Reinhardt and Doye³⁸² used umbrella sampling with the mW model to investigate nucleation at a smooth planar interface and at an ice-like surface. They found that the flat planar interface did not help nucleate ice, and that homogeneous

nucleation was the preferred pathway. One explanation given for this was that, as the density of liquid water is higher than that of ice, an attractive surface favors the liquid phase. It was also noted that the mW potential imposes an energetic penalty for non-tetrahedral triplets and by removing neighbors at the surface, this energetic penalty is decreased, and this reduction in tetrahedrality favors the liquid phase. Cabriolu and Li recently studied ice nucleation at graphitic surfaces using forward flux sampling³⁸³, again with the mW model. Under the assumption that $\Delta\mu_{V,\text{water,ice}}$ depends linearly on ΔT and that γ_S does not depend on ΔT , Cabriolu *et al.* have also extracted the values of the contact angle at different temperatures, which, along with the free energy barrier, turn out to be consistent with CNT for heterogeneous nucleation (see Sec. I A 3). Although intriguing, the generality of this finding to surfaces that include strong and localized chemical interactions remains an open question.

We have seen that for both homogeneous and heterogeneous nucleation, using the coarse grained mW model has greatly enhanced our ability to perform quantitative, systematic simulation studies of ice nucleation. We must face the fact, however, that this approach will only further our understanding of heterogeneous ice nucleation so far. As discussed for kaolinite^{361,362,371,373}, an explicit treatment of the hydrogen bonds is essential in describing heterogeneous ice nucleation. In addition to this, the mW model (as well as the majority of the fully atomistic water models) cannot take into account surface charge effects. Surfaces can polarize water molecules in the proximity of the substrate, alter their protonation state and even play a role in determining the equilibrium structure of the liquid at the interface. In light of recent studies^{370,384}, it seems that these effects can heavily affect nucleation rates of many different systems. How then, do we proceed? The answer is not clear. As discussed, enhanced sampling techniques such as umbrella sampling³⁸² and forward flux sampling³⁸³ have been applied to heterogeneous ice nucleation with the mW model, and we have seen the latter applied successfully to homogeneous nucleation with an all-atom model of water³²⁷; the computational cost, however, was huge. Although the presence of an ice nucleating agent should help reduce this cost, the parameter space that we wish to study is large and to systematically study how the various properties of a surface affect ice nucleation requires the investigation of many different surfaces.

There is another computational issue that also requires attention. Simulating heterogeneous ice nucleation under *realistic conditions* does not just mean mild supercooling – we also need realistic models of the surfaces that we wish to study! Most studies of kaolinite have only considered the planar interface, even though in nature kaolinite crystals have many step-edges and defects. Ice nucleation at AgI has also recently been studied^{385,386}, although bulk truncated structures for the exposed crystal faces were used. In the case of AgI (0001) this is problematic, as the wurtzite structure of the crystal means

that this basal face is polar and likely to undergo reconstruction³⁸⁷. Furthermore, AgI is photosensitive and it has been shown experimentally that exposure to light enhances its ice nucleating efficacy³⁸⁸, suggesting structural motifs at the surface very different from those expected from the bulk crystal structure are important. The development of computational techniques to determine surface structures, along with accurate force fields to describe the interaction with water, will be essential if we are to fully understand heterogeneous ice nucleation.

E. Nucleation from Solution

Understanding crystal nucleation from solution is a problem of great practical interest, influencing for instance pharmaceutical, chemical and food processing companies. Being able to obtain a microscopic description of nucleation and growth would allow the selection of specific crystalline polymorphs, which in turn can have an enormous impact on the final product³⁸⁹. An (in)famous case illustrating the importance of this issue is the drug Ritonavir^{390,391}, originally marketed as solid capsules to treat HIV. This compound has at least two polymorphs: the marketed and thoroughly tested polymorph (P_I) and a second more stable crystalline phase P_{II} which appeared after P_I went to market. P_{II} is basically non active as a drug because of a much lower solubility than P_I . As such, and most importantly because of the fact that P_{II} had never been properly tested, Ritonavir was withdrawn from the market in favor of a much safer alternative in the form of gel capsules. Many other examples³⁹² could be listed, as various environmental factors (such as the temperature, the degree of supersaturation, the kind of solvent or the presence of impurities) can play a role in determining the final polymorph of many classes of molecular crystals. Thus, it is highly desirable to pinpoint *a priori* the conditions leading to the formation of a specific polymorph possessing the optimal physical/chemical properties for the application of interest.

The term *nucleation from solution* encompasses a whole range of systems, from small molecules in aqueous or organic solvents to proteins, peptides or other macromolecular systems in their natural environment. These systems are very diverse and an universal nucleation framework is probably not applicable to all these cases. The review by Dadey *et al.*³⁹³ discusses the role of the solvent in determining the final crystal. Many aspects of the nucleation of solute precipitates from solution have been recently reviewed by Agarwal and Peters³⁹⁴. In this section we limit the discussion to small molecules in solution.

A central issue with MD simulations of nucleation from solution is the choice of order parameters able to distinguish different polymorphs. Many of these *collective variables* have been used in enhanced sampling simulations (see Sec. I C 2). Several examples can be

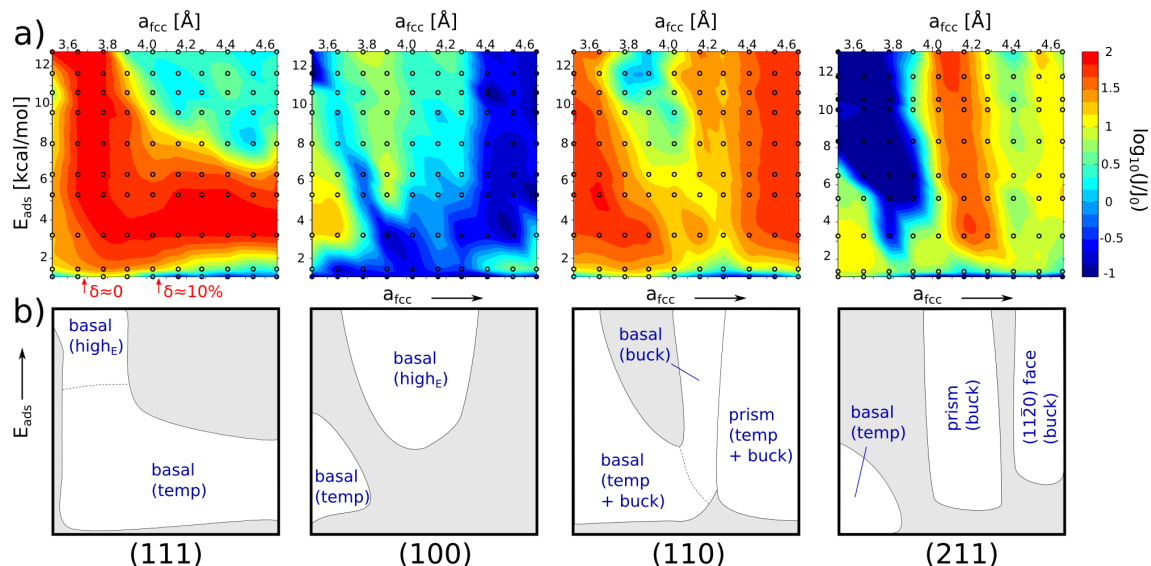


Figure 16. Interplay between surface morphology and water-surface interaction on the heterogeneous ice nucleation rate. a) Heat maps representing the values of ice nucleation rates on top of four different FCC surfaces ((111), (100), (110), (211)), plotted as a function of the adsorption energy E_{ads} and the lattice parameter a_{FCC} . The lattice mismatch δ with respect to ice on (111) is indicated below the graph. The values of the nucleation rate \mathcal{J} are reported as $\log_{10}(J/J_0)$, where J_0 refers to the homogeneous nucleation rate at the same temperature. b) Sketches of the different regions (white areas) in the (E_{ads}, a_{FCC}) space in which a significant enhancement of the nucleation rate is observed. Each region is labeled according to the face of Ih nucleating and growing on top of the surface (basal, prismatic or (11-20)), together with an indication of what it is that enhances the nucleation. "temp", "buck", and "highE" refer to the in-plane template of the first overlayer, the ice-like buckling of the contact layer, and the nucleation for high adsorption energies on compact surfaces. Reprinted with permission from Ref. 380. Copyright 2015, American Chemical Society.

found in e.g. Refs. 395–399. MD simulations of nucleation from solution are particularly challenging because of finite size effects due to the nature of the solute/solvent system^{152,400}. In the NVT and NPT ensembles, where MD simulations of nucleation are usually performed, the total number of solute molecules is constant. However, the ratio between the number of solute molecules in the crystalline phase and those within the solution varies during the nucleation events, leading to a change in the chemical potential of the system. This occurrence has negligible effects in the thermodynamic limit⁴⁰¹, but it can affect substantially the outcomes of e.g. free energy based enhanced sampling simulations. Simulations of models containing a large number (10^3 – 10^5) of molecules can alleviate the problem⁴⁰², although this is not always the case^{394,403,404}. An analytic correction to the free energy for NPT simulations of nucleation of molecules from solution has been proposed in Refs. 394,404 on the basis of a number of previous works (see e.g. Refs. 152,400,405) and applied later on in Ref. 406 as well. Alternative approaches include seeded MD simulations^{193,402} (see Sec. IC1) and simulations mimicking the grand canonical ensemble μVT ^{407,408}, where the number of constituents is not a constant and the number of molecules in - in this case - the solution is allowed to evolve in time. It is worth noticing that nucleation of molecules in solution is a challenging playground for ex-

periments as well. For instance, quantitative data about nucleation of ionic solutions are amazingly hard to find within the current literature. This is in stark contrast with the vast amount of data covering e.g. ice nucleation (as illustrated in Sec. IID).

Nucleation of Organic Crystals

Among the countless organic compounds, urea molecules can be regarded as a benchmark for MD simulation of nucleation from solution. This is because urea is a system of great practical importance which: (i) displays fast nucleation kinetics; and (ii) has only one experimentally characterized polymorph. Early studies by Piana *et al.*^{409,410} focused on the growth rate of urea crystals, which turned out to be consistent with experimental results. Years later, the inhibition of urea crystal growth by additives was investigated by Salvalaglio *et al.*^{411,412}. The investigation of the early stages of nucleation has been tackled only recently by Salvalaglio *et al.*⁴¹³ for urea molecules in aqueous or organic (ethanol, methanol and acetonitrile) solvents. In these studies the authors employed metadynamics along with the generalized Amber force field^{414,415}. The resulting free energies, modified for finite size effects related to the solvent⁴¹³, suggested that different solvents led to different nucleation mechanisms. While a single-step nucleation process is favored in methanol and ethanol, a two-step mechanism

(see Sec. I A 2) emerges for urea molecules in acetonitrile and water, as depicted in Fig. 17. In this case, the initial formation of an amorphous - albeit dense - cluster is followed by the evolution into a crystalline nucleus. Note that according to the free energy surface reported in Fig. 17a, the amorphous clusters (configurations n.2 and n.3 in Fig. 17a and Fig. 17b) are unstable with respect to the liquid phase, i.e. they are not metastable states having their own free energy bases but rather they originate from fluctuations within the liquid phase. This evidence, together with the fact that the transition state (configuration n.4 in Fig. 17a and Fig. 17b) displays a fully crystalline core, prompts the following, long-standing question: *if the critical nucleus is mostly crystalline and the amorphous precursors are unstable with respect to the liquid phase, can we truly talk about a two-steps mechanism?* Ref. 394 suggests the term *ripening regime two-step* when dealing with stable amorphous precursors and *crystallization-limited two-step* when the amorphous clusters are unstable and the limiting step is the formation of a crystalline core within the clusters. Salvalaglio *et al.*⁴¹³ also observed two polymorphs (p_I and p_{II}) in the early stages of the nucleation process. p_I corresponds to the experimental crystal structure and is the most stable structure in the limit of an infinite crystal⁴¹⁶. p_{II} , however, is more stable for small crystalline clusters. In agreement with Ostwald rule (see Sec. IIB), the small crystalline clusters that initially form in solution are of p_{II} type, and the subsequent conversion from p_{II} to p_I seems to be an almost barrierless process.

A similar approach to Ref.⁴¹³ was used to investigate crystal nucleation of 1,3,5-Tris(4-bromophenyl)benzene molecules in water and methanol. These simulations showed the emergence of prenucleation clusters, consistent with recent experimental results¹³⁷ based on single-molecule real-time transmission electron microscopy (SMRT-TEM, see Sec. IB). The formation of prenucleation clusters in the early stages of nucleation from solution has been observed in several other cases^{18,24,137,393,417}. This is of great relevance as CNT is not able to account for two (or multi) step nucleation. MD simulations have been of help in several cases, validating or supporting a particular mechanism. For instance, MD simulations have provided evidence for two-step nucleation in aqueous solutions of α -Glycine⁴¹⁸ and n -octane (or n -octanol) solutions of D-/L-norleucine⁴¹⁹.

Nucleation of Sodium Chloride

Sodium chloride (NaCl) nucleation from supersaturated brines represents an interesting challenge for simulations, as the system is relatively easy to model and experimental nucleation rates are available.

The first simulations of NaCl nucleation date back to Ohtaki et Fukushima⁴²⁰, who in the early 90's performed brute force MD simulations using very small systems (448 molecules including water molecules and ions) and exceedingly short simulation times (~ 10 ps). Thus, the formation of small crystalline clusters they observed was

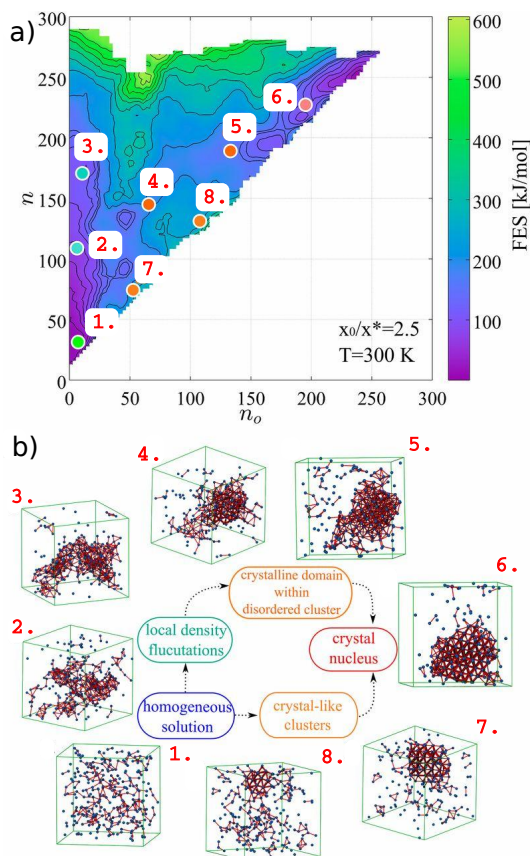


Figure 17. a) Free-energy surface (FES) associated with the early stages of nucleation of urea in aqueous solution. This has been obtained by Salvalaglio *et al.*⁴⁰⁶ from a well tempered metadynamics simulation of 300 urea molecules and 3173 water molecules, within an isothermal-isobaric ensemble at $p = 1$ bar and $T = 300$ K (simulation S2 in Ref.⁴⁰⁶, with correction term to the free-energy included in order to represent the case of a constant supersaturation of 2.5). The contour plot of the FES is reported as a function of the number of molecules belonging to the largest connected cluster (n , in ordinate) and the number of molecules in a crystal-like configuration within the largest cluster (n_o , in abscissa). Note that $n \geq n_o$ by definition, and that CNT would prescribe that the evolution of the largest cluster in the simulation box is such that $n = n_o$ (i.e., only the diagonal of the contour plot is populated). The presence of an off-diagonal basin provides evidence of a two-step nucleation of urea crystals from aqueous solutions. This is further supported by the representative states sampled during the nucleation process, shown in panel b). Urea molecules are represented as blue spheres, and red connections are drawn between urea molecules falling within a cutoff distance of 0.6 nm of each other. Reprinted with permission from Ref. 406. Copyright 2015, National Academy of Sciences.

most likely a consequence of finite size effects. More recently, the TPS simulations of Zahn⁴²¹ suggested that the centers of stability for NaCl aggregates consists of non-hydrated Na^+ ions octahedrally coordinated with Cl^- ions, albeit the results related to very small simulations

boxes (containing 310 molecules in total).

Tentative insight into the structure of the crystalline clusters came with the work of Nahtigal *et al.*⁴²², featuring simulations of 4132 molecules (4000 water molecules and 132 ions) in the 673-1073 K range for supercritical water at different densities (0.17-0.34 g/cm³). They reported a strong dependence of the crystalline cluster size distribution on the system density, with larger clusters formed at lower densities. Moreover, the clusters appeared to be amorphous. The emergence of amorphous precursors has been also reported in the work of Chakraborty and Patey^{423,424}, reporting large scale MD simulations featuring 56,000 water molecules and 4000 ion pairs in the NPT ensemble. The SPC/E model⁴²⁵ was used for water, and the ion parameters were those used in the OPLS^{426,427} force field. Their findings provided strong evidence for a two-step mechanism of nucleation, where a dense but unstructured NaCl nucleus is formed first, followed by a rearrangement into the rock salt structure, as depicted in Fig. 18a. On a similar note, metadynamics simulations performed by Giberti *et al.*⁴²⁸ using the GROMOS⁴²⁹ force field for the ions and the SPC/E⁴²⁵ model for water suggested the emergence of a wurtzite-like polymorph in the early stages of nucleation. This precursor could be an intermediate state along the path from brine to the NaCl crystal. However, Alexandre and Hansen⁴³⁰ pointed out a strong sensitivity of the nucleation mechanism on the choice of the force field.

In fact, very recent simulations by Zimmermann *et al.*⁴⁰² demonstrated that the GROMOS force field overestimates the stability of the wurtzite-like polymorph. The authors employed a seeding approach within a NVT setup for which the absence of depletion effects was explicitly verified¹⁵². The force fields used are those developed by Joung and Cheatham⁴³¹ for Na⁺ and Cl⁻, and SPC/E⁴²⁵ for water, which provide reliable solubilities and accurate chemical potential driving force⁴³². By using a methodology introduced in Ref.¹⁹³, the interfacial free energy and the attachment frequency δ_n were deduced. A thorough investigation of the latter demonstrated that the limiting factor for δ_n , which in turn strongly affects the kinetics of nucleation (see Sec. I A 1), is not the diffusion of the ions within the solution, but instead the desolvation process needed for the ions to get rid of the solvent and join the crystalline clusters. Moreover, Zimmermann *et al.*⁴⁰² evaluated the free energy barrier to nucleation as well as the nucleation rate as a function of supersaturation, providing three estimates by using different approaches. The results are compared with experiments in Fig. 18b, showing a substantial discrepancy as large as 30 orders of magnitude. Interestingly, experimental nucleation rates are much smaller than what is observed in simulations, contrary to what has been observed for e.g. colloids (see Sec. II A). We stress that the work of Zimmermann *et al.* employed state of the art computational techniques and explored NaCl nucleation in different conditions using a variety of approaches. The fact that these *tour de force* simula-

tions yielded nucleation rates that differed significantly from experiments casts yet another doubt on the possibility to compare effectively experiments and simulations. However, it must be noted that Zimmermann *et al.*⁴⁰² assumed a value of about 5.0 mol_{NaCl}/kg_{H₂O} for the NaCl solubility in water, as proposed in Ref. 432. This differs substantially from the values independently obtained by Moucka *et al.*⁴³³ (3.64 mol_{NaCl}/kg_{H₂O}) and more recently by Mester and Panagiotopoulos⁴³⁴ (3.71 mol_{NaCl}/kg_{H₂O}). This discrepancy can explain the enormous mismatch reported by Zimmermann *et al.*⁴⁰², once again demonstrating the severe sensitivity of nucleation rates with respect to any of the ingredients involved in their calculations.

On a final note, we stress that many other examples of molecular dynamics simulations looking at specific aspects of crystal nucleation from solution exist in the literature. For instance, a recent study by Anwar *et al.*⁴³⁵ describes secondary crystal nucleation, where crystalline seeds are already present within the solution. The authors suggest, for a generic solution represented by Lennard-Jones particles, a (secondary) nucleation mechanism enhanced by the existence of PNCs (see Sec. I A 2). Kawska *et al.*¹⁸⁹ underlined instead the importance of proton transfer within the early stages of nucleation of zinc oxide nano clusters from an ethanol solution. The emergence of similar ripening processes, selecting specific crystalline polymorphs according to e.g. the effect of different solvents is still fairly unexplored but bound to be of great relevance in the future. Finally, several computational studies have dealt with the crystallization of calcium carbonate, which has recently been reviewed extensively in Ref.¹⁸ and thus, together with the broad topic of crystal nucleation of biominerals, is not discussed in here.

F. Natural Gas Hydrates

Natural gas hydrates are crystalline compounds in which small gas molecules are caged (or *enclathrated*) in a host framework of water molecules. Natural gas molecules (e.g. methane, ethane, propane) are hydrophobic. They are also favored by conditions of high pressure and low temperature, and are found to occur naturally in the ocean bed and in permafrost regions⁴³⁹. With exceptionally high gas storage capabilities and the fact that it is believed that gas hydrates exceed conventional gas reserves by at least an order of magnitude⁴⁴⁰, there is interest in trying to exploit gas hydrates as a future energy resource. While gas hydrates may potentially play a positive role in the energy industry's future, they are currently considered a hindrance: if mixed phases of water and natural gas are allowed to cool in an oil pipeline, then a hydrate may form and block the line, causing production to stall. Understanding the mechanism(s) by which gas hydrates nucleate is likely to play an important role in the rational design of more effective hydrate inhibitors.

Hydrate Structures

There are two main types of natural gas hydrates: struc-

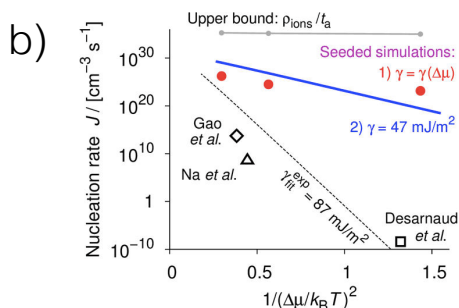
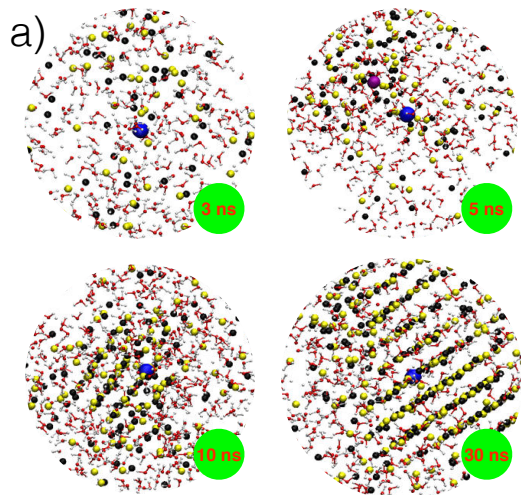


Figure 18. a) Snapshots from an MD simulation of crystal nucleation of NaCl from aqueous solution. The simulations, carried out by Chakraborty and Patey⁴²³, involved 56,000 water molecules and 4000 ion pairs (concentration is 3.97 *m*) in the NPT ensemble. All Na⁺ (black) and Cl⁻ (yellow) ions within 2 nm of a reference Na⁺ ion (larger and blue) are shown together with water molecules (oxygens and hydrogens in red and white respectively) within 0.4 nm from each ion. From the relatively homogeneous solution (3 ns) an amorphous cluster of ions emerges (5 ns). This fluctuation in the concentration of the ions leads to a subsequent ordering of the disordered cluster (10 ns) in a crystalline fashion (30 ns), consistently with a two-step nucleation mechanism. Reprinted with permission from Ref.⁴²³. Copyright 2013, American Chemical Society. b) Comparison of NaCl nucleation rates, J , as a function of the driving force for nucleation, reported as $1/(\Delta\mu/k_B T)^2$. Red dots as well as blue and gray (continuous) lines have been estimated via three different approaches by the simulations of Zimmermann *et al.*⁴⁰². Experimental data obtained employing an electrodynamic levitator trap (Na *et al.*⁴³⁶), an efflorescence chamber (Gao *et al.*⁴³⁷), and microcapillaries (Desarnaud *et al.*⁴³⁸) are also reported together with a tentative fit (γ_{fit}^{exp} , dotted line). Note the substantial (up to about 30 orders of magnitude) discrepancy between experiments and simulations. Reprinted with permission from Ref.⁴⁰². Copyright 2015, American Chemical Society.

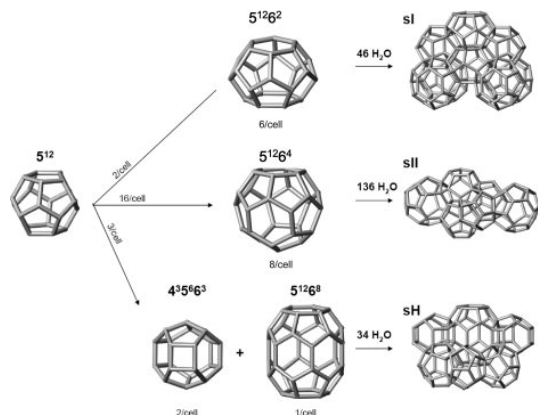


Figure 19. Crystal structure of the sI, sII and sH gas hydrates, along with the corresponding cage structures. Only the water molecule positions are shown as spheres connected by lines. Reprinted with permission from Ref. 441. Copyright 2007, John Wiley and Sons.

ture I *sI*, which has a cubic structure (space group *Pm3n*); and structure II *sII*, which also has a cubic structure (space group *Fd3m*). (There is also a third, less common type *sH*, which has an hexagonal crystal structure, but we do not discuss this any further here.) Structurally, the water frameworks of both *sI* and *sII* hydrate are similar to Ice *I_h*, with each water molecule finding itself in an approximately tetrahedral environment with its nearest neighbors. Unlike ice *I_h*, however, the water framework consists of cages, with cavities large enough to accommodate a gas molecule.

Between the *sI* and *sII* hydrate there exist three types of cages, which are denoted 5^p6^h depending upon the number of five- and six-sided faces that make up the cage. For example, common to both the *sI* and *sII* hydrate is the 5^{12} cage, where the water molecules sit on the vertices of a pentagonal dodecahedron. Along with the 5^{12} cage the *sI* hydrate also consists of a $5^{12}6^2$ cage, which has two six-sided faces and twelve five-sided faces: there are two 5^{12} cages and six $5^{12}6^2$ cages in the unit cell. The *sII* hydrate, on the other hand, has a unit cell made up of sixteen 5^{12} cages and eight $5^{12}6^4$ cages. Due to the larger size of the $5^{12}6^4$ cage, the *sII* structure forms in the presence of larger guest molecules such as propane, whereas small guest molecules such as methane favor the *sI* hydrate. (This is not to say that small guest molecules are not present in *sII*, just that the presence of larger guest molecules is necessary to stabilize the larger cavities.) The *sI*, *sII* and *sH* crystals structures are shown in Fig. 19, along with the individual cage structures. Further details regarding the crystal structures of natural gas hydrates can be found in Ref. 439.

Homogeneous Nucleation

Historically, two main molecular mechanisms for hydrate nucleation have been proposed. First, Sloan and co-workers^{442,443} proposed the *labile cluster hypothesis*

(LCH), which essentially describes the nucleation process as the formation of isolated hydrate cages which then agglomerate to form a critical hydrate nucleus. Second, the *local structure hypothesis* (LSH) was proposed after umbrella sampling simulations by Radhakrishnan and Trout⁴⁴⁴ suggested that the guest molecules first arrange themselves in a structure similar to the hydrate phase, which is accompanied by a perturbation (relative to the bulk mixture) of the water molecules around the locally ordered guest molecules. For the same reasons already outlined elsewhere (see Sec. IB), it is experimentally challenging to verify which, if either, of these two nucleation mechanisms is correct. What we will see in this section is how computer simulations of gas hydrate nucleation have been used to help shed light on this process.

Although not the first computer simulation study of natural gas hydrate formation (see e.g. Refs.^{444–447}), one of the most influential simulation works on gas hydrate formation is that of Walsh *et al.*⁴⁴⁸, in which methane hydrate formation was directly simulated under conditions of 250 K and 500 bar. It was found that nucleation proceeded *via* two methane and five water molecules cooperatively organizing into a stable structure, with the methane molecules adsorbed on opposite sides of a pentagonal ring of water molecules. This initial structure allowed the growth of more water faces and adsorbed methane, until a 5^{12} cage formed. This process took on the order of 50–100 ns to complete. After persisting for ~ 30 ns, this 5^{12} cage opened when two new water molecules were inserted into the only face without an adsorbed methane molecule, on the opposite side to that where several new full cages were completed. This opening of the original 5^{12} cage was then followed by the relatively fast growth of methane hydrate. The early stages of hydrate nucleation are shown in Fig. 20. After ~ 240 ns, the original 5^{12} cage transformed into a $5^{12}6^3$ cage, a structure not found in any equilibrium hydrate structure. Walsh *et al.* also found that 5^{12} cages dominate, in terms of abundance, during the early stages of nucleation. The formation of $5^{12}6^2$ cages (which along with the 5^{12} cages comprise the sI hydrate) are the second most abundant, although their formation occurred approximately 100 ns after the initial 5^{12} cages. A significant amount of the larger $5^{12}6^4$ cages that are found in the sII hydrate was also observed, which was rationalized by the large number of face-sharing 5^{12} cages providing an appropriate pattern. The $5^{12}6^3$ cages were also observed in an abundance close to that of the $5^{12}6^2$ cages. The final structure can be summarized as a mixture of sI and sII motifs, linked by $5^{12}6^3$ cages. A similar structure had been previously reported as a result of hydrate growth simulations^{449,450}.

Even though the work of Walsh *et al.*⁴⁴⁸ provided useful insight into the hydrate nucleation mechanism, the conclusions were based upon only two independent nucleation trajectories. Soon after the Walsh paper, Jacobson and Molinero⁴⁵¹ reported a set of twelve simu-

lations using a methane-water model⁴⁵² based on mW water under conditions of 210 K and 500 atm (the melting point of the model is approximately 300 K). Owing to the reduced computational cost of the coarse-grained model, Jacobson and Molinero were also able to study a much larger system size than Walsh *et al.* (8000 water and 1153 guest molecules⁴⁵¹ vs 2944 water and 512 guest molecules⁴⁴⁸). In agreement with Walsh *et al.*, the initial stages of the nucleation mechanism were also dominated by 5^{12} cages, and a mixture of sI and sII motifs connected by $5^{12}6^3$ cages were observed. It was also observed that solvent-separated-pairs of guest molecules were stabilized by greater numbers of guest molecules in the cluster. As gas hydrates are comprised of solvent-separated-pairs of guest molecules as opposed to contact-pairs, this suggests that a resemblance to the LSH, where the local ordering of guest molecules drives the nucleation of the hydrate. Jacobson and Molinero, however, also found a likeness to the LCH; clusters of guest molecules and their surrounding water molecules formed long-lived *blobs* that slowly diffuse in solution. These blobs could be considered large analogues of the labile clusters proposed in the LCH. Through analysis of their simulation data, Jacobson and Molinero concluded that the blob is a guest rich precursor in the nucleation pathway of gas hydrates with small guest molecules (such as methane). Note that the distinction between *blobs* and *amorphous* is that the water molecules have yet to be locked into the clathrate hydrate cages in the former. The overall nucleation mechanism is depicted in Fig. 21.

Both the work of Walsh *et al.* and Jacobson and Molinero suggest that amorphous hydrate structures are involved in the nucleation mechanism, although both studies were carried out under high driving forces. In Ref. 453, Jacobson and Molinero addressed the following two questions raised by the above studies: *how could amorphous nuclei grow into a crystalline form?*; and *are amorphous nuclei precursors intermediates for clathrate hydrates under less forcing conditions?* By considering the size-dependent melting temperature of spherical particles using the Gibbs-Thompson equation, Jacobson and Molinero found for all temperatures that the size of the crystalline critical nucleus was always smaller than the amorphous critical nucleus, with the two becoming virtually indistinguishable in terms of stability for very small nuclei of ~ 15 guest molecules (i.e. under very forcing conditions). From a thermodynamic perspective, this would suggest that nucleation would always proceed *via* a crystalline nucleus. The observation of amorphous nuclei^{445,448,451,454,455}, even at temperatures as high as 20% supercooling, hints that their formation may be favored for kinetic reasons. Employing the CNT expression for the free energy barrier suggested that the amorphous nuclei could be kinetically favored up to 17% supercooling if $\gamma_a/\gamma_x = 0.5$, where γ_a and γ_x are the liquid-amorphous and liquid-crystal surface tensions, respectively. Jacobson and Molinero estimate $\gamma_x \approx 36$ mJ/m² and $16 < \gamma_a < 32$ mJ/m², so it is certainly plausible that

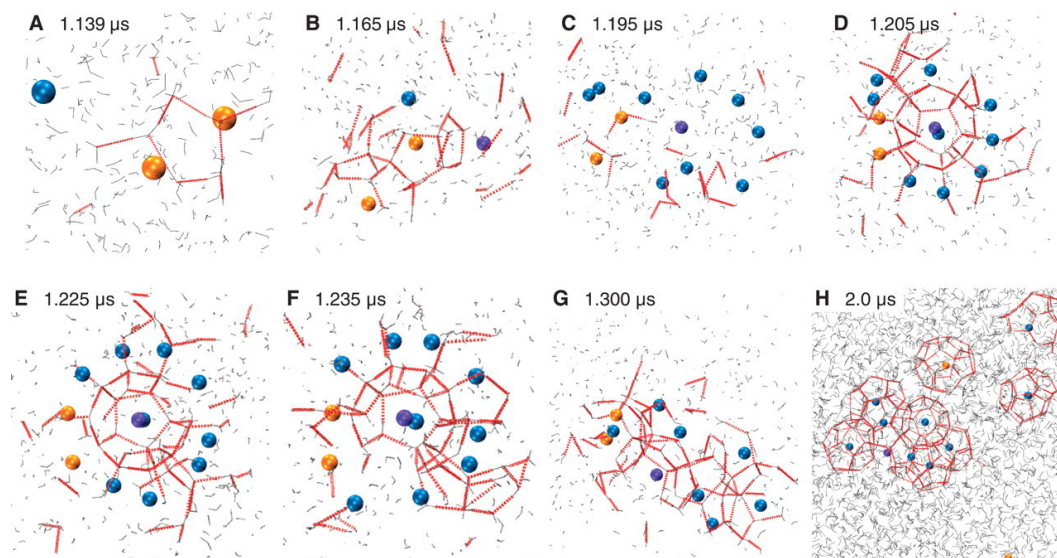


Figure 20. Early stages of hydrate nucleation observed by Walsh *et al.* (A to C) A pair of methane molecules is adsorbed on either side of a single pentagonal face of water molecules. Partial cages form around this pair, near the eventual central violet methane molecule, only to dissociate over several nanoseconds. (D and E) A small cage forms around the violet methane and other methane molecules adsorb at 11 of the 12 pentagonal faces of the cage, creating the bowl-like pattern shown. (F and G) The initial central cage opens on the end opposite to the formation of a network of face-sharing cages, and rapid hydrate growth follows. (H) A snapshot of the system after hydrate growth, showing the fates of those methane molecules that make up the initial bowl-like structure (other cages not shown). Reprinted with permission from Ref. 448. Copyright 2009, The American Association for the Advancement of Science.

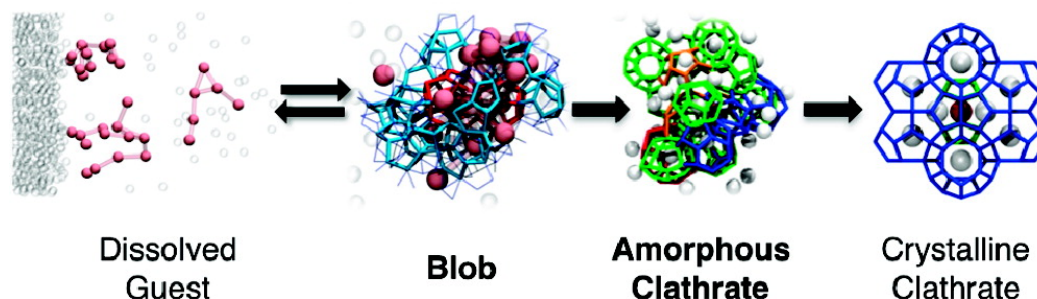


Figure 21. Sketch of the nucleation mechanism of methane hydrates proposed in Ref. 451. Clusters of guest molecules aggregate in *blobs*, which transform in to amorphous clathrates as soon as the water molecules arrange themselves in the cages characteristic of crystalline clathrate, which eventually for upon the re-ordering of the guest molecules - and thus of the cages - in a crystalline fashion. Note that the difference between the *blob* and *amorphous clathrate* is that the water molecules have yet to be locked into clathrate hydrate cages in the former. Reprinted with permission from Ref. 451. Copyright 2010, American Chemical Society.

amorphous precursors are intermediates for clathrate hydrates under certain conditions. The growth of clathrate hydrates from amorphous and crystalline seeds was also studied, where it was found that crystalline clathrate can grow from amorphous nuclei. As the simulation led to fast mass-transport, the growth of post critical nuclei was relatively quick, and the amorphous seed became encapsulated by a (poly)crystalline shell. Under conditions where an amorphous nucleus forms first due to a smaller free energy barrier, but where diffusion of the guest species becomes a limiting factor, it is likely that

small nuclei would have long enough to anneal to structures of greater crystallinity before growing to the macroscopic crystal phase.

It thus appears that gas hydrates may exhibit a multi-step nucleation process involving amorphous precursors for reasonably forcing conditions, but for temperatures close to coexistence, it seems that nucleation should proceed *via* a single crystalline nucleus. By assuming a CNT expression for the free energy (as well as the total rate), Knott *et al.*⁴⁵⁶ used the *seeding technique* (See Sec. IC 1) to compute the nucleation rate for sI methane hydrate

with relatively mild supersaturation of methane, in a similar manner to Espinosa *et al.*³²⁶ for homogeneous ice nucleation as discussed in Sec. IID 1. They found vanishingly small homogeneous nucleation rates of 10^{-111} nuclei $\text{cm}^{-3} \text{s}^{-1}$, meaning that even with all of Earth's ocean waters, the induction time to form one crystal nucleus homogeneously would be $\sim 10^{80}$ years! Knott *et al.* therefore conclude that under mild conditions, hydrate nucleation must occur heterogeneously.

Heterogeneous Nucleation

Compared to homogeneous nucleation, the heterogeneous nucleation of gas hydrates is little studied. Liang *et al.*⁴⁵⁴ investigated the steady state growth of a hydrate crystal in the presence of silica surfaces, finding that the crystal preferentially grew in the bulk solution rather than at the interface with the solid. It was also observed that in one simulation, local methane density fluctuations led to the spontaneous formation of a methane bubble from solution, which was located at the silica interface. This had two effects on the observed growth: (i) the methane bubble depleted most of the methane from solution, leading to an overall slowing down of the crystal growth rate; and (ii) due to the location of the methane bubble, the silica surface effectively acts like a source of methane, promoting growth of the crystal closer to the interface relative to the bulk.

Bai *et al.* investigated the heterogeneous nucleation of CO_2 hydrate in the presence of a fully hydroxylated silica surface, first in a two-phase system where the water and CO_2 are well mixed⁴⁵⁷, and then in a three-phase system where the CO_2 and water are initially phase separated⁴⁵⁸. In the two-phase system, the authors report the formation of an ice-like layer at the silica surface, above which a layer comprised of *semi-5*¹² *cage-like* structures mediates the structural mismatch between the ice-like contact layer and the sI hydrate structure above. In the three-phase system, nucleation is observed at the three-phase contact line, along which the crystal nucleus also grows. This is attributed to the stabilizing effect of the silica on the hydrate cages, plus the requirement for the availability of both water and CO_2 . In a later paper, Bai *et al.*⁴⁵⁹ investigated the effect of surface hydrophilicity (by decreasing the percentage of surface hydroxyl groups) and crystallinity on the nucleation of CO_2 hydrate. They found that in the case of decreased hydrophilicity, the ice-like layer at the crystalline surface vanishes, replaced instead by a single liquid-like layer upon which the hydrate directly nucleates. Whereas shorter induction times to nucleation at the less hydrophilic surfaces are reported, little dependence upon the crystallinity of the surface is observed. While certainly an interesting observation, as only a single trajectory was performed for each system, studies in which multiple trajectories are used to obtain a distribution of induction times would be desirable and, as the hydrate actually appears to form away from the surface in all cases, a full comparison of the heterogeneous and homogeneous rates would also be a worthwhile pur-

suit.

There have also been a number of studies investigating the potential role of ice in the nucleation of gas hydrates. Pirzadeh and Kusalik⁴⁶⁰ performed MD simulations of methane hydrate nucleation in the presence of ice surfaces, and reported that an increased density of methane at the interface induced structural defects (coupled 5-8 rings) in the ice that facilitated the formation of hydrate cages. Nguyen *et al.*⁴⁶¹ used MD simulations to directly investigate the interface between a gas hydrate and ice, and found the existence of an *interfacial transition layer* (ITL) between the two crystal structures. The water molecules in the ITL, which was found to be disordered and 2-3 layers of water in thickness, have a tetrahedrality and potential energy that is intermediate between that of either of the crystal structures and liquid water. The authors suggest that the ITL could assist the heterogeneous nucleation of gas hydrates from ice by providing a lower surface free energy than either of the ice-liquid and hydrate-liquid interfaces. Differential scanning calorimetry experiments by Zhang *et al.*⁴⁶² found that ice and hydrate formation to occur simultaneously (on the experimental timescale), which was attributed to the heterogeneous nucleation of ice, which in turn facilitated hydrate formation. Poon and Peters⁴⁶³ provide a possible explanation for ice acting as a heterogeneous nucleating agent for gas hydrates, aside from the structural considerations of Refs. 460 and 462: At a growing ice front, the local supersaturation of methane can be dramatically increased, to the extent that induction times to nucleation are reduced by as much as a factor 10^{100} .

Computer simulations of hydrate nucleation have certainly contributed to our understanding of the underlying mechanisms, especially in the case of homogeneous nucleation. One fairly consistent observation across many simulation studies^{444,445,447,448,451,453,464} suggests that some kind of ordering of dissolved guest molecules precedes the formation of hydrate cages. Another is that amorphous nuclei, consisting of structural elements of both sI and sII hydrate form when conditions are forcing enough. Nevertheless, open questions still remain. In particular, the prediction that homogeneous nucleation rates are vanishingly small under mild conditions⁴⁵⁶ emphasizes the need to better understand heterogeneous nucleation. To this end, enhanced sampling techniques such as FFS, which has recently been applied to methane hydrate nucleation at 220 K and 500 bar⁴⁶⁴, are likely to be useful, although directly simulating nucleation under mild conditions is still likely to be a daunting task. Another complicating factor is that, aside from the presence of solid particles, the conditions from which natural gas hydrates form are often highly complex; for example in an oil or gas line there is a fluid flow and understanding how this affects the methane distribution in water, is likely to be an important factor in determining how fast gas hydrates form⁴⁶⁵. In this respect, the formation of natural gas hydrates is a truly multi-scale phenomenon.

III. FUTURE PERSPECTIVES

We have described only a fraction of the many computer simulation studies of crystal nucleation in supercooled liquids and solutions. Still, we have learned that MD simulations have dramatically improved our fundamental understanding of nucleation. For instance, several studies on colloidal particles (see Sec. II A) provided evidence for two-step nucleation mechanisms, and the investigation of LJ liquids has yielded valuable insight into the effect of confinement (see Sec. II B). In addition, the investigation of more realistic systems has delivered outcomes directly related to problems of great relevance. For example, the influence of different solvents on the early stages of urea crystallization (see Sec. II E) has important consequences in fine chemistry and in the fertilizer industry, and the molecular details of clathrate nucleation (see Sec. II E) could help to rationalize and prevent hydrate formation in oil or natural gas pipelines. Thus, it is fair to say that MD simulations have been and will remain a powerful complement to experiments.

However, simulations are presently affected by several shortcomings, which hinder a reliable comparison with experimental nucleation rates and limit nucleation studies to systems and/or conditions often far away from those investigated experimentally. These weaknesses can be classified in to two main categories: (i) limitations related to the accuracy of the computational model used to represent the system; and (ii) shortcomings due to the computational techniques employed to simulate nucleation events.

(i) In an ideal world, *ab initio* calculations would be the tool of the trade. Unfortunately, in all but a handful of cases such as the phase change materials presented in Sec. II C, the timescale problem makes *ab initio* simulations of crystal nucleation unfeasible (see Fig. 5). As this will be the *status quo* for the next few decades, we are forced to focus our efforts on improving the current classical force fields and on developing novel classical interatomic potentials. This is a fundamental issue that affects computer simulations of materials as a whole. While for nucleation of simple systems like colloids (Sec. II A) this is not really an issue, things start to fall apart when dealing with more realistic systems (see e.g. Sec. II E and II F), and become even worse in the case of heterogeneous nucleation (see e.g. Sec. II D 2), as the description of the interface requires extremely transferable and reliable force fields. Machine learning techniques⁴⁶⁶ such as neural network potentials (see Sec. II C and Refs. 467,468) are emerging as possible candidates to allow for classical MD simulations with an accuracy closer to first principles calculations, but the field is constantly looking for other options that are capable of bringing simulations closer to reality.

(ii) The limitations of the computational techniques currently employed to study crystal nucleation are those characteristic of rare events sampling. Brute force MD simulations (see Sec. I C 1) allow for an unbiased inves-

tigation of nucleation events, but the timescale problem limits this approach to very few systems, typically very distant from realistic materials (see e.g. Sec. II A and Sec. II B) - although notable exceptions exist (see Sec. II C). It is also worth noticing that while brute force MD is not able to provide a full characterization of the nucleation process, useful insight can still be gained into e.g. pre-nucleation events^{18,469}. Enhanced sampling techniques (see Sec. I C 2) are rapidly evolving and have the potential to take the field to the next level. However, free energy methods as they are do not give access to nucleation kinetics and in the case of complex systems (see e.g. Sec. II D 1 and Sec. II E) are strongly dependent on the choice of the order parameter. On the other hand, in light of the body of work reviewed it seems that path sampling methods can provide a more comprehensive picture of crystal nucleation. However, at the moment these techniques are computationally expensive and a general implementation is not available yet, albeit consistent efforts have been recently put in place. We believe that the development of efficient enhanced sampling methods specific to crystal nucleation is one of the crucial challenges ahead.

At the moment, simulations of crystal nucleation of complex liquids are restricted to small (10^2 - 10^4 particles) systems, most often in idealized conditions. For instance, it is presently very difficult to take into account impurities or, in the case of heterogeneous nucleation, defects of the substrate. Indeed defects seem to be ubiquitous in many different systems, such as ice, hard spheres crystals, LJ crystals and organic crystals as well. Defects are also often associated with polymorphism, but possibly because of the inherent difficulties in modeling them (or in characterizing them experimentally), they are under represented within the current literature. These are important aspects that almost always impact experimental measurements, and that should thus be included in simulations as well. In general, simulations of nucleation should allow us not only to provide microscopic insight, but also to make useful predictions and/or to provide a general understanding to be applied to a variety of systems. These two ambitious goals are particularly challenging for simulations of heterogeneous nucleation. In light of the literature we have reviewed in here, we believe that much of the effort has to be devoted in the future to i) enable atomistic simulations of heterogeneous nucleation dealing with increasingly realistic interfaces and to ii) obtain general, maybe non material-specific trends able to point the community into the right direction, even at the cost of sacrificing accuracy to a certain extent. On the other hand, we hope that the body of work reviewed here will inspire future experiments targeting *cleaner*, well defined systems by means of novel techniques, possibly characterized by better temporal and spatial resolution. Improving on the current limitations of the computational models and techniques would enable simulations of much larger systems over much longer timescales, with a degree of accuracy that would allow a

much more fruitful comparison with experiments. We think this should be the long term objective for the field. Up to now, the only way to connect simulations and experiments has been through the comparison of crystal nucleation rates, which even now still exhibit substantial discrepancies for every single class of systems we have reviewed. This is true not only for complex liquids like water (see Sec. IID 1), but even for model systems such as colloids (Sec. IIA). This, together with the fact that in some cases even experimental data are scattered across several orders of magnitude, suggests that we are dealing with crystal nucleation in liquids within a flawed theoretical framework.

As a matter of fact, CNT is now 90 years old. It is thus no wonder that every aspect of this battered theory has been criticized at some point. However, some aspects have been questioned more frequently than others. For instance, the emergence of two-step (or even multi-step) mechanisms for nucleation, has been reported for many different systems (see Sec. IIA, IIB, IIE and IIF) and cannot be easily embedded in CNT as it is, albeit several improvement upon the original CNT formulation appeared within the last decade (see Sec. IA 2). Nonetheless, CNT is basically the only theory invoked by both experiments and simulations when dealing with crystal nucleation from the liquid phase. CNT is widely used because it offers a simple and unified picture for nucleation and it is often very useful. However, as demonstrated by both experiment and simulations, even the basic rules governing the formation of the critical nucleus can change drastically from one system to another. Thus, we believe that any sort of theoretical universal approach, a brand new CNT, so to say, will be unlikely to significantly further the field. Indeed we fear that the same reasoning will hold for the computational methods required. We cannot think of a single enhanced sampling technique capable of tackling the complexity of crystal nucleation as a whole. The interesting but uncomfortable truth is that each class of supercooled liquids often possess a unique behavior, which in turn results into specific features ruling the crystal nucleation process. Thus, it is very much possible that different systems within different conditions could require different, *ad hoc* flavors of CNT. While the latter has been evolving for decades, we believe that a sizable fraction of the new developments in the field should aim at producing particular flavors of CNT, specifically tailored to the problem at hand.

In conclusion, it is clear that MD simulations have proven themselves to be of the utmost importance in unraveling the microscopic details of crystal nucleation in liquids. We have reviewed important advances which provided valuable insight into fundamental issues and diverse nucleation scenarios, complementing experiments and furthering our understanding of nucleation as a whole. Whether CNT can be effectively improved in a universal fashion is unclear. We feel that the ultimate goal for simulations would be to get substantially closer to the reality probed by experiments, and that in order

to do so we have to sharpen our computational and possibly theoretical tools. In particular, we believe that the community should invest in improving the classical interatomic potentials available as well as the enhanced sampling techniques currently used, enabling accurate simulations of crystal nucleation for systems of practical relevance.

ACKNOWLEDGEMENT

This work was supported by the European Research Council under the European Union's Seventh Framework Programme (FP/2007-2013)/ERC Grant Agreement number 616121 (HeteroIce project). A.M. is also supported by the Royal Society through a Royal Society Wolfson Research Merit Award. We gratefully acknowledge Dr. Matteo Salvalaglio, Dr. Gareth Tribello, Dr. Richard Sear and Prof. Daan Frenkel for insightful discussions and for reading an earlier version of the manuscript.

REFERENCES

- ¹T. Bartels-Rausch, *Nature* **494**, 27 (2013).
- ²B. J. Murray, T. W. Wilson, S. Dobbie, Z. Cui, S. M. R. K. Al-Jumr, O. Möhler, M. Schnaiter, R. Wagner, S. Benz, M. Niemand, H. Saathoff, V. Ebert, S. Wagner, and B. Kärcher, *Nat. Geosci.* **3**, 233 (2010).
- ³P. Mazur, *Science* **168**, 939 (1970).
- ⁴A. Lintunen, T. Hölttä, and M. Kulmala, *Sci. Rep.* **3**, 2031 (2013).
- ⁵D. Erdemir, A. Y. Lee, and A. S. Myerson, *Curr. Opin. Drug. Discov. Devel.* **10**, 746 (2007).
- ⁶J. R. Cox, L. A. Ferris, and V. R. Thalladi, *Angew. Chem. Int. Edit.* **46**, 4333 (2007).
- ⁷E. D. Sloan, *Nature* **426**, 353 (2003).
- ⁸E. G. Hammerschmidt, *Ind. Eng. Chem.* **26**, 851 (1934).
- ⁹R. Velazquez-Castillo, J. Reyes-Gasca, D. I. Garcia-Gutierrez, and M. Jose-Yacamán, *J. Mat. Res.* **21**, 1484 (2006), wOS:000238191300018.
- ¹⁰J. D. Harper, C. M. Lieber, and P. T. Lansbury Jr, *Chem. Bio.* **4**, 951 (1997).
- ¹¹D. M. Walsh, A. Lomakin, G. B. Benedek, M. M. Condrón, and D. B. Teplow, *J. Bio. Chem.* **272**, 22364 (1997).
- ¹²P. G. Debenedetti, *Metastable Liquids. Concepts And Principles* (Princeton Univ. Press, Princeton, NJ, USA, 1996) pp. 105–121.
- ¹³J. D. Stevenson and P. G. Wolynes, *J. Phys. Chem. A* **115**, 3713 (2011).
- ¹⁴(), many supercooled liquids in certain conditions take a more chaotic path towards amorphous systems⁴⁷⁰. However, this topic, involving the uncanny phenomenon of the glass transition³¹⁵, rests outside the scope of this work.
- ¹⁵W. J. E. M. Habraken, J. Tao, L. J. Brylka, H. Friedrich, L. Bertineti, A. S. Schenk, A. Verch, V. Dmitrovic, P. H. H. Bomans, P. M. Frederik, J. Laven, P. van der Schoot, B. Aichmayer, G. de With, J. J. DeYoreo, and N. A. J. M. Sommerdijk, *Nat. Comm.* **4**, 1507 (2013).
- ¹⁶B. J. Murray, D. O'Sullivan, J. D. Atkinson, and M. E. Webb, *Chem. Soc. Rev.* **41**, 6519 (2012).
- ¹⁷M. Volmer and A. Weber, *Zeit. Phys. Chem.* **119**, 277 (1926).
- ¹⁸D. Gebauer, M. Kellermeier, J. D. Gale, L. Bergström, and H. Cölfen, *Chem. Soc. Rev.* **43**, 2348 (2014).
- ¹⁹R. P. Sear, *Cryst. Eng. Comm.* **16**, 6506 (2014).
- ²⁰P. G. Vekilov, *Crys. Gro. Des.* **10**, 5007 (2010).
- ²¹X. Xu, C. L. Ting, I. Kusaka, and Z.-G. Wang, *Ann. Rev. Phys. Chem.* **65**, 449 (2014).
- ²²P. Yi and G. C. Rutledge, *Ann. Rev. Chem. Biomol. Eng.* **3**, 157 (2012).
- ²³J. Anwar and D. Zahn, *Angew. Chem. Int. Ed.* **50**, 1996 (2011).
- ²⁴D. Zahn, *Chem. Phys. Chem.* **16**, 2069 (2015).
- ²⁵(), in most cases, simulations of crystal nucleation do not embrace Classical Nucleation Theory as a whole, taking into account instead only selected elements of the theory. Common examples include i) assuming the size of the largest crystalline cluster as the only relevant order parameter to describe the nucleation process, ii) assuming the critical nuclei to be of spherical shape and iii) assuming a perfectly sharp interface between the crystalline and the liquid phase.
- ²⁶K. Kelton and A. Greer, in *Nucleation in Condensed Matter: Applications in Materials and Biology*, Pergamon Materials Series, Vol. 15, edited by K. Kelton and A. Greer (Pergamon, 2010) pp. 279 – 329.
- ²⁷V. Kalikmanov, *Nucleation Theory*, Lecture Notes in Physics, Vol. 860 (Springer Netherlands, Dordrecht, 2013).
- ²⁸H. Vehkamäki, *Classical Nucleation Theory In Multicomponent Systems* (Springer, Berlin ; New York, 2006).
- ²⁹L. Farkas, *Zeit. Phys. Chem.* **125**, 236 (1927).
- ³⁰(), farkas, forced to flee Nazi Germany in 1933, was the first one to develop a real theory of nucleation, as acknowledged by Becker and Döring³¹ in 1935. Interestingly, Farkas wrote in Ref. 29 that his work was in turn inspired by an idea of Leo Szilard, who apparently never bothered to write anything on the topic.
- ³¹R. Becker and W. Döring, *Ann. Phys.* **416**, 719 (1935).
- ³²J. B. Zeldovich, *Acta Physicochim. URSS* **18**, 1 (1943).
- ³³J. W. Gibbs, *The Collected Works of J. Willard Gibbs* (New York Longmans, Green and Co., 1928).
- ³⁴(), in several cases, including for instance the aggregation of amyloid fibrils⁴⁷¹, nucleation effectively happens in two dimensions.
- ³⁵(), a number of additional assumptions have to be made in order to write down the steady-state nucleation rate. See e.g. Ref. 472.
- ³⁶V. G. Baidakov and A. O. Tipsev, *J. Chem. Phys.* **136**, 074510 (2012).
- ³⁷J. D. Hoffman, *J. Chem. Phys.* **29**, 1192 (1958).
- ³⁸C. V. Thompson and F. Spaepen, *Acta Metall.* **27**, 1855 (1979).
- ³⁹S. Auer and D. Frenkel, *Nature* **409**, 1020 (2001).
- ⁴⁰J. W. P. Schmelzer, *J. Non-Cryst. Sol. Crystallization in Glasses in Liquids (Crystallization 2009)*, **356**, 2901 (2010).
- ⁴¹H. Vehkamäki, A. Määttä, A. Lauri, I. Napari, and M. Kulmala, *Atmos. Chem. Phys.* **7**, 309 (2007).
- ⁴²S. Raoux and M. Wuttig, *Phase change materials: Science and applications* (New York : Springer, 2009).
- ⁴³H. Fredriksson and U. Akerlind, *Solidification and Crystallization Processing in Metals and Alloys* (John Wiley & Sons, Ltd, Chichester, West Sussex ; Hoboken, N.J. : Wiley, 2012).
- ⁴⁴D. Porter, K. Easterling, and M. Sherif, *Phase Transformations in Metals and Alloys* (CRC press, Boca Raton, FL, 2009).
- ⁴⁵D. Kashchiev, *Nucleation: Basic Theory With Applications*, 1st ed. (Butterworth-Heinemann, Oxford; Boston, 2000).
- ⁴⁶P. Wette and H. J. Schöpe, *Phys. Rev. E* **75**, 051405 (2007).
- ⁴⁷S. Angioletti-Uberti, M. Ceriotti, P. D. Lee, and M. W. Finnis, *Phys. Rev. B* **81**, 125416 (2010).
- ⁴⁸R. L. Davidchack, R. Handel, J. Anwar, and A. V. Brukhno, *J. Chem. Theory Comput.* **8**, 2383 (2012).
- ⁴⁹M. N. Joshiak, N. Duff, M. F. Doherty, and B. Peters, *J. Phys. Chem. Letters* **4**, 4267 (2013).
- ⁵⁰R. G. Pereyra, I. Szeifer, and M. A. Carignano, *J. Chem. Phys.* **135**, 034508 (2011).
- ⁵¹E. Sanz, C. Vega, J. R. Espinosa, R. Caballero-Bernal, J. L. F. Abascal, and C. Valeriani, *J. Am. Chem. Soc.* **135**, 15008 (2013).
- ⁵²P. G. Vekilov, *Nanoscale* **2**, 2346 (2010).
- ⁵³J. De Yoreo, *Nat. Mat.* **12**, 284 (2013).
- ⁵⁴W. Pan, A. B. Kolomeisky, and P. G. Vekilov, *J. Chem. Phys.* **122**, 174905 (2005).
- ⁵⁵P. G. Vekilov, *Rev. Chem. Eng.* **27**, 1 (2011).
- ⁵⁶Q. Hu, M. H. Nielsen, C. L. Freeman, L. M. Hamm, J. Tao, J. R. I. Lee, T. Y. J. Han, U. Becker, J. H. Harding, P. M. Dove, and J. J. D. Yoreo, *Farad. Discuss.* **159**, 509 (2013).
- ⁵⁷(), to be clear, it is perfectly legitimate to measure the contact angle of a water droplet of several mm on a macroscopically planar surface. In contrast, defining a contact angle for a critical crystalline nucleus containing just a few hundred molecules on a surface characterized by a roughness of the same extent, is clearly much more difficult, if meaningful at all.
- ⁵⁸F. Cardinaux, T. Gibaud, A. Stradner, and P. Schurtenberger, *Phys. Rev. Lett.* **99**, 118301 (2007).
- ⁵⁹(), cNT is still expected to capture nucleation on very short timescales at strong supercooling when the free energy barrier for nucleation, albeit being non-zero, is of the order of $k_B \cdot T$.
- ⁶⁰K. Binder and P. Fratzl, "Spinodal decomposition," in *Phase Transformations In Materials* (Wiley-VCH Verlag GmbH & Co. KGaA, 2005) pp. 409–480.
- ⁶¹L. S. Bartell and D. T. Wu, *J. Chem. Phys.* **127**, 174507 (2007).
- ⁶²F. Trudu, D. Donadio, and M. Parrinello, *Phys. Rev. Lett.* **97**, 105701 (2006).
- ⁶³L. J. Peng, J. R. Morris, and Y. C. Lo, *Phys. Rev. B* **78**, 012201 (2008).
- ⁶⁴(), a complete list of the approximations contained in CNT would deserve a book chapter itself. The reader is referred to

the e.g. Ref. 472.

- ⁶⁵G. K. Schenter, S. M. Kathmann, and B. C. Garrett, *Phys. Rev. Lett.* **82**, 3484 (1999).
- ⁶⁶V. I. Kalikmanov, *J. Chem. Phys.* **124**, 124505 (2006).
- ⁶⁷K. C. Russell, *Acta Metall.* **16**, 761 (1968).
- ⁶⁸B. Peters, *J. Chem. Phys.* **135**, 044107 (2011).
- ⁶⁹P. F. Wei, K. F. Kelton, and R. Falster, *J. App. Phys.* **88**, 5062 (2000).
- ⁷⁰K. F. Kelton, *Acta Mater.* **48**, 1967 (2000).
- ⁷¹L. Gránásy, *J. Non-Cryst. Sol.* **162**, 301 (1993).
- ⁷²L. Gránásy and D. M. Herlach, *J. Non-Cryst. Sol. Structure of Non-Crystalline Materials* **6**, **192-193**, 470 (1995).
- ⁷³S. Prestipino, A. Laio, and E. Tosatti, *Phys. Rev. Lett.* **108**, 225701 (2012).
- ⁷⁴G. Kahl and H. Löwen, *J. Phys. Cond. Matt.* **21**, 464101 (2009).
- ⁷⁵H. Löwen, C. N. Likos, L. Assoud, R. Blaak, and S. V. Teeffelen, *Phil. Mag. Lett.* **87**, 847 (2007).
- ⁷⁶T. Neuhaus, A. Härtel, M. Marechal, M. Schmiedeberg, and H. öwen, *The European Physical Journal Special Topics* **223**, 373 (2014).
- ⁷⁷J. F. Lutsko, in *Advances in Chemical Physics*, edited by S. A. Rice (John Wiley & Sons, Inc., 2010) pp. 1-92.
- ⁷⁸R. M. Martin, *Electronic Structure: Basic Theory And Practical Methods (Vol 1)* (Cambridge University Press, 2004).
- ⁷⁹K. Kelton and A. L. Greer, *Nucleation In Condensed Matter: Applications In Materials And Biology* (Elsevier, 2010).
- ⁸⁰(), by *microscopic* we refer to insight into the smallest entities that make up the liquid phase.
- ⁸¹P. N. Pusey and W. van Meegen, *Nature* **320**, 340 (1986).
- ⁸²T. H. Zhang and X. Y. Liu, *Chem. Soc. Rev.* **43**, 2324 (2014).
- ⁸³U. Gasser, E. R. Weeks, A. Schofield, P. N. Pusey, and D. A. Weitz, *Science* **292**, 258 (2001).
- ⁸⁴A. D. Dinsmore, E. R. Weeks, V. Prasad, A. C. Levitt, and D. A. Weitz, *Appl. Opt.* **40**, 4152 (2001).
- ⁸⁵M. Sleutel, J. Lutsko, A. E. S. Van Driessche, M. A. Durán-Olivencia, and D. Maes, *Nat. Comm.* **5** (2014), 10.1038/ncomms6598.
- ⁸⁶E. M. Pouget, P. H. H. Bomans, J. A. C. M. Goos, P. M. Frederik, G. d. With, and N. A. J. M. Sommerdijk, *Science* **323**, 1455 (2009).
- ⁸⁷M. H. Nielsen, S. Aloni, and J. J. D. Yoreo, *Science* **345**, 1158 (2014).
- ⁸⁸S.-Y. Chung, Y.-M. Kim, J.-G. Kim, and Y.-J. Kim, *Nat. Phys.* **5**, 68 (2009).
- ⁸⁹J. Baumgartner, A. Dey, P. H. H. Bomans, C. Le Coadou, P. Fratzl, N. A. J. M. Sommerdijk, and D. Faivre, *Nat. Mat.* **12**, 310 (2013).
- ⁹⁰J. A. Sellberg, C. Huang, T. A. McQueen, N. D. Loh, H. Laksmono, D. Schlesinger, R. G. Sierra, D. Nordlund, C. Y. Hampton, D. Starodub, D. P. DePonte, M. Beye, C. Chen, A. V. Martin, A. Barty, K. T. Wikfeldt, T. M. Weiss, C. Caronna, J. Feldkamp, L. B. Skinner, M. M. Seibert, M. Messerschmidt, G. J. Williams, S. Boutet, L. G. M. Pettersson, M. J. Bogan, and A. Nilsson, *Nature* **510**, 381 (2014).
- ⁹¹H. Laksmono, T. A. McQueen, J. A. Sellberg, N. D. Loh, C. Huang, D. Schlesinger, R. G. Sierra, C. Y. Hampton, D. Nordlund, M. Beye, A. V. Martin, A. Barty, M. M. Seibert, M. Messerschmidt, G. J. Williams, S. Boutet, K. Amann-Winkel, T. Loerting, L. G. M. Pettersson, M. J. Bogan, and A. Nilsson, *J. Phys. Chem. Letters* **6**, 2826 (2015).
- ⁹²J. M. Campbell, F. C. Meldrum, and H. K. Christenson, *J. Phys. Chem. C* **119**, 1164 (2015).
- ⁹³K. Li, S. Xu, W. Shi, M. He, H. Li, S. Li, X. Zhou, J. Wang, and Y. Song, *Langmuir* **28**, 10749 (2012).
- ⁹⁴P. N. Pusey, W. van Meegen, P. Bartlett, B. J. Ackerson, J. G. Rarity, and S. M. Underwood, *Phys. Rev. Lett.* **63**, 2753 (1989).
- ⁹⁵J. Zhu, M. Li, R. Rogers, W. Meyer, R. H. Ottewill, STS-73 Space Shuttle Crew, W. B. Russel, and P. M. Chaikin, *Nature* **387**, 883 (1997).
- ⁹⁶D. Ehre, E. Lavert, M. Lahav, and I. Lubomirsky, *Science* **327**, 672 (2010).
- ⁹⁷M. Ildefonso, E. Revalor, P. Punniyam, J. Salmon, N. Candoni, and S. Veessler, *J. Cryst. Growth* **342**, 9 (2012).
- ⁹⁸S. S. Kadam, S. A. Kulkarni, R. C. Ribera, A. I. Stankiewicz, J. H. ter Horst, and H. J. Kramer, *Chem. Eng. Sci.* **72**, 10 (2012).
- ⁹⁹N. Kubota, *J. of Cryst. Growth* **310**, 629 (2008).
- ¹⁰⁰D. Kashchiev, A. Borissova, R. B. Hammond, and K. J. Roberts, *J. Cryst. Growth* **312**, 698 (2010).
- ¹⁰¹K. Sangwal, *J. Cryst. Growth* **318**, 103 (2011).
- ¹⁰²B. Peters, *J. Cryst. Growth* **317**, 79 (2011).
- ¹⁰³K. Sangwal, *Cryst. Growth Des.* **9**, 942 (2009).
- ¹⁰⁴D. Kashchiev, A. Borissova, R. B. Hammond, and K. J. Roberts, *J. Phys. Chem. B* **114**, 5441 (2010).
- ¹⁰⁵D. Kashchiev, D. Verdoes, and G. Van Rosmalen, *J. Cryst. Growth* **110**, 373 (1991).
- ¹⁰⁶C. Lindenberg and M. Mazzotti, *J. Cryst. Growth* **311**, 1178 (2009).
- ¹⁰⁷C. M. Roelands, R. R. Roestenberg, J. H. ter Horst, H. J. Kramer, and P. J. Jansens, *Cryst. Growth Des.* **4**, 921 (2004).
- ¹⁰⁸C. M. Roelands, J. H. ter Horst, H. J. Kramer, and P. J. Jansens, *Cryst. Growth Des.* **6**, 1380 (2006).
- ¹⁰⁹S. Jiang and J. H. ter Horst, *Cryst. Growth Des.* **11**, 256 (2010).
- ¹¹⁰S. Teychené and B. Biscans, *Cryst. Growth Des.* **8**, 1133 (2008).
- ¹¹¹D. Kashchiev and G. Van Rosmalen, *Cryst. Res. Tech.* **38**, 555 (2003).
- ¹¹²R. J. Davey, S. L. Schroeder, and J. H. ter Horst, *Angew. Chem. Int. Edit.* **52**, 2166 (2013).
- ¹¹³T. Vetter, M. Iggländ, D. R. Ochsenbein, F. S. Hanseler, and M. Mazzotti, *Cryst. Growth Des.* **13**, 4890 (2013).
- ¹¹⁴S. A. Kulkarni, S. S. Kadam, H. Meekes, A. I. Stankiewicz, and J. H. ter Horst, *Cryst. Growth Des.* **13**, 2435 (2013).
- ¹¹⁵N. Kubota, *J. Cryst. Growth* **345**, 27 (2012).
- ¹¹⁶C. A. Stan, G. F. Schneider, S. S. Shevkoplyas, M. Hashimoto, M. Ibanescu, B. J. Wiley, and G. M. Whitesides, *Lab on a Chip* **9**, 2293 (2009).
- ¹¹⁷G. Bogoeva-Gaceva, A. Janevski, and E. Mader, *Polymer* **42**, 4409 (2001).
- ¹¹⁸S. R. Davies, K. C. Hester, J. W. Lachance, C. A. Koh, and E. Dendy Sloan, *Chem. Eng. Sci.* **64**, 370 (2009).
- ¹¹⁹S. Charoenrein and D. S. Reid, *Thermochim. Acta* **156**, 373 (1989).
- ¹²⁰C. Marcolli, S. Gedamke, T. Peter, and B. Zobrist, *Atmos. Chem. Phys.* **7**, 5081 (2007).
- ¹²¹V. Pinti, C. Marcolli, B. Zobrist, C. R. Hoyle, and T. Peter, *Atmos. Chem. Phys.* **12**, 5859 (2012).
- ¹²²D. H. Rasmussen and C. R. Loper Jr., *Acta Metall.* **24**, 117 (1976).
- ¹²³E. Ochshorn and W. Cantrell, *J. Chem. Phys.* **124**, 054714 (2006).
- ¹²⁴A. Manka, H. Pathak, S. Tanimura, J. Wölk, R. Strey, and B. E. Wyslouzil, *Phys. Chem. Chem. Phys.* **14**, 4505 (2012).
- ¹²⁵A. Bhabhe, H. Pathak, and B. E. Wyslouzil, *J. Phys. Chem. A* **117**, 5472 (2013).
- ¹²⁶X. Yang, J. Lu, X.-J. Wang, and C.-B. Ching, *J. Cryst. Growth* **310**, 604 (2008).
- ¹²⁷M. Fujiwara, P. S. Chow, D. L. Ma, and R. D. Braatz, *Crys. Gro. Des.* **2**, 363 (2002).
- ¹²⁸D. Gebauer, A. Völkel, and H. Cölfen, *Science* **322**, 1819 (2008).
- ¹²⁹D. C. Rogers, P. J. DeMott, S. M. Kreidenweis, and Y. Chen, *J. Atm. Oceanic Tech.* **18**, 725 (2001).
- ¹³⁰P. J. DeMott, K. Sassen, M. R. Poellot, D. Baumgardner, D. C. Rogers, S. D. Brooks, A. J. Prenni, and S. M. Kreidenweis, *Geophys. Res. Lett.* **30**, 1732 (2003).
- ¹³¹Y. Tobo, P. J. DeMott, M. Raddatz, D. Niedermeier, S. Hartmann, S. M. Kreidenweis, F. Stratmann, and H. Wex, *Geophys. Res. Lett.* **39**, L19803 (2012).
- ¹³²H. Lihavainen, Y. Viisanen, and M. Kulmala, *J. Chem. Phys.* **114**, 10031 (2001).

- ¹³³P. Konstantinov, T. Agopian, and I. Tchokova, *Bulg. J. Meteor. Hydro.*, **13** (2000).
- ¹³⁴W. G. Finnegan and S. K. Chai, *J. Atm. Sci.* **60**, 1723 (2003).
- ¹³⁵N. Hiranuma, O. Möhler, K. Yamashita, T. Tajiri, A. Saito, A. Kiselev, N. Hoffmann, C. Hoose, E. Jantsch, T. Koop, and M. Murakami, *Nat. Geosci.* **8**, 273 (2015).
- ¹³⁶D. L. Gard, *Devel. Bio.* **143**, 346 (1991).
- ¹³⁷K. Harano, T. Homma, Y. Niimi, M. Koshino, K. Suenaga, L. Leibler, and E. Nakamura, *Nat. Mat.* **11**, 877 (2012).
- ¹³⁸E. Nakamura, *Angew. Chem. Int. Edit.* **52**, 236 (2013).
- ¹³⁹O. Regev, *Langmuir* **12**, 4940 (1996).
- ¹⁴⁰S. Bauerecker, P. Ulbig, V. Buch, L. Vrbka, and P. Jungwirth, *J. Phys. Chem. C* **112**, 7631 (2008).
- ¹⁴¹Z. K. Nagy, M. Fujiwara, X. Y. Woo, and R. D. Braatz, *Ind. Eng. Chem. Res.* **47**, 1245 (2008).
- ¹⁴²H. Bluhm, D. F. Ogletree, C. S. Fadley, Z. Hussain, and M. Salmeron, *J. Phys. Cond. Matt.* **14**, L227 (2002).
- ¹⁴³G. Ketteler, S. Yamamoto, H. Bluhm, K. Andersson, D. E. Starr, D. F. Ogletree, H. Ogasawara, A. Nilsson, and M. Salmeron, *J. Phys. Chem. C* **111**, 8278 (2007).
- ¹⁴⁴F. Barrere, M. M. E. Snel, C. A. van Blitterswijk, K. de Groot, and P. Layrolle, *Biomat.* **25**, 2901 (2004).
- ¹⁴⁵F. Zimmermann, S. Weinbruch, L. Schütz, H. Hofmann, M. Ebert, K. Kandler, and A. Worringer, *J. Geophys. Res.* **113**, D23204 (2008).
- ¹⁴⁶S. Auer and D. Frenkel, *J. Chem. Phys.* **120**, 3015 (2004).
- ¹⁴⁷T. Schilling, S. Dorosz, H. J. Schöpe, and G. Opletal, *J. Phys. Condens. Matt.* **23**, 194120 (2011).
- ¹⁴⁸S. Punnathanam and P. A. Monson, *J. Chem. Phys.* **125**, 024508 (2006).
- ¹⁴⁹(), for instance, in the case of sodium acetate crystal nucleation it is used to craft hand warmers⁴⁷³.
- ¹⁵⁰Z. Zhang, M. R. Walsh, and G.-J. Guo, *Phys. Chem. Chem. Phys.* (2015), 10.1039/C5CP00098J.
- ¹⁵¹A. Pérez and A. Rubio, *J. Chem. Phys.* **135**, 244505 (2011).
- ¹⁵²J. Wedekind, D. Reguera, and R. Strey, *J. Chem. Phys.* **125**, 214505 (2006).
- ¹⁵³G. Bussi, D. Donadio, and M. Parrinello, *J. Chem. Phys.* **126**, 014101 (2007).
- ¹⁵⁴D. W. Oxtoby, *Phil. Trans. R. Soc. A* **361**, 419 (2003).
- ¹⁵⁵P. Nielaba, M. Mareschal, and G. Ciccotti, *Bridging Time Scales: Molecular Simulations For The Next Decade* (Springer, Berlin; New York, 2002).
- ¹⁵⁶C. Abrams and G. Bussi, *Entropy* **16**, 163 (2013).
- ¹⁵⁷K. Yasuoka and M. Matsumoto, *J. Chem. Phys.* **109**, 8451 (1998).
- ¹⁵⁸V. P. Skripov, *Metastable Liquids [By] V.P. Skripov. Translated From Russian By R. Kondor. Translation Edited By D. Shultzkin.* (Wiley, New York, 1974).
- ¹⁵⁹J. H. t. Horst and D. Kashchiev, *J. Chem. Phys.* **119**, 2241 (2003).
- ¹⁶⁰P. Yi, C. R. Locker, and G. C. Rutledge, *Macromol.* **46**, 4723 (2013).
- ¹⁶¹J. Wedekind, R. Strey, and D. Reguera, *J. Chem. Phys.* **126**, 134103 (2007).
- ¹⁶²T. S. Van Erp, in *Kinetics And Thermodynamics Of Multistep Nucleation And Self-Assembly In Nanoscale Materials*, edited by G. Ncolis (John Wiley & Sons, Inc., 2012) pp. 27–60.
- ¹⁶³C. Dellago and P. G. Bolhuis, in *Advanced Computer Simulation Approaches For Soft Matter Sciences III*, Advances in Polymer Science, edited by P. C. Holm and P. K. Kremer (Springer Berlin Heidelberg, 2009) pp. 167–233.
- ¹⁶⁴T. Schlick, *F1000 Bio. Rep.* **1** (2009), 10.3410/B1-51.
- ¹⁶⁵G. M. Torrie and J. P. Valleau, *Chem. Phys. Lett.* **28**, 578 (1974).
- ¹⁶⁶G. M. Torrie and J. P. Valleau, *J. Comp. Phys.* **23**, 187 (1977).
- ¹⁶⁷S. Kumar, J. M. Rosenberg, D. Bouzida, R. H. Swendsen, and P. A. Kollman, *J. Comp. Chem.* **13**, 1011 (1992).
- ¹⁶⁸A. Laio and M. Parrinello, *Proc. Natl. Acad. Sci. U.S.A.* **99**, 12562 (2002).
- ¹⁶⁹A. Laio and F. L. Gervasio, *Rep. Prog. Phys.* **71**, 126601 (2008).
- ¹⁷⁰A. Barducci, G. Bussi, and M. Parrinello, *Phys. Rev. Lett.* **100**, 020603 (2008).
- ¹⁷¹H. Eyring, *J. Chem. Phys.* **3**, 107 (1935).
- ¹⁷²E. Wigner, *Trans. Faraday Soc.* **34**, 29 (1938).
- ¹⁷³J. B. Anderson, *J. Chem. Phys.* **58**, 4684 (1973).
- ¹⁷⁴P. Hnggi, P. Talkner, and M. Borkovec, *Rev. Mod. Phys.* **62**, 251 (1990).
- ¹⁷⁵D. Chandler, *J. Chem. Phys.* **68**, 2959 (1978).
- ¹⁷⁶CHARLES H. BENNETT, in *Algorithms Chem. Comp.*, ACS Symposium Series, Vol. 46 (AMERICAN CHEMICAL SOCIETY, 1977) pp. 63–97.
- ¹⁷⁷T. S. v. Erp, D. Moroni, and P. G. Bolhuis, *J. Chem. Phys.* **118**, 7762 (2003).
- ¹⁷⁸D. Moroni, T. S. van Erp, and P. G. Bolhuis, *Physica A News and Expectations in Thermostatistics*, **340**, 395 (2004).
- ¹⁷⁹J. Juraszek, G. Saladino, T. S. van Erp, and F. L. Gervasio, *Phys. Rev. Lett.* **110**, 108106 (2013).
- ¹⁸⁰R. J. Allen, D. Frenkel, and P. R. t. Wolde, *J. Chem. Phys.* **124**, 024102 (2006).
- ¹⁸¹R. J. Allen, C. Valeriani, and P. Rein ten Wolde, *J. Phys. Cond. Matt.* **21**, 463102 (2009).
- ¹⁸²C. Dellago, P. G. Bolhuis, and D. Chandler, *J. Chem. Phys.* **108**, 9236 (1998).
- ¹⁸³P. G. Bolhuis, C. Dellago, and D. Chandler, *Faraday Disc.* **110**, 421 (1998).
- ¹⁸⁴P. L. Geissler, C. Dellago, and D. Chandler, *J. Phys. Chem. B* **103**, 3706 (1999).
- ¹⁸⁵J. G. Kirkwood, *J. Chem. Phys.* **3**, 300 (1935).
- ¹⁸⁶A. Gavezzotti, G. Filippini, J. Kroon, B. P. van Eijck, and P. Klewinghaus, *Chem. Eur. J.* **3**, 893 (1997).
- ¹⁸⁷A. Gavezzotti, *Chem. Eur. J.* **5**, 567 (1999).
- ¹⁸⁸A. Kawska, J. Brickmann, R. Knip, O. Hochrein, and D. Zahn, *J. Chem. Phys.* **124**, 024513 (2006).
- ¹⁸⁹A. Kawska, P. Duchstein, O. Hochrein, and D. Zahn, *Nano Lett.* **8**, 2336 (2008).
- ¹⁹⁰A. Cacciuto, S. Auer, and D. Frenkel, *Nature* **428**, 404 (2004).
- ¹⁹¹A. R. Browning, M. F. Doherty, and G. H. Fredrickson, *Phys. Rev. E* **77**, 041604 (2008).
- ¹⁹²J. Kalikka, J. Akola, J. Larrucea, and R. O. Jones, *Phys. Rev. B* **86**, 144113 (2012).
- ¹⁹³B. C. Knott, V. Molinero, M. F. Doherty, and B. Peters, *J. Am. Chem. Soc.* **134**, 19544 (2012).
- ¹⁹⁴W. G. Hoover and F. H. Ree, *J. Chem. Phys.* **49**, 3609 (1968).
- ¹⁹⁵L. Antl, J. W. Goodwin, R. D. Hill, R. H. Ottewill, S. M. Owens, S. Papworth, and J. A. Waters, *Coll. Surf.* **17**, 67 (1986).
- ¹⁹⁶S.-E. Phan, W. B. Russel, Z. Cheng, J. Zhu, P. M. Chaikin, J. H. Dunsmaier, and R. H. Ottewill, *Phys. Rev. E* **54**, 6633 (1996).
- ¹⁹⁷T. Palberg, *Curr. Opin. Coll. Int. Sci.* **2**, 607 (1997).
- ¹⁹⁸T. Palberg, *J. Phys. Condens. Matt.* **11**, R323 (1999).
- ¹⁹⁹V. J. Anderson and H. N. W. Lekkerkerker, *Nature* **416**, 811 (2002).
- ²⁰⁰R. P. Sear, *J. Phys. Condens. Matt.* **19**, 033101 (2007).
- ²⁰¹U. Gasser, *J. Phys. Condens. Matt.* **21**, 203101 (2009).
- ²⁰²T. Palberg, *J. Phys. Condens. Matt.* **26**, 333101 (2014).
- ²⁰³B. S. John, A. Stroock, and F. A. Escobedo, *J. Chem. Phys.* **120**, 9383 (2004).
- ²⁰⁴A. Haji-Akbari, M. Engel, A. S. Keys, X. Zheng, R. G. Petschek, P. Palfy-Muhoray, and S. C. Glotzer, *Nature* **462**, 773 (2009).
- ²⁰⁵P. F. Damasceno, M. Engel, and S. C. Glotzer, *Science* **337**, 453 (2012).
- ²⁰⁶U. Agarwal and F. A. Escobedo, *Nat. Mater.* **10**, 230 (2011).
- ²⁰⁷R. Ni and M. Dijkstra, *J. Chem. Phys.* **134**, 034501 (2011).
- ²⁰⁸V. Thapar and F. A. Escobedo, *Phys. Rev. Lett.* **112**, 048301 (2014).
- ²⁰⁹S. Auer and D. Frenkel, *J. Phys. Cond. Matt.* **14**, 7667 (2002).
- ²¹⁰P. Wette, H. J. Schöpe, and T. Palberg, *J. Chem. Phys.* **122**, 144901 (2005).

- ²¹¹S. Punnathanam and P. Monson, J. Chem. Phys. **125**, 024508 (2006).
- ²¹²P. Wette and H. J. Schöpe, Phys. Rev. E **75**, 051405 (2007).
- ²¹³S. R. Williams, C. P. Royall, and G. Bryant, Phys. Rev. Lett. **100**, 225502 (2008).
- ²¹⁴B. Peters, J. Chem. Phys. **131**, 244103 (2009).
- ²¹⁵K. Schätzel and B. J. Ackerson, Phys. Rev. E **48**, 3766 (1993).
- ²¹⁶H. J. Schöpe, G. Bryant, and W. van Meegen, Phys. Rev. Lett. **96**, 175701 (2006).
- ²¹⁷H. J. Schöpe, G. Bryant, and W. v. Meegen, J. Chem. Phys. **127**, 084505 (2007).
- ²¹⁸J. L. Harland, S. I. Henderson, S. M. Underwood, and W. van Meegen, Phys. Rev. Lett. **75**, 3572 (1995).
- ²¹⁹Z. Cheng, J. Zhu, W. B. Russel, W. V. Meyer, and P. M. Chaikin, Appl. Opt. **40**, 4146 (2001).
- ²²⁰P. S. Francis, S. Martin, G. Bryant, W. v. Meegen, and P. A. Wilksch, Rev. Sci. Instr. **73**, 3878 (2002).
- ²²¹T. Schilling, H. J. Schöpe, M. Oettel, G. Opletal, and I. Snook, Phys. Rev. Lett. **105**, 025701 (2010).
- ²²²L. Filion, M. Hermes, R. Ni, and M. Dijkstra, J. Chem. Phys. **133**, 244115 (2010).
- ²²³L. Filion, R. Ni, D. Frenkel, and M. Dijkstra, J. Chem. Phys. **134**, 134901 (2011).
- ²²⁴T. Kawasaki and H. Tanaka, Proc. Natl. Acad. Sci. U.S.A. **107**, 14036 (2010).
- ²²⁵(), brownian dynamics⁴⁷⁴ differs from molecular dynamics mainly with respect to the dynamics of the system at short times. This difference is thus not expected to play a role in the estimate of nucleation rates, which depend chiefly on the long-time dynamics of the system.
- ²²⁶A. Shirayev and J. D. Gunton, J. Chem. Phys. **120**, 8318 (2004).
- ²²⁷D. F. Rosenbaum and C. F. Zukoski, J. Cryst. Growth **169**, 752 (1996).
- ²²⁸R. Piazza, Curr. Opin. Coll. Int. Sci. **5**, 38 (2000).
- ²²⁹A. Lomakin, N. Asherie, and G. B. Benedek, Proc. Natl. Acad. Sci. U.S.A. **100**, 10254 (2003).
- ²³⁰Y. Liu, X. Wang, and C. B. Ching, Crys. Gro. Des. **10**, 548 (2010).
- ²³¹H. Liu, S. K. Kumar, and J. F. Douglas, Phys. Rev. Lett. **103**, 018101 (2009).
- ²³²A. George and W. W. Wilson, Acta Cryst. D **50**, 361 (1994).
- ²³³J. P. K. Doye, A. A. Louis, I.-C. Lin, L. R. Allen, E. G. Noya, A. W. Wilber, H. C. Kok, and R. Lyus, Phys. Chem. Chem. Phys. **9**, 2197 (2007).
- ²³⁴N. M. Dixit and C. F. Zukoski, J. Coll. Int. Sci. **228**, 359 (2000).
- ²³⁵N. M. Dixit, A. M. Kulkarni, and C. F. Zukoski, Coll. Surf. A **190**, 47 (2001).
- ²³⁶J. Chang, A. M. Lenhoff, and S. I. Sandler, J. Chem. Phys. **120**, 3003 (2004).
- ²³⁷J. E. Jones, Proc. Roy. Soc. Lond. A **106**, 463 (1924).
- ²³⁸V. G. Baidakov, A. O. Tipsev, K. S. Bobrov, and G. V. Ionov, J. Chem. Phys. **132**, 234505 (2010).
- ²³⁹M. A. v. d. Hoef, J. Chem. Phys. **113**, 8142 (2000).
- ²⁴⁰F. W. de Wette, R. E. Allen, D. S. Hughes, and A. Rahman, Phys. Lett. A **29**, 548 (1969).
- ²⁴¹S. A. Khrapak and G. E. Morfill, J. Chem. Phys. **134**, 094108 (2011).
- ²⁴²S.-N. Luo, A. Strachan, and D. C. Swift, J. Chem. Phys. **120**, 11640 (2004).
- ²⁴³J. R. Morris and X. Song, J. Chem. Phys. **119**, 3920 (2003).
- ²⁴⁴R. L. Davidchack and B. B. Laird, J. Chem. Phys. **118**, 7651 (2003).
- ²⁴⁵J. Q. Broughton and G. H. Gilmer, J. Chem. Phys. **84**, 5759 (1986).
- ²⁴⁶P. G. Bolhuis, D. Frenkel, S.-C. Mau, and D. A. Huse, Nature **388**, 235 (1997).
- ²⁴⁷C. Desgranges and J. Delhommelle, Phys. Rev. Lett. **98**, 235502 (2007).
- ²⁴⁸A. Rahman, Phys. Rev. **136**, A405 (1964).
- ²⁴⁹L. Verlet, Phys. Rev. **159**, 98 (1967).
- ²⁵⁰D. J. McGinty, J. Chem. Phys. **58**, 4733 (1973).
- ²⁵¹M. J. Mandell, J. P. McTague, and A. Rahman, J. Chem. Phys. **64**, 3699 (1976).
- ²⁵²P. R. t. Wolde, M. J. Ruiz-Montero, and D. Frenkel, J. Chem. Phys. **104**, 9932 (1996).
- ²⁵³P. R. t. Wolde, M. J. Ruiz-Montero, and D. Frenkel, J. Chem. Phys. **110**, 1591 (1999).
- ²⁵⁴W. Lechner and C. Dellago, J. Chem. Phys. **129**, 114707 (2008).
- ²⁵⁵V. I. Kalikmanov, J. Wölk, and T. Kraska, J. Chem. Phys. **128**, 124506 (2008).
- ²⁵⁶X.-M. Bai and M. Li, J. Chem. Phys. **122**, 224510 (2005).
- ²⁵⁷X.-M. Bai and M. Li, J. Chem. Phys. **124**, 124707 (2006).
- ²⁵⁸H. Wang, H. Gould, and W. Klein, Phys. Rev. E **76**, 031604 (2007).
- ²⁵⁹D. Moroni, P. R. ten Wolde, and P. G. Bolhuis, Phys. Rev. Lett. **94**, 235703 (2005).
- ²⁶⁰H. Huitema, J. van der Eerden, J. Janssen, and H. Human, Phys. Rev. B **62**, 14690 (2000).
- ²⁶¹L. J. Peng, J. R. Morris, and R. S. Aga, J. Chem. Phys. **133**, 084505 (2010).
- ²⁶²W. Klein and F. Leyvraz, Phys. Rev. Lett. **57**, 2845 (1986).
- ²⁶³P. ten Wolde, M. Ruiz-Montero, and D. Frenkel, Phys. Rev. Lett. **75**, 2714 (1995).
- ²⁶⁴P. R. t. Wolde and D. Frenkel, Phys. Chem. Chem. Phys. **1**, 2191 (1999).
- ²⁶⁵C. Desgranges and J. Delhommelle, J. Am. Chem. Soc. **128**, 10368 (2006).
- ²⁶⁶X. Wang, J. Mi, and C. Zhong, J. Chem. Phys. **138**, 164704 (2013).
- ²⁶⁷(), as early as 1897, Ostwald asserted⁴⁷⁵ that the critical cluster nucleating from a supercooled liquid is not necessarily the thermodynamically most stable crystalline polymorph. In fact, it could very well be the polymorph closest in energy to the liquid phase. A nice review of the *Ostwald rule* can be found in e.g. Ref. 264.
- ²⁶⁸J. Delhommelle, Molecular Simulation **37**, 613 (2011).
- ²⁶⁹(), in this case the equilibrium crystalline phase that forms upon homogeneous nucleation is a RHCP made of stacked of hexagonal layers.
- ²⁷⁰D. Turnbull and B. Vonnegut, Ind. Eng. Chem. **44**, 1292 (1952).
- ²⁷¹J. P. Mithen and R. P. Sear, J. Chem. Phys. **140**, 084504 (2014).
- ²⁷²S. Jungblut and C. Dellago, Europhys. Lett. **96**, 56006 (2011).
- ²⁷³A. J. Page and R. P. Sear, J. Am. Chem. Soc. **131**, 17550 (2009).
- ²⁷⁴H. Zhang, S. Peng, X. Long, X. Zhou, J. Liang, C. Wan, J. Zheng, and X. Ju, Phys. Rev. E **89**, 032412 (2014).
- ²⁷⁵J. D. Honeycutt and H. C. Andersen, J. Phys. Chem. **90**, 1585 (1986).
- ²⁷⁶W. Swope and H. Andersen, Phys. Rev. B **41**, 7042 (1990).
- ²⁷⁷(), we are referring to the average population of critical nuclei at a given temperature and pressure. In other words, the number of critical nuclei expected per unit volume, which should not be confused with the density of the crystalline phase within the nuclei.
- ²⁷⁸A. P. Sutton and J. Chen, Phil. Mag. Lett. **61**, 139 (1990), <http://dx.doi.org/10.1080/09500839008206493>.
- ²⁷⁹F. Fumi and M. Tosi, J. Phys. Chem. Sol. **25**, 31 (1964).
- ²⁸⁰F. H. Stillinger and T. A. Weber, Phys. Rev. B **31**, 5262 (1985).
- ²⁸¹J. Tersoff, Phys. Rev. B **37**, 6991 (1988).
- ²⁸²J. Tersoff, Phys. Rev. B **39**, 5566 (1989).
- ²⁸³D. W. Brenner, O. A. Shenderova, J. A. Harrison, S. J. Stuart, B. Ni, and S. B. Sinnott, J. Phys. Cond. Matt. **14**, 783 (2002).
- ²⁸⁴G. J. Ackland and R. Thetford, Phil. Mag. A **56**, 15 (1987), <http://dx.doi.org/10.1080/01418618708204464>.
- ²⁸⁵M. S. Daw, S. M. Foiles, and M. I. Baskes, Mat. Sci. Rep. **9**, 251 (1993).
- ²⁸⁶F. Ercolessi and J. B. Adams, Europhys. Lett. **26**, 583 (1994).
- ²⁸⁷F. Ercolessi, E. Tosatti, and M. Parrinello, Phys. Rev. Lett. **57**, 719 (1986).

- ²⁸⁸Z. Hou, Z. Tian, R. Liu, K. Dong, and A. Yu, *Comp. Mat. Sci.* **99**, 256 (2015).
- ²⁸⁹Y. Shibuta, K. Oguchi, T. Takaki, and M. Ohno, *Sci. Rep.* **5**, 13534 (2015).
- ²⁹⁰Y. Shibuta, K. Oguchi, and M. Ohno, *Scripta Mater.* **86**, 20 (2014).
- ²⁹¹A. Aguado and M. F. Jarrold, *Ann. Rev. Phys. Chem.* **62**, 151 (2011).
- ²⁹²Y. Shibuta, *J. Therm. Sci. Tech.* **7**, 45 (2012).
- ²⁹³A. V. Yakubovich, G. Sushko, S. Schramm, and A. V. Solov'yov, *Phys. Rev. B* **88**, 035438 (2013).
- ²⁹⁴T. Milek and D. Zahn, *Nano Lett.* **14**, 4913 (2014).
- ²⁹⁵H. Pan and W. Shou, *J. Phys. D* **48**, 225302 (2015).
- ²⁹⁶Y. Lü and M. Chen, *Acta Mater.* **60**, 4636 (2012).
- ²⁹⁷T. Li, D. Donadio, L. M. Ghiringhelli, and G. Galli, *Nat. Mat.* **8**, 726 (2009).
- ²⁹⁸V. Molinero and E. B. Moore, *The Journal of Physical Chemistry B* **113**, 4008 (2008).
- ²⁹⁹A. Haji-Akbari, R. S. DeFever, S. Sarupria, and P. G. Debenedetti, *Phys. Chem. Chem. Phys.* **16**, 25916 (2014).
- ³⁰⁰M. M. Gianetti, A. Haji-Akbari, M. Paula Longinotti, and P. G. Debenedetti, *Phys. Chem. Chem. Phys.* **18**, 4102 (2016).
- ³⁰¹T. Li, D. Donadio, and G. Galli, *Nat. Commun.* **4**, 1887 (2013).
- ³⁰²T. Li, D. Donadio, and G. Galli, *J. Chem. Phys.* **131**, 224519 (2009).
- ³⁰³C. Valeriani, E. Sanz, and D. Frenkel, *J. Chem. Phys.* **122**, 194501 (2005).
- ³⁰⁴S. Raoux, W. W. , and D. Ielmini, *Chem. Rev.* **110**, 240 (2010).
- ³⁰⁵D. Lencer, M. Salinga, and M. Wuttig, *Adv. Mater.* **23**, 2030 (2011).
- ³⁰⁶M. Wuttig and N. Yamada, *Nat. Mat.* **6**, 824 (2007).
- ³⁰⁷J. Orava, A. L. Greer, B. Gholipour, D. W. Hewak, and C. E. Smith, *Nat. Mat.* **11**, 279 (2012).
- ³⁰⁸P. Zalden, A. von Hoegen, P. Landreman, M. Wuttig, and A. M. Lindenberg, *Chem. Mat.* **27**, 5641 (2015).
- ³⁰⁹J. Hegedüs and S. R. Elliott, *Nat. Mat.* **7**, 399 (2008).
- ³¹⁰T. H. Lee and S. R. Elliott, *Phys. Rev. Lett.* **107**, 145702 (2011).
- ³¹¹G. C. Sossio, G. Miceli, S. Caravati, J. Behler, and M. Bernasconi, *Phys. Rev. B* **85**, 174103 (2012).
- ³¹²J. Behler and M. Parrinello, *Phys. Rev. Lett.* **98**, 146401 (2007).
- ³¹³G. C. Sossio, G. Miceli, S. Caravati, F. Giberti, J. Behler, and M. Bernasconi, *J. Phys. Chem. Letters* **4**, 4241 (2013).
- ³¹⁴G. C. Sossio, M. Salvalaglio, J. Behler, M. Bernasconi, and M. Parrinello, *J. Phys. Chem. C* (2015), 10.1021/acs.jpcc.5b00296.
- ³¹⁵P. G. Debenedetti and F. H. Stillinger, *Nature* **410**, 259 (2001).
- ³¹⁶G. C. Sossio, J. Behler, and M. Bernasconi, *Phys. Stat. Sol. B* **249**, 1880 (2012).
- ³¹⁷M. G. Potapczuk, *J. Aerospace Eng.* **26**, 260 (2013).
- ³¹⁸Z. Ye, J. Wu, N. E. Ferradi, and X. Shi, *Canadian J. Civil Eng.* **40**, 11 (2013).
- ³¹⁹K. Padayachee, M. Watt, N. Edwards, and D. Mycock, *South. Forests: J. Forest. Sci.* **71**, 165 (2009).
- ³²⁰M. Baker, *Science* **276**, 1072 (1997).
- ³²¹K. Carslaw, R. Harrison, and J. Kirkby, *Science* **298**, 1732 (2002).
- ³²²T. Li, D. Donadio, G. Russo, and G. Galli, *Phys. Chem. Chem. Phys.* **13**, 19807 (2011).
- ³²³E. B. Moore and V. Molinero, *Nature* **479**, 506 (2011).
- ³²⁴A. Reinhardt and J. P. K. Doye, *J. Chem. Phys.* **136**, 054501 (2012).
- ³²⁵J. Russo, F. Romano, and H. Tanaka, *Nat. Mater.* **13**, 733 (2014).
- ³²⁶J. R. Espinosa, E. Sanz, C. Valeriani, and C. Vega, *J. Chem. Phys.* **141**, 18C529 (2014).
- ³²⁷A. Haji-Akbari and P. G. Debenedetti, *Proc. Natl. Acad. Sci. U.S.A.* , 201509267 (2015).
- ³²⁸D. E. Hagen, R. J. Anderson, and J. L. Kassner Jr, *J. Atmosph. Sci.* **38**, 1236 (1981).
- ³²⁹P. Taborek, *Phys. Rev. B* **32**, 5902 (1985).
- ³³⁰P. J. DeMott and D. C. Rogers, *J. Atm. Sci.* **47**, 1056 (1990).
- ³³¹H. Pruppacher, *J. Atm. Sci.* **52**, 1924 (1995).
- ³³²B. Krämer, O. Hübner, H. Vortisch, L. Wöste, T. Leisner, M. Schwell, E. Rühl, and H. Baumgärtel, *J. Chem. Phys.* **111**, 6521 (1999).
- ³³³L. S. Bartell and Y. G. Chushak, in *Water in Confining Geometries* (Springer, 2003) pp. 399–424.
- ³³⁴P. Stöckel, I. M. Weidinger, H. Baumgärtel, and T. Leisner, *J. Phys. Chem. A* **109**, 2540 (2005).
- ³³⁵C. A. Stan, G. F. Schneider, S. S. Shevkoplyas, M. Hashimoto, M. Ibanescu, B. J. Wiley, and G. M. Whitesides, *Lab on a Chip* **9**, 2293 (2009).
- ³³⁶E. B. Moore and V. Molinero, *J. Chem. Phys.* **132**, 244504 (2010).
- ³³⁷M. Avrami, *J. Chem. Phys.* **7**, 1103 (1939).
- ³³⁸M. Avrami, *J. Chem. Phys.* **8**, 212 (1940).
- ³³⁹W. Hage, A. Hallbrucker, E. Mayer, and G. P. Johari, *J. Chem. Phys.* **100**, 2743 (1994).
- ³⁴⁰W. Hage, A. Hallbrucker, E. Mayer, and G. P. Johari, *J. Chem. Phys.* **103**, 545 (1995).
- ³⁴¹L. Filion, M. Hermes, R. Ni, and M. Dijkstra, *J. Chem. Phys.* **133**, 244115 (2010).
- ³⁴²L. Gránásy, T. Pusztai, and P. F. James, *J. Chem. Phys.* **117**, 6157 (2002).
- ³⁴³T. L. Malkin, B. J. Murray, A. V. Brukhno, J. Anwar, and C. G. Salzmann, *Proc. Natl. Acad. Sci. U.S.A.* **109**, 1041 (2012).
- ³⁴⁴C. Angell, J. Shuppert, and J. Tucker, *J. Phys. Chem.* **77**, 3092 (1973).
- ³⁴⁵N. J. English and S. T. John, *Phys. Rev. E* **92**, 032132 (2015).
- ³⁴⁶M. Matsumoto, S. Saito, and I. Ohmine, *Nature* **416**, 409 (2002).
- ³⁴⁷L. Vrbka and P. Jungwirth, *J. Phys. Chem. B* **110**, 18126 (2006).
- ³⁴⁸E. B. Moore and V. Molinero, *Phys. Chem. Chem. Phys.* **13**, 20008 (2011).
- ³⁴⁹J. L. F. Abascal, E. Sanz, R. G. Fernández, and C. Vega, *J. Chem. Phys.* **122**, 234511 (2005).
- ³⁵⁰J. C. Palmer, F. Martelli, Y. Liu, R. Car, A. Z. Panagiotopoulos, and P. G. Debenedetti, *Nature* **510**, 385 (2014).
- ³⁵¹D. Chandler, *arXiv preprint arXiv:1407.6854* (2014).
- ³⁵²J. C. Palmer, P. G. Debenedetti, R. Car, and A. Z. Panagiotopoulos, *arXiv preprint arXiv:1407.7884* (2014).
- ³⁵³E. Sanz, C. Vega, J. R. Espinosa, R. Caballero-Bernal, J. L. F. Abascal, and C. Valeriani, *J. Am. Chem. Soc.* **135**, 15008 (2013), <http://dx.doi.org/10.1021/ja4028814>.
- ³⁵⁴R. J. Herbert, B. J. Murray, S. J. Dobbie, and T. Koop, *Geophys. Res. Lett.* **42**, 1599 (2015).
- ³⁵⁵J. Carrasco, A. Hodgson, and A. Michaelides, *Nature Mater.* **11**, 667 (2012).
- ³⁵⁶B. J. Murray, D. O'Sullivan, J. D. Atkinson, and M. E. Webb, *Chem. Soc. Rev.* **41**, 6519 (2012).
- ³⁵⁷S. Nie, P. J. Feibelman, N. C. Bartelt, and K. Thürmer, *Phys. Rev. Lett.* **105**, 026102 (2010).
- ³⁵⁸D. R. Nutt and A. J. Stone, *J. Chem. Phys.* **117**, 800 (2002).
- ³⁵⁹D. R. Nutt and A. J. Stone, *Langmuir* **20**, 8715 (2004).
- ³⁶⁰V. Sadtchenko, G. E. Ewing, D. R. Nutt, and A. J. Stone, *Langmuir* **18**, 4632 (2002).
- ³⁶¹X. L. Hu and A. Michaelides, *Surf. Sci.* **601**, 5378 (2007).
- ³⁶²X. L. Hu and A. Michaelides, *Surf. Sci.* **602**, 960 (2008).
- ³⁶³H. R. Pruppacher and J. D. Klett, *Microphysics Of Clouds And Precipitation - Second Revised And Enlarged Edition with an Introduction to Cloud Chemistry and Cloud Electricity* (Kluwer Academic Publishers, Dordrecht, The Netherlands, 1997).
- ³⁶⁴T. Croteau, A. K. Bertram, and G. N. Patey, *J. Phys. Chem. A* **112**, 10708 (2008).
- ³⁶⁵T. Croteau, A. K. Bertram, and G. N. Patey, *J. Phys. Chem. A* **113**, 7826 (2009).
- ³⁶⁶R. T. Cygan, J. J. Liang, and A. G. Kalinichev, *J. Phys. Chem. B* **108**, 1255 (2004).
- ³⁶⁷H. J. C. Berendsen, J. R. Grigera, and T. P. Straatsma, *J. Phys. Chem.* **91**, 6269 (1987).

- ³⁶⁸S. J. Cox, S. M. Kathmann, J. A. Purton, M. J. Gillan, and A. Michaelides, *Phys. Chem. Chem. Phys.* **14**, 7944 (2012).
- ³⁶⁹W. L. Jorgensen, J. Chandrasekhar, J. D. Madura, R. W. Impey, and M. L. Klein, *J. Chem. Phys.* **79**, 926 (1983).
- ³⁷⁰J. Y. Yan and G. N. Patey, *J. Phys. Chem. Lett.* **2**, 2555 (2011).
- ³⁷¹S. J. Cox, Z. Raza, S. M. Kathmann, B. Slater, and A. Michaelides, *Faraday Discuss.* **167**, 389 (2013).
- ³⁷²J. L. F. Abascal and C. Vega, *J. Chem. Phys.* **123**, 234505 (2005).
- ³⁷³S. A. Zielke, A. K. Bertram, and G. N. Patey, *J. Phys. Chem. B* **0**, null (0), pMID: 26524230, <http://dx.doi.org/10.1021/acs.jpcc.5b09052>.
- ³⁷⁴L. Lupi, A. Hudait, and V. Molinero, *J. Am. Chem. Soc.* **136**, 3156 (2014).
- ³⁷⁵L. Lupi and V. Molinero, *J. Phys. Chem. A* **118**, 7330 (2014).
- ³⁷⁶S. J. Cox, S. M. Kathmann, B. Slater, and A. Michaelides, *J. Chem. Phys.* **142**, 184704 (2015), <http://dx.doi.org/10.1063/1.4919714>.
- ³⁷⁷S. J. Cox, S. M. Kathmann, B. Slater, and A. Michaelides, *J. Chem. Phys.* **142**, 184705 (2015).
- ³⁷⁸T. F. Whale, M. Rosillo-Lopez, B. J. Murray, and C. G. Salzmann, *J. Phys. Chem. Letters* **6**, 3012 (2015).
- ³⁷⁹X.-X. Zhang, M. Chen, and M. Fu, *J. Chem. Phys.* **141**, 124709 (2014).
- ³⁸⁰M. Fitzner, G. C. Sosso, S. J. Cox, and A. Michaelides, *J. Am. Chem. Soc.* **137**, 13658 (2015), pMID: 26434775, <http://dx.doi.org/10.1021/jacs.5b08748>.
- ³⁸¹Y. Bi, R. Cabriolu, and T. Li, *J. Phys. Chem. C* **120**, 1507 (2016).
- ³⁸²A. Reinhardt and J. P. K. Doye, *J. Chem. Phys.* **141**, 084501 (2014).
- ³⁸³R. Cabriolu and T. Li, *Phys. Rev. E* **91**, 052402 (2015).
- ³⁸⁴J. E. Aber, S. Arnold, B. A. Garetz, and A. S. Myerson, *Phys. Rev. Lett.* **94**, 145503 (2005).
- ³⁸⁵S. A. Zielke, A. K. Bertram, and G. N. Patey, *J. Phys. Chem. B* **119**, 9049 (2015), pMID: 25255062, <http://dx.doi.org/10.1021/jp508601s>.
- ³⁸⁶G. Fraux and J. P. K. Doye, *J. Chem. Phys.* **141**, 216101 (2014), <http://dx.doi.org/10.1063/1.4902382>.
- ³⁸⁷P. W. Tasker, *J. Phys. C* **12**, 4977 (1979).
- ³⁸⁸B. J. Anderson and J. Hallett, *J. Atmos. Sci.* **33**, 822 (1976).
- ³⁸⁹S. L. Price, *Chem. Soc. Rev.* **43**, 2098 (2014).
- ³⁹⁰J. Bauer, S. Spanton, R. Henry, J. Quick, W. Dziki, W. Porter, and J. Morris, *Pharm. Res.* **18**, 859 (2001).
- ³⁹¹S. Datta and D. J. W. Grant, *Nat. Rev. Drug Disc.* **3**, 42 (2004).
- ³⁹²E. H. Lee, *Asian J. Pharma. Sci.* **9**, 163 (2014).
- ³⁹³R. J. Davey, S. L. M. Schroeder, and J. H. ter Horst, *Angew. Chem. Int. Edit.* **52**, 2166 (2013).
- ³⁹⁴V. Agarwal and B. Peters, in *Advances In Chemical Physics: Volume 155*, edited by S. A. Rice and A. R. Dinner (John Wiley & Sons, Inc., 2014) pp. 97–160.
- ³⁹⁵E. E. Santiso and B. L. Trout, *J. Chem. Phys.* **134**, 064109 (2011).
- ³⁹⁶T.-Q. Yu, P.-Y. Chen, M. Chen, A. Samanta, E. Vanden-Eijnden, and M. Tuckerman, *J. Chem. Phys.* **140**, 214109 (2014).
- ³⁹⁷N. Duff and B. Peters, *J. Chem. Phys.* **135**, 134101 (2011).
- ³⁹⁸B. Peters, *J. Chem. Phys.* **131**, 244103 (2009).
- ³⁹⁹R. Shetty, F. A. Escobedo, D. Choudhary, and P. Clancy, *J. Chem. Phys.* **117**, 4000 (2002).
- ⁴⁰⁰R. Grossier and S. Veessler, *Crys. Gro. Des.* **9**, 1917 (2009).
- ⁴⁰¹(), statistical mechanics tells us that macroscopic thermodynamic variables are well behaved for a system with a number of molecules of the order of N_A , with N_A being Avogadro's number.
- ⁴⁰²N. E. R. Zimmermann, B. Vorselaars, D. Quigley, and B. Peters, *J. Am. Chem. Soc.* **137**, 13352 (2015).
- ⁴⁰³N. Duff and B. Peters, *J. Chem. Phys.* **131**, 184101 (2009).
- ⁴⁰⁴V. Agarwal and B. Peters, *J. Chem. Phys.* **140**, 084111 (2014).
- ⁴⁰⁵D. Reguera, R. K. Bowles, Y. Djikaev, and H. Reiss, *J. Chem. Phys.* **118**, 340 (2003).
- ⁴⁰⁶M. Salvalaglio, C. Perego, F. Giberti, M. Mazzotti, and M. Parrinello, *Proc. Natl. Acad. Sci. U.S.A.* **112**, E6 (2015).
- ⁴⁰⁷A. Agarwal, H. Wang, C. Schütte, and L. D. Site, *J. Chem. Phys.* **141**, 034102 (2014).
- ⁴⁰⁸C. Perego, M. Salvalaglio, and M. Parrinello, *J. Chem. Phys.* **142**, 144113 (2015).
- ⁴⁰⁹S. Piana and J. D. Gale, *J. Am. Chem. Soc.* **127**, 1975 (2005).
- ⁴¹⁰S. Piana, M. Reyhani, and J. D. Gale, *Nature* **438**, 70 (2005).
- ⁴¹¹M. Salvalaglio, T. Vetter, F. Giberti, M. Mazzotti, and M. Parrinello, *J. Am. Chem. Soc.* **134**, 17221 (2012).
- ⁴¹²M. Salvalaglio, T. Vetter, M. Mazzotti, and M. Parrinello, *Angew. Chem. Int. Ed.* **52**, 13369 (2013).
- ⁴¹³M. Salvalaglio, M. Mazzotti, and M. Parrinello, *Faraday Discuss.* **179**, 291 (2015).
- ⁴¹⁴W. D. Cornell, P. Cieplak, C. I. Bayly, I. R. Gould, K. M. Merz, D. M. Ferguson, D. C. Spellmeyer, T. Fox, J. W. Caldwell, and P. A. Kollman, *J. Am. Chem. Soc.* **117**, 5179 (1995).
- ⁴¹⁵J. Wang, R. M. Wolf, J. W. Caldwell, P. A. Kollman, and D. A. Case, *J. Comput. Chem.* **25**, 1157 (2004).
- ⁴¹⁶F. Giberti, M. Salvalaglio, M. Mazzotti, and M. Parrinello, *Chem. Eng. Sci. 2013 Danckwerts Special Issue on Molecular Modelling in Chemical Engineering*, **121**, 51 (2015).
- ⁴¹⁷A. Dey, P. H. H. Bomans, F. A. Müller, J. Will, P. M. Frederik, G. de With, and N. A. J. M. Sommerdijk, *Nat. Mat.* **9**, 1010 (2010).
- ⁴¹⁸Y. Yani, P. S. Chow, and R. B. H. Tan, *Crys. Gro. Des.* **12**, 4771 (2012).
- ⁴¹⁹P. Ectors, P. Duchstein, and D. Zahn, *Cryst. Eng. Comm.* **17**, 6884 (2015).
- ⁴²⁰H. Ohtaki and N. Fukushima, *Pure Appl. Chem.* **63** (1991), 10.1351/pac199163121743.
- ⁴²¹D. Zahn, *Phys. Rev. Lett.* **92**, 040801 (2004).
- ⁴²²I. G. Nahtigal, A. Y. Zaslavsky, and I. M. Svishchev, *J. Phys. Chem. B* **112**, 7537 (2008).
- ⁴²³D. Chakraborty and G. N. Patey, *J. Phys. Chem. Lett.* **4**, 573 (2013).
- ⁴²⁴D. Chakraborty and G. N. Patey, *Chem. Phys. Lett.* **587**, 25 (2013).
- ⁴²⁵H. J. C. Berendsen, J. R. Grigera, and T. P. Straatsma, *J. Phys. Chem.* **91**, 6269 (1987).
- ⁴²⁶J. Chandrasekhar, D. C. Spellmeyer, and W. L. Jorgensen, *J. Am. Chem. Soc.* **106**, 903 (1984).
- ⁴²⁷J. Aqvist, *J. Phys. Chem.* **94**, 8021 (1990).
- ⁴²⁸F. Giberti, G. A. Tribello, and M. Parrinello, *J. Chem. Theory Comput.* **9**, 2526 (2013).
- ⁴²⁹C. Oostenbrink, A. Villa, A. E. Mark, and W. F. Van Gunsteren, *J. Comput. Chem.* **25**, 1656 (2004).
- ⁴³⁰J. Alejandre and J.-P. Hansen, *Phys. Rev. E* **76**, 061505 (2007).
- ⁴³¹I. S. Joung and T. E. Cheatham, *J. Phys. Chem. B* **113**, 13279 (2009).
- ⁴³²J. L. Aragones, E. Sanz, and C. Vega, *J. Chem. Phys.* **136**, 244508 (2012).
- ⁴³³F. Mouka, M. Lsal, J. Kvor, J. Jirsk, I. Nezbeda, and W. R. Smith, *J. Phys. Chem. B* **115**, 7849 (2011).
- ⁴³⁴Z. Mester and A. Z. Panagiotopoulos, *J. Chem. Phys.* **143**, 044505 (2015).
- ⁴³⁵J. Anwar, S. Khan, and L. Lindfors, *Angew. Chem. Int. Ed.* **54**, 14681 (2015).
- ⁴³⁶H.-S. Na, S. Arnold, and A. S. Myerson, *J. Cryst. Growth* **139**, 104 (1994).
- ⁴³⁷Y. Gao, L. E. Yu, and S. B. Chen, *J. Phys. Chem. A* **111**, 10660 (2007).
- ⁴³⁸J. Desarnaud, H. Derluyn, J. Carmeliet, D. Bonn, and N. Shahidzadeh, *J. Phys. Chem. Lett.* **5**, 890 (2014).
- ⁴³⁹E. D. Sloan and C. A. Koh, *Clathrate Hydrates Of Natural Gases, Third Edition* (CRC Press, Boca Raton, Florida, USA, 2008).

- ⁴⁴⁰J. B. Klauda, , and S. I. Sandler, *Energy & Fuels* **19**, 459 (2005), <http://dx.doi.org/10.1021/ef049798o>.
- ⁴⁴¹C. A. Koh and E. D. Sloan, *AIChE Journal* **53**, 1636 (2007).
- ⁴⁴²B. Muller-Bongartz, T. Wildeman, and E. Sloan Jr, in *The Second International Offshore and Polar Engineering Conference* (International Society of Offshore and Polar Engineers, 1992).
- ⁴⁴³E. D. Sloan and F. Fleyfel, *AIChE J.* **37**, 1281 (1991).
- ⁴⁴⁴R. Radhakrishnan and B. L. Trout, *J. Chem. Phys.* **117**, 1786 (2002).
- ⁴⁴⁵R. W. Hawtin, D. Quigley, and P. M. Rodger, *Phys. Chem. Chem. Phys.* **10**, 4853 (2008).
- ⁴⁴⁶C. Moon, R. W. Hawtin, and P. M. Rodger, *Faraday Discuss.* **136**, 367 (2007).
- ⁴⁴⁷C. Moon, P. C. Taylor, and P. M. Rodger, *J. Am. Chem. Soc.* **125**, 4706 (2003).
- ⁴⁴⁸M. R. Walsh, C. A. Koh, E. D. Sloan, A. K. Sum, and D. T. Wu, *Science* **326**, 1095 (2009).
- ⁴⁴⁹J. Vatamanu, , and P. G. Kusalik, *J. Am. Chem. Soc.* **128**, 15588 (2006), pMID: 17147358, <http://dx.doi.org/10.1021/ja066515t>.
- ⁴⁵⁰L. C. Jacobson, W. Hujo, and V. Molinero, *J. Phys. Chem. B* **113**, 10298 (2009), pMID: 19585976, <http://dx.doi.org/10.1021/jp903439a>.
- ⁴⁵¹L. C. Jacobson, W. Hujo, and V. Molinero, *J. Am. Chem. Soc.* **132**, 11806 (2010).
- ⁴⁵²L. C. Jacobson and V. Molinero, *J. Phys. Chem. B* **114**, 7302 (2010).
- ⁴⁵³L. C. Jacobson and V. Molinero, *J. Am. Chem. Soc.* **133**, 6458 (2011).
- ⁴⁵⁴S. Liang and P. G. Kusalik, *Chem. Sci.* **2**, 1286 (2011).
- ⁴⁵⁵S. Sarupria and P. G. Debenedetti, *J. Phys. Chem. Lett.* **3**, 2942 (2012).
- ⁴⁵⁶B. C. Knott, V. Molinero, M. F. Doherty, and B. Peters, *J. Am. Chem. Soc.* **134**, 19544 (2012).
- ⁴⁵⁷D. Bai, G. Chen, X. Zhang, and W. Wang, *Langmuir* **27**, 5961 (2011).
- ⁴⁵⁸D. Bai, G. Chen, X. Zhang, and W. Wang, *Langmuir* **28**, 7730 (2012).
- ⁴⁵⁹D. Bai, G. Chen, X. Zhang, A. K. Sum, and W. Wang, *Sci. Rep.* **5** (2015).
- ⁴⁶⁰P. Pirzadeh and P. G. Kusalik, *J. Am. Chem. Soc.* **135**, 7278 (2013).
- ⁴⁶¹A. H. Nguyen, M. A. Koc, T. D. Shepherd, and V. Molinero, *J. Phys. Chem. C* **119**, 4104 (2015).
- ⁴⁶²Y. Zhang, P. G. Debenedetti, R. K. Prud'homme, and B. A. Pethica, *J. Phys. Chem. B* **108**, 16717 (2004).
- ⁴⁶³G. G. Poon and B. Peters, *Cryst. Growth Des.* **13**, 4642 (2013).
- ⁴⁶⁴Y. Bi and T. Li, *J. Phys. Chem. B* **118**, 13324 (2014).
- ⁴⁶⁵M. R. Walsh, G. T. Beckham, C. A. Koh, E. D. Sloan, D. T. Wu, and A. K. Sum, *J. Phys. Chem. C* **115**, 21241 (2011).
- ⁴⁶⁶C. M. Handley and J. Behler, *Europ. Phys. J. B* **87**, 1 (2014).
- ⁴⁶⁷J. Behler, *J. Phys. Cond. Matt.* **26**, 183001 (2014).
- ⁴⁶⁸A. P. Bartók, M. C. Payne, R. Kondor, and G. Csányi, *Phys. Rev. Lett.* **104**, 136403 (2010).
- ⁴⁶⁹G. A. Tribello, F. Bruneval, C. Liew, and M. Parrinello, *J. Phys. Chem. B* **113**, 11680 (2009).
- ⁴⁷⁰R. Zallen, *The Physics Of Amorphous Solids (Wiley Classics Library)* (Wiley-VCH, 1998).
- ⁴⁷¹R. Cabriolu, D. Kashchiev, and S. Auer, *J. Chem. Phys.* **137**, 204903 (2012).
- ⁴⁷²R. P. Sear, *Int. Mat. Rev.* **57**, 328 (2012).
- ⁴⁷³N. Menon, *Am. J. Phys.* **67**, 1109 (1999).
- ⁴⁷⁴Z. Schuss, *Brownian dynamics at boundaries and interfaces : in physics, chemistry, and biology* (New York Springer, 2013) includes bibliographical references and index.
- ⁴⁷⁵W. Ostwald, *Zeit. Phys. Chem.* **22**, 289 (1897).